Title

GENETIC-PHYSICAL MAPPING OF A PHOTOSYNTHETIC GENE CLUSTER IN Rhodopseudomonas capsulata

Author

Zsebo, K.M.

Publication Date

1984-04-01

LBL-17654

Lawrence Berkeley Laboratory
UNIVERSITY OF CALIFORNIA

CHEMICAL BIODYNAMICS DIVISION

GENETIC-PHYSICAL MAPPING OF A PHOTOSYNTHETIC GENE CLUSTER IN *Rhodopseudomonas capsulata*

K.M. Zsebo
(Ph.D. Thesis)

April 1984

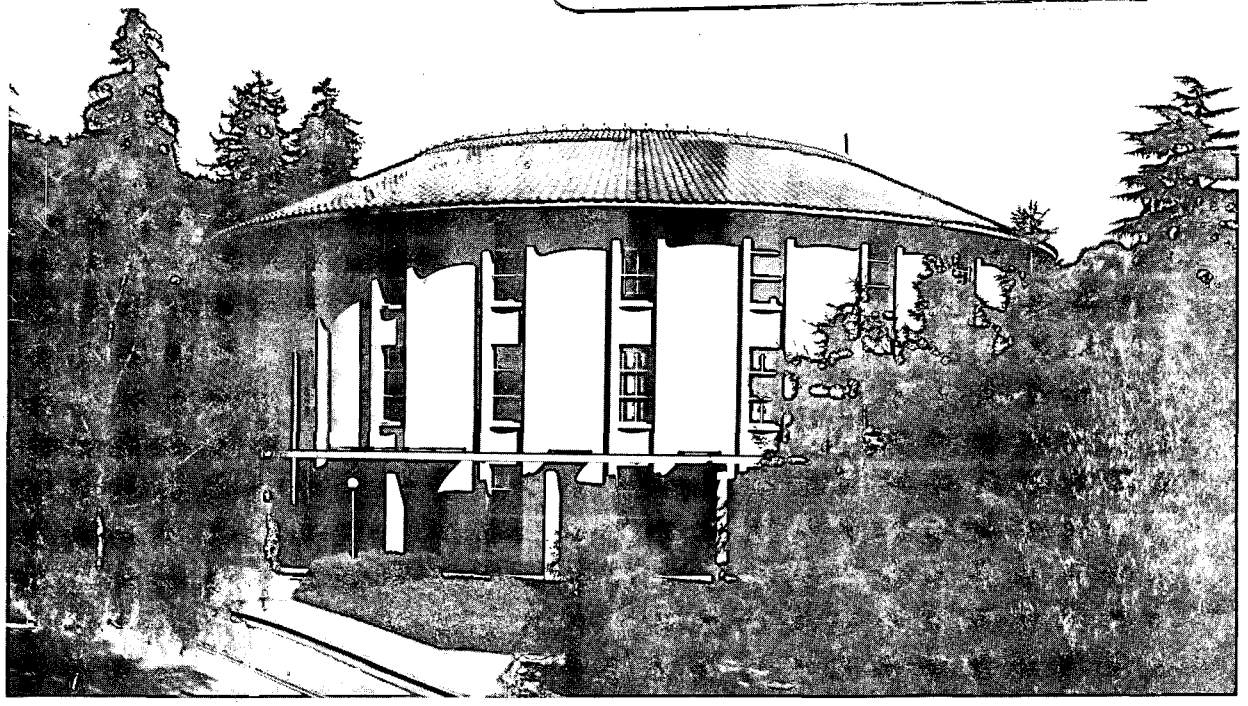

Prepared for the U.S. Department of Energy under Contract DE-AC03-76SF00098

LBL-17654

DISCLAIMER

LBL-17654

GENETIC-PHYSICAL MAPPING OF A PHOTOSYNTHETIC GENE CLUSTER IN *Rhodopseudomonas capsulata*

Krisztina Maria Zsebo
(Ph.D. Thesis)

Chemical Biodynamics Division
Lawrence Berkeley Laboratory
University of California
Berkeley, CA 94720

April 1984

This work was supported by the U.S. Department of Energy under Contract No. DE-AC03-76SF00098.

Abstract

The photosynthesis genes of Rhodopseudomonas capsulata are investigated using transposon mutagenesis, phenotypic characterization of transposon induced mutants, and complementation analysis. The genes investigated are located on an R-prime plasmid, pRPS404, containing 50 kilobase pairs of R. capsulata DNA. A gene replacement scheme is described utilizing the antibiotic resistance markers from Tn7 and the instability of pRPS404 in a recombination proficient background.

A transposon, Tn5.7, has been constructed incorporating the antibiotic resistance markers from Tn7 and the transposition functions from Tn5. It was used to mutagenize the plasmid pRPS404. In conjunction with the mutagenesis, physical mapping of the restriction endonuclease recognition sites for XhoI, BglII, KpnI, and SstI on pRPS404 has been accomplished. Sixty insertions of Tn5.7 into the R. capsulata DNA on the plasmid were isolated and thirty-one of these were crossed into the R. capsulata chromosome with subsequent deletion of wild type alleles. Mutants were characterized by absorption spectroscopy, SDS-PAGE, and determination of capability for photosynthetic growth. Many mutations in the bacteriochlorophyll and the carotenoid biosynthesis genes were isolated. A regulatory mutation was isolated affecting reaction centers as well as a 44kd heme containing polypeptide. Mature bacteriochlorophyll, carotenoids, and light harvesting complexes are made in this mutant. Complementation analysis using various pRPS404::Tn5.7 plasmids has led to the postulation of transcriptional units including bacteriochlorophyll and carotenoid biosynthetic genes as well as reaction center structural genes.

Acknowledgements

I am especially endebted to John Hearst for his support and enthusiasm during the good times as well as the bad. I would also like to acknowledge Nick Panopolous and Barry Marrs for contributing bacterial strains and helpful discussions during the course of this thesis work. Most of all, I would like to thank my husband, Dennis, who for the last three years had to be a part time mother as well as a full time father.

Table of Contents

Abbreviations

ALA	α-aminolevulinate
ADP	adenosine diphosphate
ATP	adenosine triphosphate
Bchl	bacteriochlorophyll
Bpheo	bacteriopheophytin
CMA	chromosome mobilizing ability
DMS	dimethyl sulfide
DMSO	dimethyl sulfoxide
DNA	deoxyribonucleic acid
$E°'$	reduction potential at pH7 with all other activities unity
IS21	insertion sequence 21
Km	kanamycin
LH	light harvesting
NAD+	nicotinamide adenine dinucleotide, oxidized
NADH	nicotinamide adenine ditucleotide, reduced
P_i	inorganic phosphate
PS+/-	photosynthetic growth positive/negative
PSA	photosynthetic apparatus
RC	reaction center
SDS-PAGE	sodium dodecyl sulfate polyacrylamide gel electrophoresis
Sm	streptomycin
Sp	spectinomycin
TMAO	trimethylamine N-oxide
TMA	trimethylamine
Tn	transposon
Tp	trimethoprim

CHAPTER 1: A REVIEW OF RHODOPSEUDOMONAS CAPSULATA

I. Comparative Biochemistry of Rhodopseudomonas capsulata

According to Richard Dickerson, "Human beings are the metabolic offspring of defective photosynthetic bacteria." This statement originates from analysis of molecular data in relation to evolution, mainly analysis of cytochrome c structure (Dickerson, 1980) and ribosomal RNA sequences (Fox et al., 1980). Paracoccus denitrificans is most like the probable ancestor of mitochondria and on the basis of ribosomal RNA and cytochrome c structure it is a close descendent of Rhodopseudomonas sp. According to modern concepts of evolution, oxygen respiration arose independently in several lines of photosynthetic bacteria that adapted a heme protein to shunt electrons from a cyclic electron transport chain to oxygen instead of bacteriochlorophyll (BChl). In support of this theory is the fact that cytochrome oxidases represent the most diverse group of proteins in the electron transport chain.

The metabolic versatility of many Rhodopseudomonads is indicative of their existence during a variety of atmospheric conditions. The multiple modes of growth seem to parallel the evolution of the earth's atmosphere starting from H_2, NH_4, and CO_2 through the build up of organic acids and finally development of an oxidizing medium through the action of Cyanobacteria. Rhodopseudomonas capsulata is capable of six distinct modes of growth: anaerobic phototrophy growing on H_2 plus CO_2 with light as the energy source, anaerobic photoheterotrophy utilizing organic carbon sources and light energy, anaerobic chemoheterotrophy in the dark utilizing a variety of substrates but using an anaerobic form

of respiration for energy production with a terminal electron acceptor such as dimethyl sulfoxide (DMSO), dark aerobic chemoautotrophy utilizing H_2 as the sole source of energy and reducing power, ordinary aerobic chemoheterotrophy utilizing a diverse group of carbon compounds and primarily oxidative phosphorylation for the production of energy, and anaerobic dark fermentation growing on fructose and using substrate level phosphorylation as a source of energy.

One of the earily dilemmas facing researchers involved in bacterial photosynthesis was understanding how reduced pyridine nucleotides were generated during photoheterotrophic growth. In higher plant photosynthesis, NADPH is generated from photosystem I via ferredoxin. Except when growing on H_2, Rhodopseudomonads lack a photosystem which directly generates a compound with a low enough potential to reduce NAD+, since the NAD+/NADH couple is $E^{o'}$ = -320mV. Organic acids such as succinate and malate support photoheterotrophic growth of R. capsulata and chromatophore fractions support succinate linked photoreduction of NAD+ (Jones, 1972). The Chlorobiaceae, green sulfur bacteria, are distinctive in that they produce a reductant of $E^{o'}$=-540mV in the light which is capable of reducing NAD+ directly (Buchanan and Evans, 1969). In R. capsulata as in other purple non-sulfur bacteria, the NAD+ photoreduction proceeds via ATP dependent reverse electron flow similar to the process found in mitochondria (Bose and Gest, 1962; Horio et al., 1963). The fumarate/succinate couple has a reduction potential $E^{o'}$ = +31mV. Highly coupled mitochondria can reduce NAD+ with succinate only if $[ATP]/[ADP][P_i]>10^4$ (Wilson et al., 1974). Under these conditions $\Delta G'$ for reduction of NAD+ by succinate becomes approximately zero and may proceed, given that [ATP] remains high.

During growth on H_2, there is no longer a thermodynamic problem in reducing NAD+ since the $H_2/H+$ redox couple has a potential of $E^{o'} = -420mV$. However, in R. capsulata the reduction of NAD+ by H_2 is ATP dependent, and is summarized in Fig. 1-1. A high potential cytochrome c is reduced by H_2 and ATP is required to pump the electrons from the redox potential of cytochrome c to the one of NAD+ (Klemme and Schlegel, 1967; Madigan and Gest, 1979).

Another interesting area in bacterial photosynthetic metabolism involves the Krebs cycle. The cycle is shown in Fig. 1-2 for reference. During aerobic chemoheterotropic growth the cycle functions to generate reduced pyridine nucleotides which support oxidative phosphorylation and supply biosynthetic intermediates. Glucose and fructose are two sugars utilized which feed into the Krebs cycle from the Entner-Doudoroff and the Embden Meyerhof pathways, respectively (Madigan and Gest, 1978). The rate of the cycle turnover required to support the bioenergetic function is much higher than that necessary to support the biosynthetic demand during aerobic growth. The biosynthetic intermediates needed during aerobic growth are oxaloacetate, for aspartate; succinyl-CoA, for heme and the aspartate family amino acids; and αketoglutaric acid, for glutamate utilization of N_2 or NH_4 as sole N source (Johansson and Gest, 1976). In cells growing photoautotrophically or photoheterotrophically, the Krebs cycle is significant only from a biosynthetic standpoint. However, there is an increase in demand for biosynthetic purposes, namely for succinyl-CoA since it is a precursor for BChl (Lascelles, 1978). Succinyl-CoA synthesis, which proceeds at rates of $0.7 nmol \cdot min^{-1} \cdot mg\ prot^{-1}$ during optimal photosynthetic rates occurs oxidatively from αketoglutarate rather than by reductive

Figure 1-1

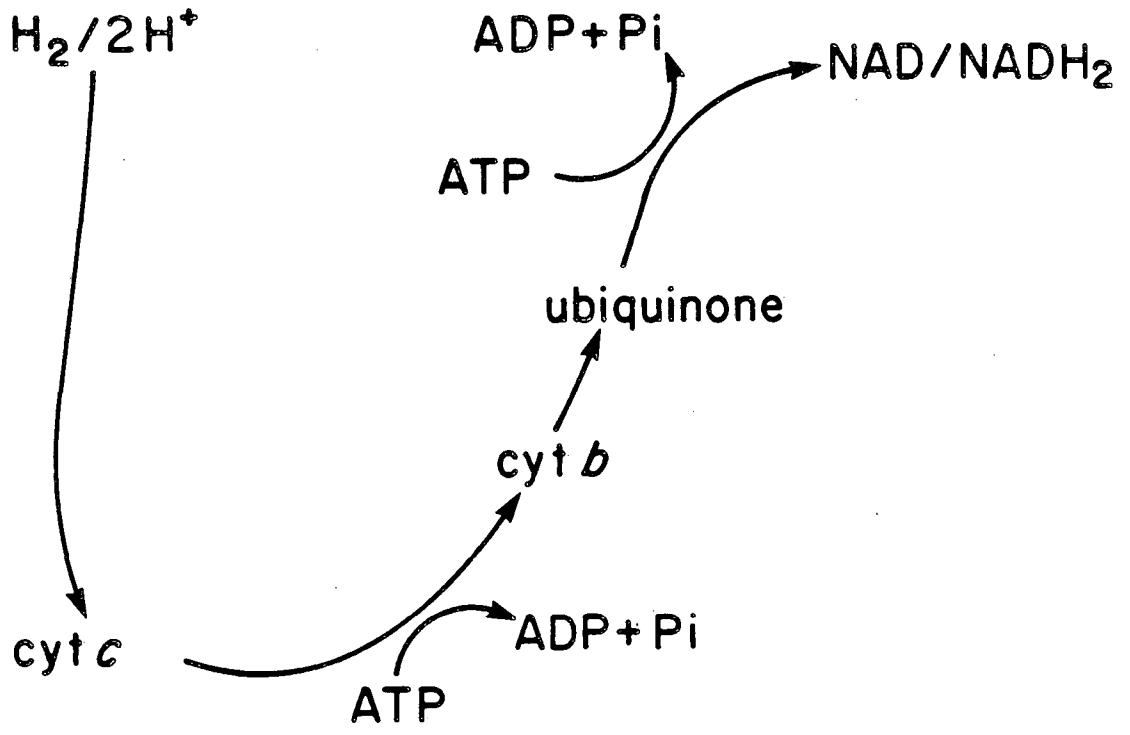

ATP-Dependent Reduction of NAD by H_2

XBL 842-647

Figure 1-2. The tricarboxylic acid cycle. The intermediates are shown as their free acids. The end products are boxed. From Lehninger, 1978.

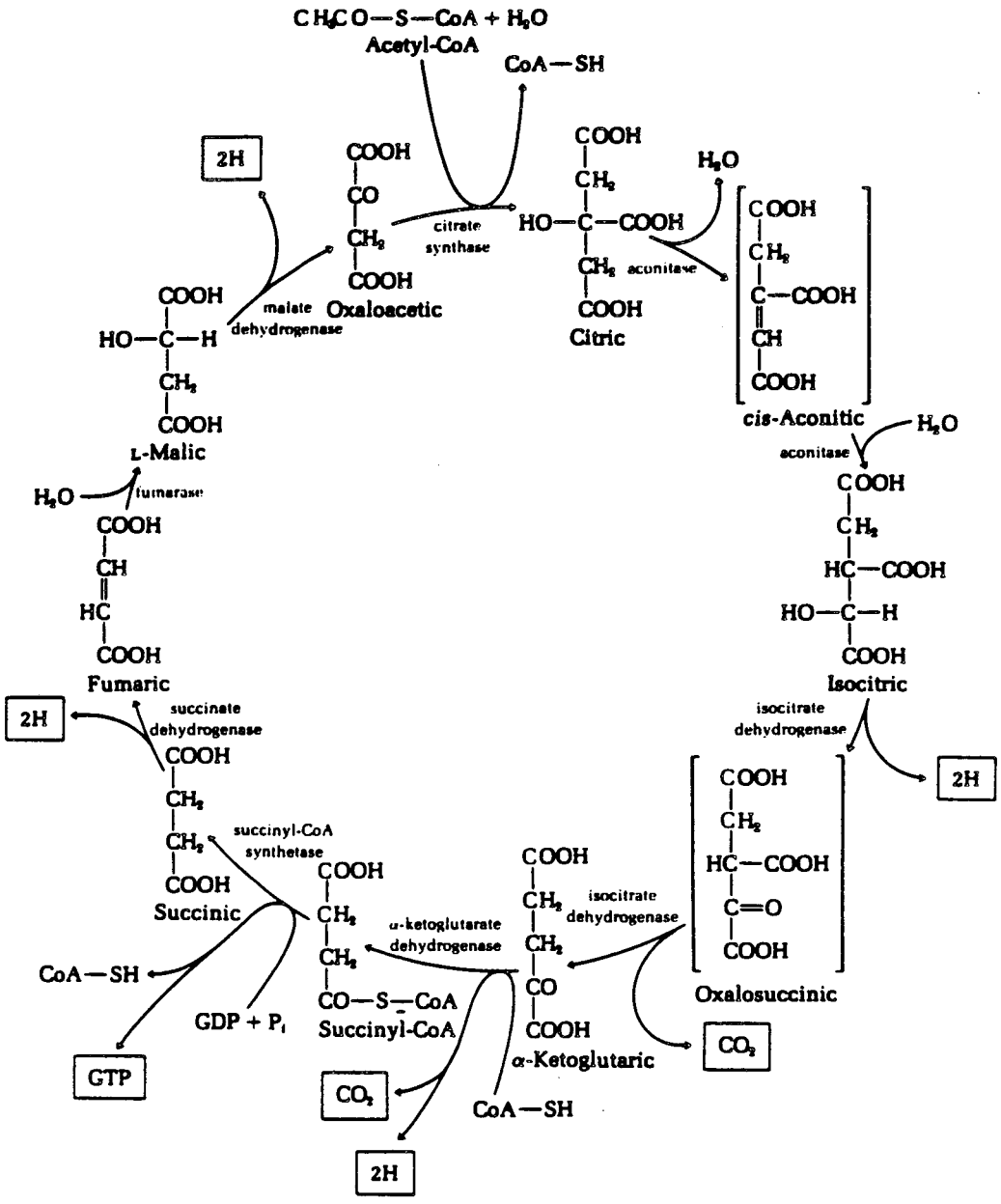
CH3CO—S—CoA + H2O
Acetyl-CoA
CoA—SH
2H
COOH
CO
CH2
COOH
Oxaloacetic
citrate synthase
COOH
CH2
HO—C—COOH
CH2
COOH
Citric
H2O
aconitase
COOH
CH2
C—COOH
CH
COOH
cis-Aconitic
malate dehydrogenase
COOH
HO—C—H
CH2
COOH
L-Malic
H2O
fumarase
COOH
CH
HC
COOH
Fumaric
aconitase
H2O
COOH
CH2
HC—COOH
HO—C—H
COOH
Isocitric
isocitrate dehydrogenase
2H
succinate dehydrogenase
2H
COOH
CH2
CH2
COOH
Succinic
succinyl-CoA synthetase
COOH
CH2
CH2
CO—S—CoA
Succinyl-CoA
α-ketoglutarate dehydrogenase
COOH
CH2
CH2
CO
COOH
α-Ketoglutaric
isocitrate dehydrogenase
COOH
CH2
HC—COOH
C=O
COOH
Oxalosuccinic
CoA—SH
GDP + Pi
GTP
CO2
CO2
CoA—SH
2H

XBL 842-644

metabolism of fumarate (Beatty and Gest, 1981). Still, there is a five fold higher activity of αketoglutarate dehydrogenase in aerobic cells than photosynthetic ones (Beatty and Gest, 1981).

R. capsulata is able to grow under dark anaerobic chemoheterotrophic conditions only in the presence of an accesory oxidant such as DMSO or trimethylamine-N-oxide (TMAO). Neither NADH dehydrogenase nor terminal oxidase activities are required for the function of DMSO (Yen and Marrs, 1977). There has been some controversy over the role of DMSO or TMAO during these growth conditions. Madigan et al., (1980) contend that the role of TMAO is to function as an electron sink to maintain fermentative redox balance, rather than acting as an electron acceptor for electron transport driven phosphorylation. They present evidence which suggests that during anaerobic dark growth on fructose and TMAO, ATP is generated by substrate level phosphorylation associated with glycolysis and pyruvate dissimilation. In their hands, only fermentable substrates supported TMAO related growth, but not organic acids such as succinate or malate. Cell fractionation studies indicated that the TMAO reductase resides in the cytoplasmic fraction and is not membrane bound as in E. coli (Cox et al., 1980). Schultz and Weaver (1982) demonstrated growth of R. capsulata on succinate, malate, and acetate in the presence of DMSO and TMAO and showed accumulation of dimethyl sulfide (DMS) and trimethylamine (TMA). However, they say that growth on TMAO resulted in inhibition during the latter stages of growth by the alkalinity of the TMA produced; 20mM resulted in a final pH of 9. Possibly, some of the discrepancies involving TMAO supported growth are due to the difficulty of maintaining a physiological pH in the medium. Growth on DMSO produces a volatile gas, dimethyl sulfide (DMS), as the by-product and is

therefore the preferred substrate for dark anaerobic growth. Recently, Schultz and Weaver (to be published) have isolated and characterized a membrane bound cytochrome $\underline{c}_{555}$ which functions as an electron transport mediator fully reduced by succinate and oxidized by DMSO, TMAO, and methionine sulfoxide. It is produced only during dark anaerobic growth with DMSO or potassium nitrate. The cytochrome has a molecular weight of 44kd and contains two hemes with midpoint potentials of +6 and -230 mV. The $E^{o'}$ for the DMSO/DMS couple is +160 mV (Wood, 1981) and therefore the cyt $\underline{c}_{555}$ could easily function to reduce DMSO. However, it was found that the DMSO reductase is in the periplasm, possibly coupled to the cyt $\underline{c}_{555}$. It is not known where this cytochrome fits in with the rest of the electron transport chain, however, during oxidation of cyt $\underline{c}_{555}$ by DMSO, cyt $\underline{c}_2$ remains reduced.

<u>R. capsulata</u> is not well adapted to dark anaerobic fermentation. Schultz and Weaver (1982) determined a doubling time of 26h during anaerobic fermentation of fructose. This is in comparison to a 6h doubling time under similar conditions but in the presence of DMSO. The fermentative end products, indicative of a strict mixed-acid fermentation, were lactate, acetate, succinate, H_2, and CO_2. The basic disadvantage for <u>R. capsulata</u> growing fermentatively is that it has not evolved a mechanism to shut down the synthesis of the very energetically expensive photosynthetic apparatus (PSA) and has to support itself by the few ATP's per carbohydrate produced from substrate level phosphorylation. In fact, fermentative growth is a successful enrichment for photosynthetic mutants since cells which no longer synthesize the PSA rapidly outgrow the wild type cells.

II. Biosynthesis of Bacteriochlorophyll

The synthesis of BChl is interesting from a biochemical standpoint as well as in relation to the synthesis of the other components of the PSA, namely the structural polypeptides of the light harvesting (LH) complexes and reaction center (RC). The proposed biosynthetic pathway to mature BChl in *R. capsulata* is shown in Fig. 1-3. The pathway from δ-aminolevulinate (ALA) to protoporphyrin is in common with heme biosynthesis. A major regulatory site for tetrapyrrole synthesis is ALA synthetase which appears to exist in both high and low activity forms (Rebeiz and Lascelles, 1982). A detailed review, through 1981, of the steps involved in both BChl and carotenoid biosynthesis is available in "Photosynthesis I: Energy Conversion by Plants and Bacteria", Chapter 15 (Rebeiz and Lascelles, 1982).

New findings concerning the BChl biosynthetic pathway include identification of additional intermediates in the pathway from protoporphyrin IX to BChl, purification of additional synthetic enzymes in the pathway, identification of an alternate synthetic route to ALA, and determination of additional regulatory factors controlling the rate of formation of mature BChl.

Through the use of mutational analysis, absorption and emission spectroscopy, and thin layer chromatography, 2-desacetyl-2-vinyl bacteriochlorophylide *a* has been placed in the biosynthetic route to BChl (Biel and Marrs, 1983). It appears that in the conversion of chlorophyllide *a* to 2-desacetyl-2-hydroxyethyl bacteriochlorophyllide *a*, the hydration and reduction steps in *R. capsulata* can occur in either order, Fig. 1-3. The accumulation of porphyrin molecules by a mutant is

Figure 1-3. Biosynthesis of Bacteriochlorophyll. I. From 2-oxyglutarate or succinyl-CoA and glycine to Protoporphyrin IX. II. Protoporphyrin IX to Bacteriochlorophyll a. The pathway to Protoporphyrin IX is common to heme biosynthesis.

Bacteriochlorophyll Synthesis

To Protoporphyrin IX

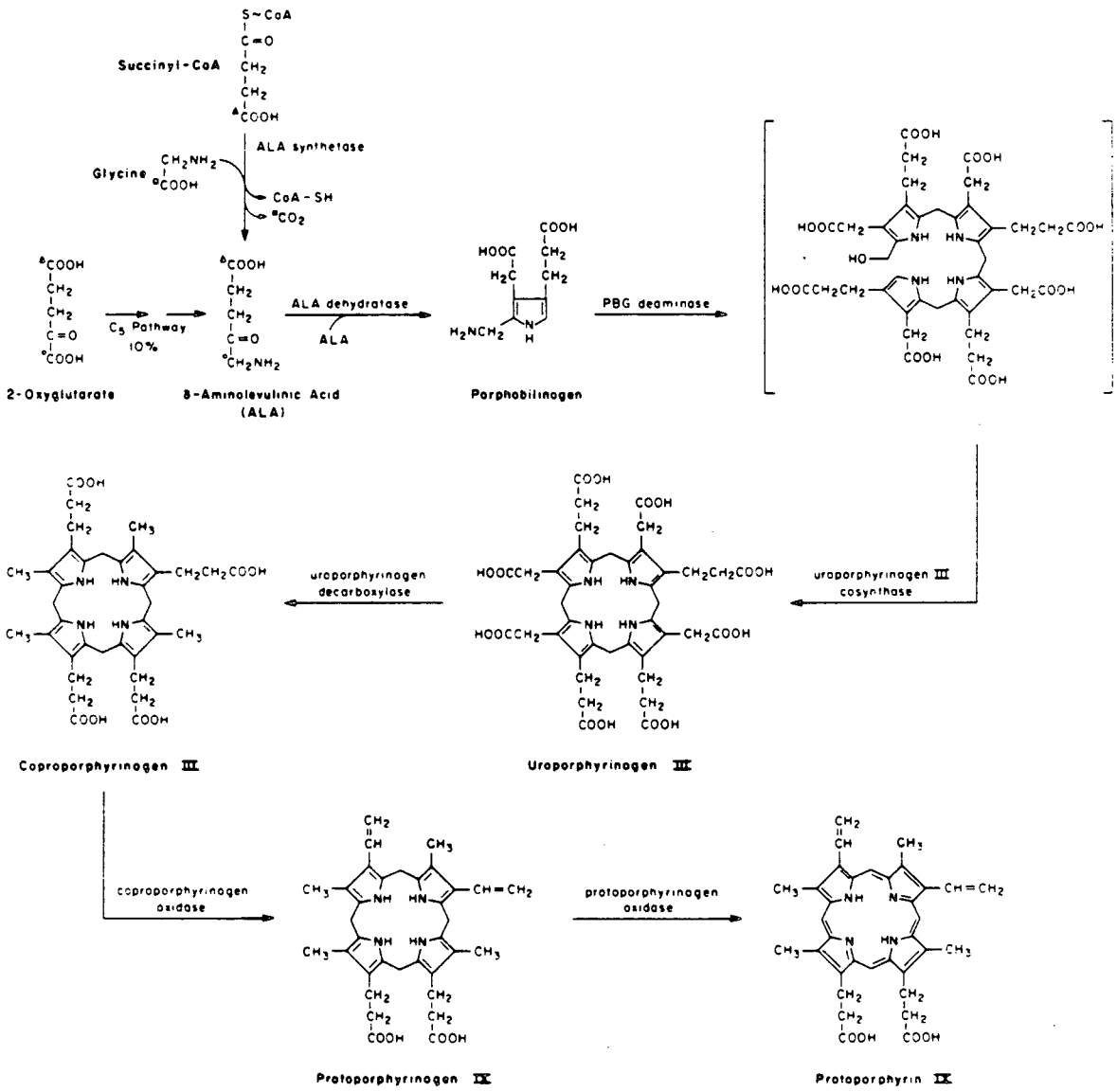

Bacteriochlorophyll Synthesis

Protoporphyrin IX to Bacteriochlorophyll *a*

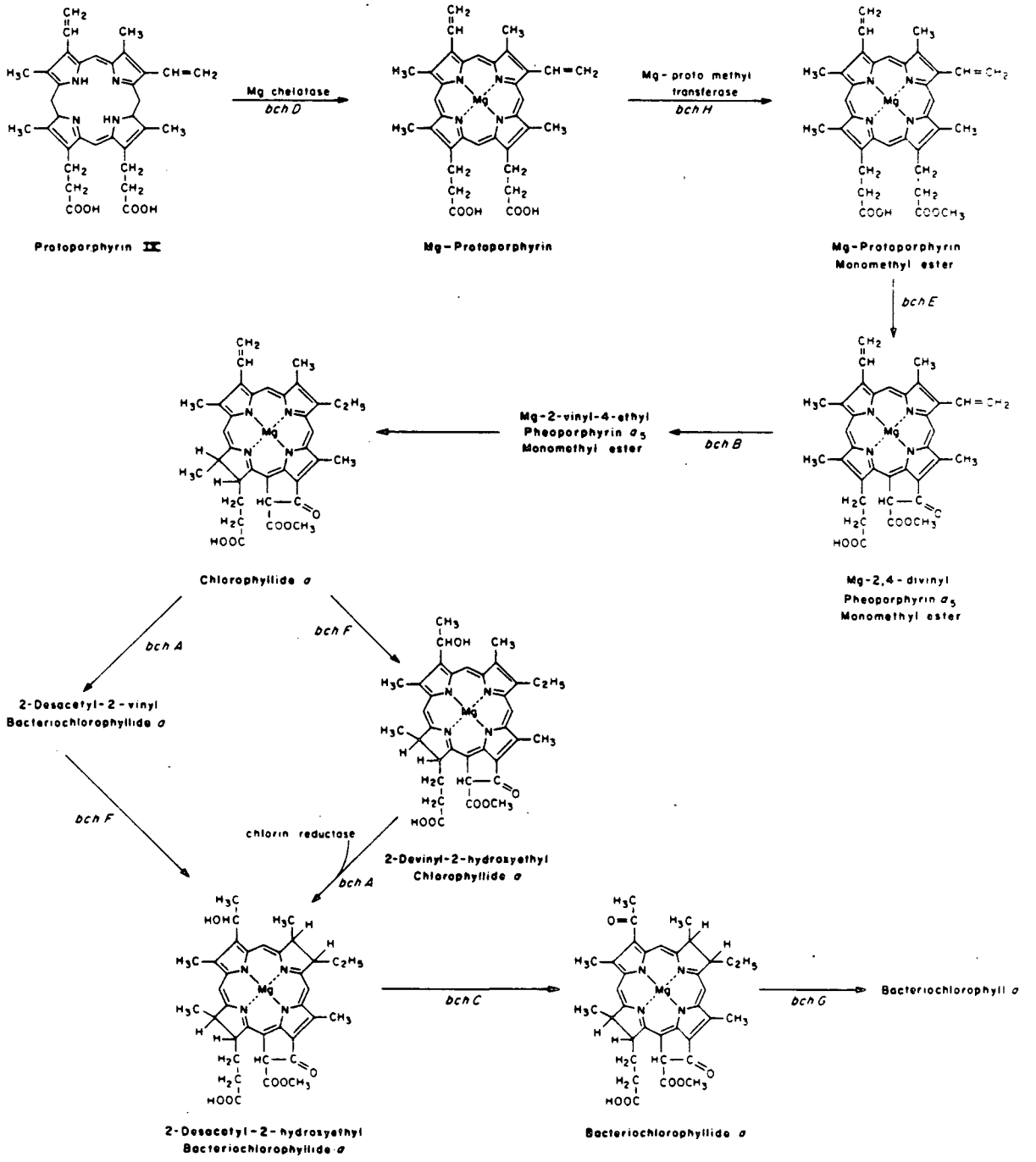

not necessarily proof that that compound is a true intermediate in the pathway. However, the more thorough method of showing conversion of a putative intermediate to mature BChl is hampered by the fact that early in the biosynthetic pathway the porphyrins become complexed to proteins, carbohydrates, and membranes, therefore, externally added free tetrapyrroles are not active. Many BChl biosynthetic mutants accumulate more than one compound, suggesting that enzyme complexes exist and are stable only when all components of the complex are present.

Recent improvements in methodology for preparation of porphobilinogens have advanced the understanding of the stereochemistry of Bchl synthesis. The stereochemistry of coproporphyrinogen III oxidases of R. spheroides, which convert porphobilinogen to protoporphyrin IX, were determined by stereospecific labelling with ^{3}H (Seehra et al., 1983). The stereochemistry of vinyl group formation from porphobilinogen by aerobic and anaerobic coproporphyrinogen II oxidases are identical with those reported from chicken reticulocyte and plant systems.

Ferrochelatase inserts ferrous iron into protoporphyrin IX during the biosynthesis of heme. Recently, a membrane bound ferrochelatase from R. spheroides was purified to apparent homogeneity (Dailey, 1982). The enzyme has a molecular weight of 115kd, is sensitive to sulfhydryl agents and, like ALA synthetase, is inhibited by heme.

The first intermediate specific to the tetrapyrrole biosynthetic pathway is ALA. Until recently, it had been assumed that ALA was formed solely, as in the Shemin pathway for heme synthesis, by the condensation of succinyl-CoA and glycine. Through the use of ^{14}C tracer methods, Klein and Porra (1982) demonstrated the operation of an additional

pathway to ALA from the C_5 compound 2-oxoglutarate. It was determined that in R. spheroides, the Shemin pathway and the C_5 pathways contribute 90 and 10%, respectively, to ALA synthesis. This is consistent with the finding that an ALA synthetase deficient mutant of R. spheroides can form BChl in the absence of exogenous ALA (Chen et al., 1981).

BChl synthesis has been assumed to be regulated mainly at the level of ALA synthetase and ALA dehydratase since both enzymes are four to five times less active in cell free extracts from aerobic dark-grown cells compared to those from semi-anaerobic light grown cells (Lacelles, 1978). However, recent studies with direct ^{13}C nuclear magnetic resonance spectroscopy (Burton et al., 1981) suggest that control also lies with coporphyrinogen III oxidase since coproporphyrin III accumulates in large quantities under anaerobic light conditions. In addition, ALA dehydratase, which in cell free extracts is extremely O_2 sensitive, still remains substantially active under aerobic conditions in whole cells.

The presence of ferredoxin in R. capsulata (Hellenbeck, 1982; Yakunin and Gogotov, 1983) and in R. spheroides (Clement-Metral, 1981) has been demonstrated. In R. spheroides, a partially purified preparation of thioredoxin activated both forms of ALA synthetase when reduced as well as DTT itself.

The mode of interaction between the synthesis of BChl and the structural polypeptides of the RC and LH complexes is not known. However, when mature BChl is not made, the photosynthetic membrane is not synthesized. This interaction may occur post-translationally by degradation of the structural polypeptides in the absence of mature BChl. This would be the most energetically expensive control mechanism.

Alternatively, the control may be exerted at the level of transcription or translation.

Transcriptional control of some of the bch genes by O_2 has recently been demonstrated (Biel and Marrs, 1983). The authors demonstrated that some BChl genes are regulated at the level of transcription by O_2 but not by light. Additional discussion of this problem is reserved for Chapter 4 of this thesis.

In the higher plant Lemna gibba, the synthesis of the Chl a/b apoprotein is regulated by a light dependent step at the level of translation (Slovin and Tobin, 1982). In prokaryotic systems, control at the level of translation has also been demonstrated. Some ribosomal proteins can inhibit the translation of their own messenger RNA (mRNA) (Nomura, 1980; Miura et al., 1981).

III. Biosynthesis of Carotenoids

Carotenoids serve dual functions in a photosynthetic membrane. They protect the organism from photooxidative damage and extend the absorption spectrum in the 400-500nm range. Photooxidative damage may result from singlet O_2 which is formed via the BChl triplet state (Krinsky, 1978). The BChl triplet state has a greater chance of being populated during high light intensities. The BChl can transfer its triplet state energy to form a carotenoid triplet which is harmless. Photosynthetic bacterial mutants which lack carotenoids are viable unlike higher plants, since the bacteria participate in anoxygenic photosynthesis. These carotenoidless mutants show pleiotropic effects, mainly abolishing LH II absorption at 800 and 855nm.

Carotenoids are C_{40} tetraterpenoids consisting of eight isoprene units. Until the advent of genetic analysis, carotenoid biosynthesis was studied with the use of inhibitors such as diphenylamine, which inhibits desaturation of carotenoids. Carotenoid biosynthesis is reviewed in "The Photosynthetic Bacteria" (Schmidt, 1978). Genetic analysis can potentially provide intermediates from all of the biosynthetic steps, not only sites of inhibitor action. The biosynthetic scheme to spheroidenone is shown in Fig. 1-4. Initial steps were determined by Pandian et al. (1981) by incorporation of ^{14}C acetate and lactate into isoprenoid compounds. Mevalonic acid is the precursor of the isoprene unit (Folkers et al., 1959) and isopentenyl pyrophosphate is a key intermediate in the metabolic pathway. The first C_{40} compound is phytoene and is formed from a condensation of two molecules of geranyl-geranyl pyrophosphate. Through a series of desaturations,

neurosporene is formed. The biosynthetic pathway from neurosporene to spheroidenone was postulated by Scolnik et al. (1980) through analysis of carotenoid mutants. Biosynthetic intermediates were determined by visible and mass spectroscopy, derivatization, and chemical analysis.

Figure 1-4. Carotenoid Biosynthesis. I. Acetolactate to Isopentenyl pyrophosphate. II. Isopentenyl pyrophosphate to Phytoene. III. Phytoene to Spheroidenone. From Schmidt, 1978; Pandian et al., 1981.

Carotenoid Biosynthesis

I Acetolactate to Isopentenyl Pyrophosphate

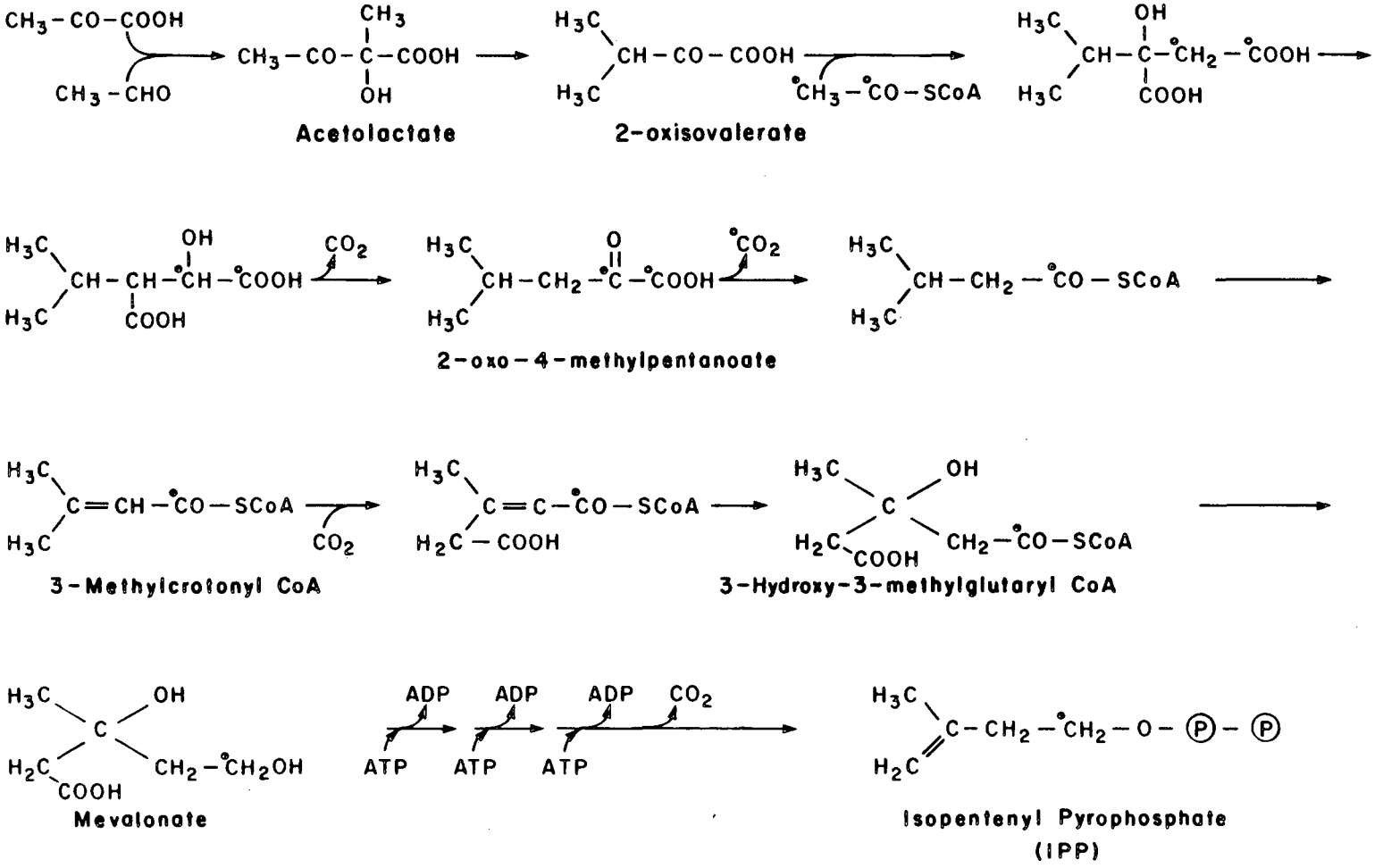

XBL 842-650

II Isopentenyl Pyrophosphate to Phytoene

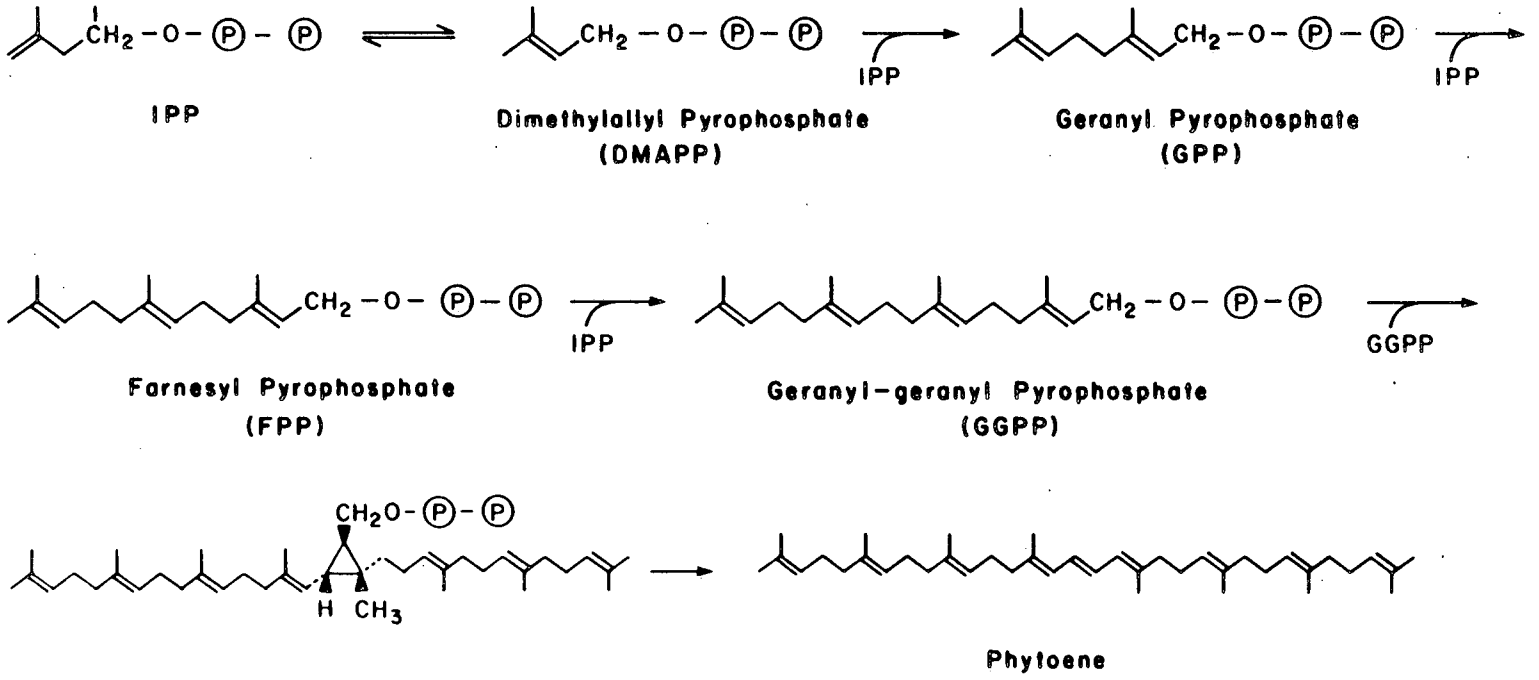

XBL 842-649

III Phytoene to Spheroidenone

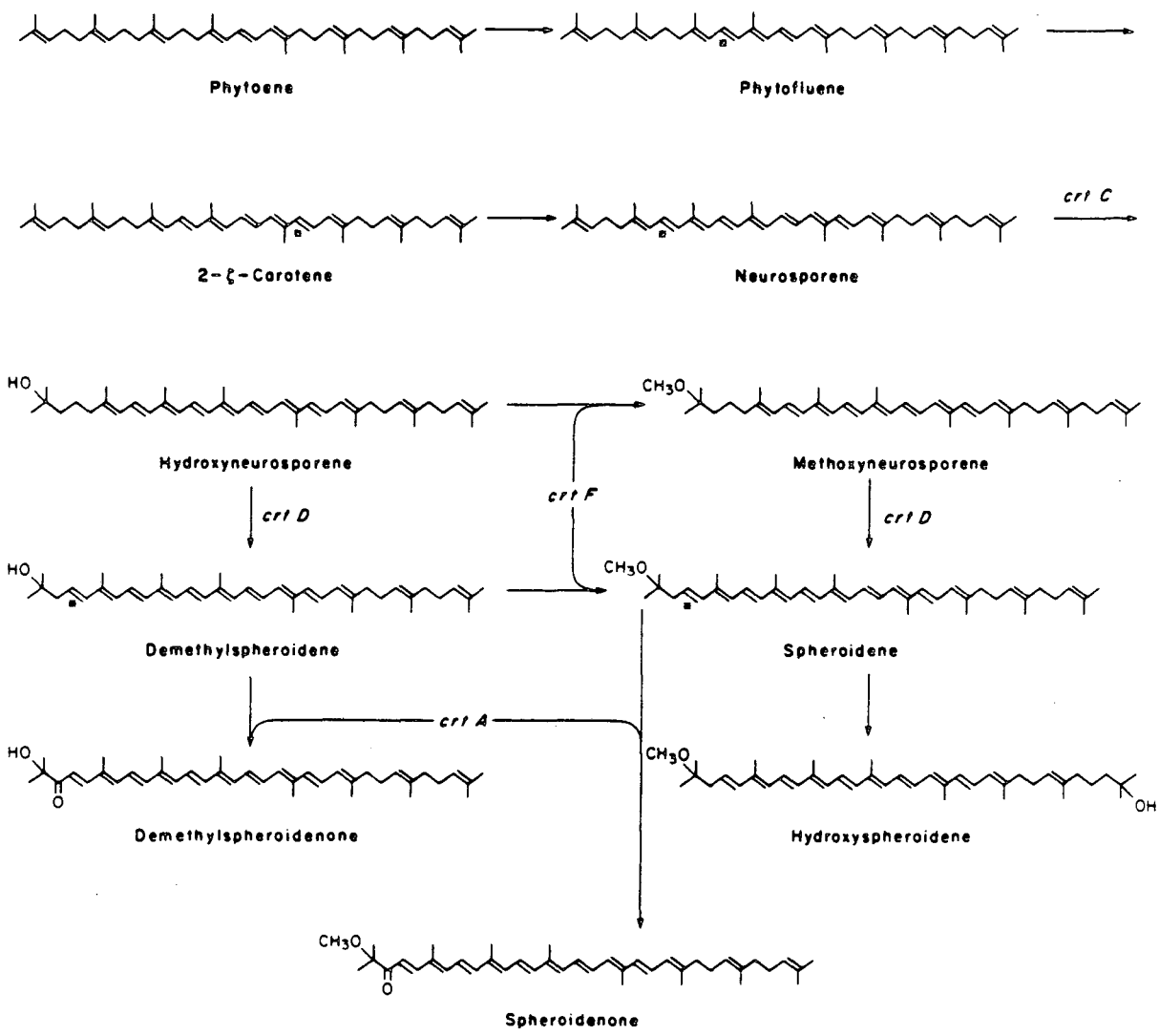

IV. The Photosynthetic Apparatus

For R. capsulata, the photosynthetic membrane is the result of invaginations of the cytoplasmic membrane in response to a lowering of the oxygen tension to below 10mm Hg. The minimum structures which are assembled into the invaginations are the LH II, LH I, RC, and cytochrome b-c complexes. The development of the photosynthetic membrane has recently been reviewed (Kaplan and Arntzen, 1982). The LH II complex consists of one molecule of each of three polypeptides (MW 12, 9.3, and 5.1kd), three molecules of BChl, and one molecule of carotenoid. The two molecules of BChl are associated with the 9.3kd subunit and the one molecule BChl associated with the 5.1kd subunit are believed to be responsible for the absorption maxima at 855 and 802nm, respectively (Cogdell and Crofts, 1978; Feick and Drews, 1979; and Sauer and Austin, 1978). The carotenoid is probably associated with the lower MW polypeptide (Webster et al., 1980). The LH I complex consists of two polypeptides (MW 7.6 and 5.6kd), two molecules of BChl, and one carotenoid and has an absorption maximum at 870nm (Broglie et al., 1980) Each polypeptide is thought to bind one molecule of BChl (H. Zuber, personal communication) The RC consists of three polypeptides (MW 28, 24, and 20kd), four molecules of BChl, two bacteriopheophytins (Bpheophytin=BChl without the Mg), two ubiquinones, one Fe^{+2}, and one spheroidene (Youvan et al., in press; Feher and Okamura, 1977; Cogdell et al., 1976) The two low molecular weight L and M subunits are thought to bind all of the pigments.

In addition to the RC and LH complexes, the photosynthetic membrane contains a ubiquinol-cytc_2 oxidoreductase complex. A composite

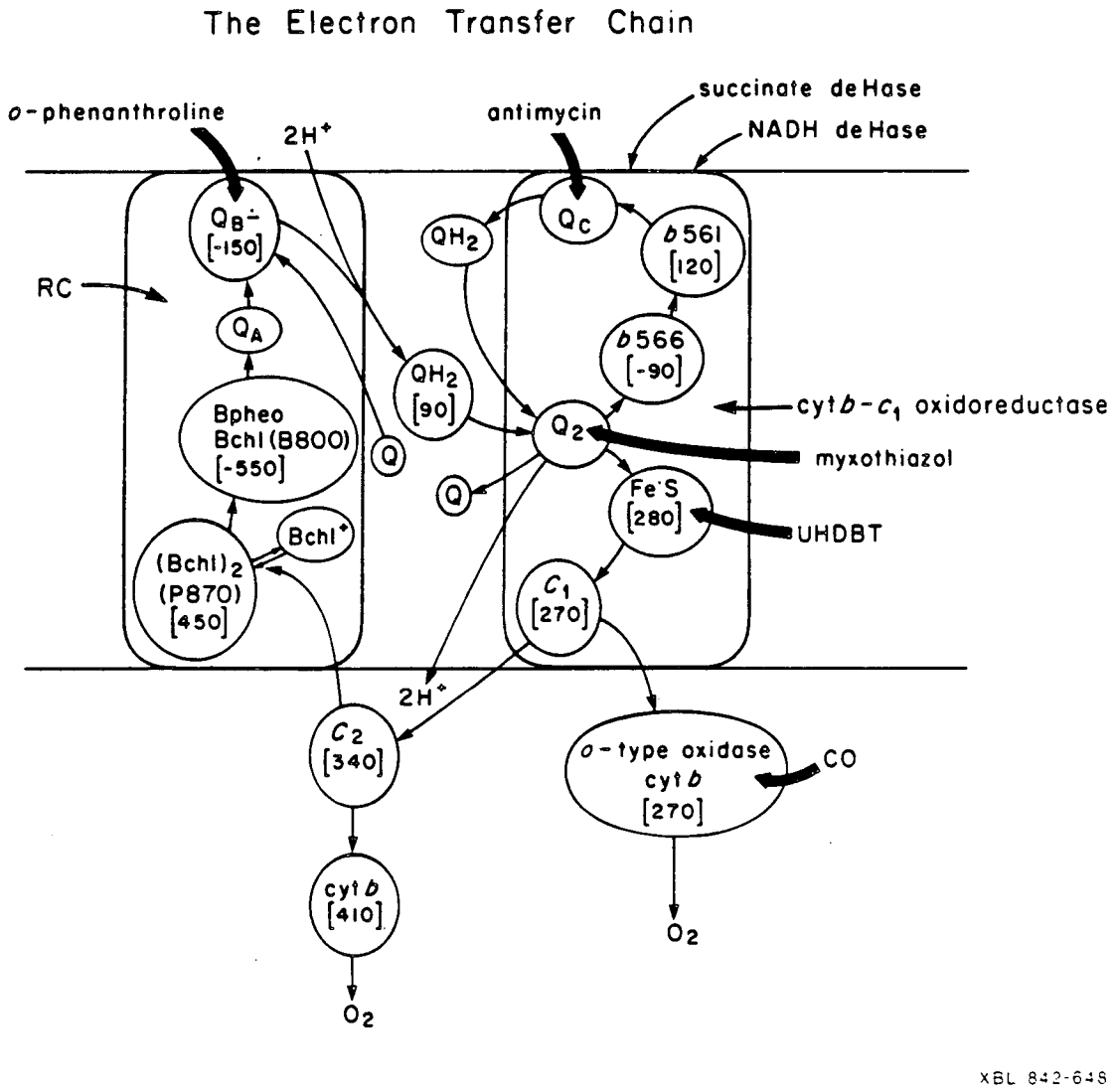

Figure 1-5. Electron Tranfer Chain. The membrane is shown with the RC and cyt$\underline{b}$-$\underline{c}_1$ oxidoreductase complex. The light harvesting complexes are not shown. Narrow arrows show electron transfers and are discussed in the text. Wide arrows show sites of binding and inhibition. From Cramer and Crofts, 1982; Zannoni et. al., 1976, 1978.

Figure 1-5. Electron Transfer Chain. The membrane is shown with the RC and cyt$\underline{b}$-$\underline{c}_1$ oxidoreductase complex. The light harvesting complexes are not shown. Narrow arrows show electron transfers and are discussed in the text. Wide arrows show sites of binding and inhibition. From Cramer and Crofts, 1982; Zannoni et. al., 1976, 1978.

diagram of the electron transport chain is shown in Fig. 1-5. During any given growth mode, only parts of this scheme operate. The RC electron transfer reactions have been reviewed by Okamura et al. (1982). Light is absorbed by Bchl in the RC via photon transfer reactions from LHII to LHI to RC, LHII to RC, or by direct absorption of a photon by the RC. An electron is transfered from the BChl to Bpheo, the intermediate electron acceptor. The unpaired electron in the oxidized donor is shared by a pair of BChl molecules. The reduced Bpheo transfers its electron to a ubiquinone, Q_A. This primary electron acceptor transfers its electrons to a secondary acceptor ubiquinone, Q_B. A non-heme iron is associated with both quinones and is thought to facilitate electron transfer from the primary to the secondary quinone. Q_B acts as a two electron gate in that it exists as a stable semiquinone until reduced a second time by Q_A. At this point, the electrons are transfered to the quinone pool along with a pair of protons from the cytoplasm. The quinone pool transfers electrons and protons to the ubiquinol-cyt$\underline{c}_2$ oxidoreductase complex. Passage of the electrons and protons through this complex is reviewed by Cramer and Crofts (1982). The complex consists of bound quinones, cytochromes $\underline{b}_{566}$ and $\underline{b}_{561}$, a Rieske iron-sulfur center, and cyt$\underline{c}_2$. The complex in Fig. 1-5 is arranged so as to act as a two-electron transferring complex. The stoichiometry of components is thought to be .5 complex/RC. One electron is thought to be transferred and 2H+ transported per RC turnover. During cyclic electron transport, cyt$\underline{c}_2$ re-reduces the BChl+ in the RC which is then ready to accept another photon. If the photon arrives when the RC is in an oxidized state, the photon is emitted as fluorescence.

During aerobic respiration, succinate dehydrogenase and/or NADH

dehydrogenase donate electrons to the ubiquinol-cyt $\underline{c}_2$ oxidoreductase complex, some components which are thought to be shared with the cyclic electron transport system (Zannoni et al., 1978, 1981; Smith and Pinder, 1978). The exact nature of this interaction is not understood. *R. capsulata* contains a branched respiratory chain and contains two terminal oxidases, cyt$\underline{b}_{410}$ and cyt$\underline{b}_{260}$ (Zannoni et al., 1974, 1976).

V. Genetics and Molecular Biology

The study of photosynthesis in R. capsulata is aided by the multiple growth modes of this organism, described above. Basically, photosynthetic mutants may be propagated by aerobic or anaerobic chemoheterotrophic growth. Recently, the molecular biology of R. spheroides and R. capsulata has been reviewed (Marrs, 1984). In R. capsulata, genetic analysis became a reality when capsduction was discovered by Marrs (1974). The particles that serve as vectors for capsduction are called gene transfer agents (GTA) and transfer 4.3kb of DNA at a time. The isolation of GTA allowed for the fine structure mapping of several genes involved in BChl and carotenoid biosynthesis (Yen and Marrs, 1976). Once point mutants were isolated and mapped, an entire region of DNA coding for various photosynthesis genes was isolated (Marrs, 1981). The method of isolation of photosynthesis genes is outlined in Figs. 1-6 and 1-7. The method is based on the ability of certain DNA elements, IS elements, to mobilize foreign DNA. pRPS404 was derived from RP1, a broad host range conjugative plasmid shown in Fig. 1-6. A series of insertions and a duplication of the IS21 element produced pBLM2 containing chromosome mobilizing ability (CMA). Once these elements are introduced into an organism, desired regions were mobilized through the use of suitable selectable markers. For R. capsulata, these markers provided capability for photosynthetic growth, since genes involved in photosynthesis were to be isolated. The isolation scheme outlined in Fig. 1-7 starts with a strain containing a crtD mutation (green phenotype, PS+) and a bchA mutation (wild type carotenoids, PS-). The plasmid pBLM2 contains two

Figure 1-6. Lineage of pRPS404. The plasmid RP1 is the ancestor of pRPS404. Chromosome mobilizing ability (CMA) in pBLM2 results from a duplication of IS21.

Figure 1-7. Isolation of R. capsulata photosynthesis genes using pBLM2.

Figure 1-6

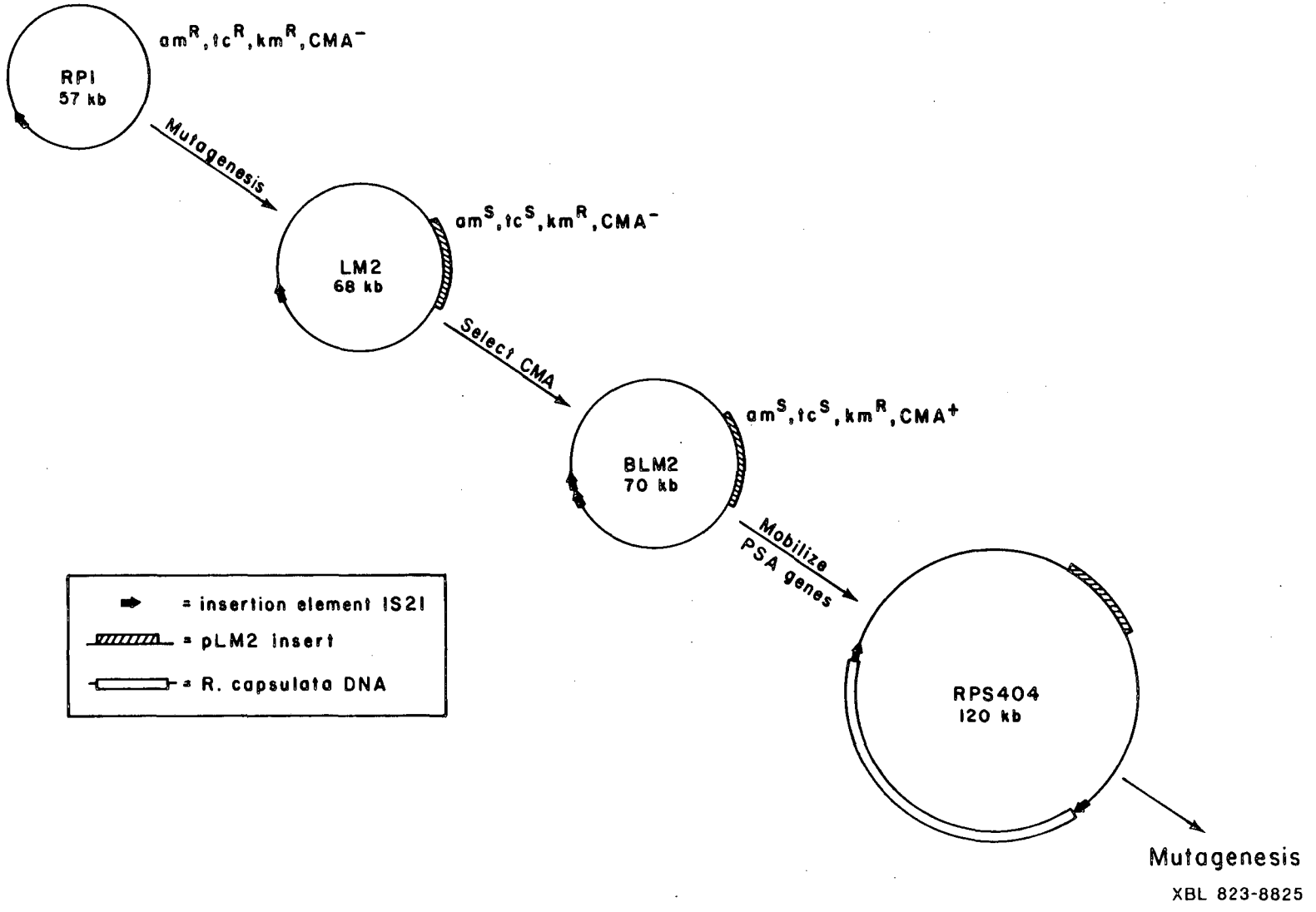

XBL 823-8825

Figure 1-7

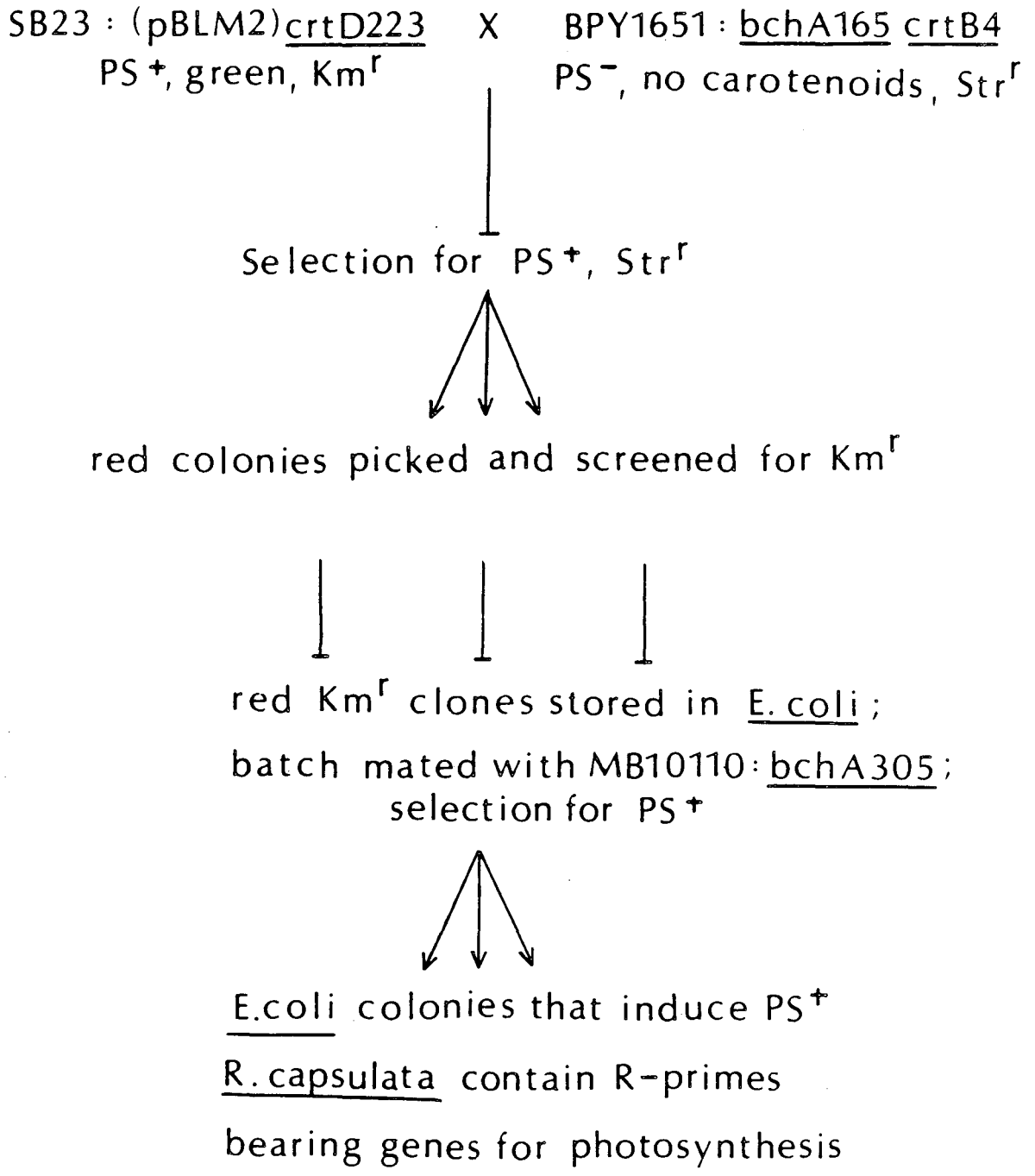

XBL 842-645

IS21 elements and is capable of mobilizing large segments of DNA, relatively at random. A mating between the two strains allowed for transfer of pBLM2 to the PS- strain at roughly 10^{-1} frequency. The selection was for photosynthetic growth, carried by the donor of pBLM2, and resistance to rifampicin, carried by the recipient. The small red unstable PS+ colonies, result from complementation of the bchA gene in trans. Some of these colonies when further repurified, sector green due to recombination of the crtD gene into the chromosome. Since the bchA and crtD genes are greater than 4.3kb apart, the only way that a PS+, carotenoid+ recombinant could arise is by the transfer of a segment of DNA by a mechanism different from GTA. The presence of the kanamycin (Km) marker in the recipient suggests that the DNA was transfered via pBLM2. These strains each carried an R-prime plasmid with photosynthesis genes, at least the bchA gene. They were then tested for complementation of a number of other genes involved in photosynthesis by similar matings with PS- mutants. It was found that the genes for BChl and carotenoid biosynthesis were tightly clustered on the R. capsulata chromosome since all of the R-prime plasmids isolated by original complementation of the bchA gene complemented all of the other known photosynthetic mutants. This by no means indicates that all of the genes necessary for the differientation of the PSA is coded for by the R-prime pRPS404.

With the isolation of a large segment of DNA carrying photosynthesis genes, the door was opened for the genetic analysis of these genes irrespective of whether mutations in them existed or not. Therefore, the genetic analysis of this DNA segment was undertaken via transposon mutagenesis. The aims were to locate as many new genes as possible contained on the R-prime plasmid. In particular, the reaction

center structural genes were sought for sequencing purposes since the primary protein structure of the RC could not be determined by protein sequencing due to hydrophobicity. In addition, with the possibility of complementation analysis, transcriptional units could be determined.

Transposon mutagenesis has been used for the analysis of a number of gene clusters, among them are nitrogen fixation genes in Rhizobium meliloti (Ruvkun et al., 1982) and the virulence region of the Agrobacterium tumefaciens Ti plasmid (Lundquist et al., 1984). A transposon is a segment of DNA which codes for enzymes which catalyze the breaking and joining of covalent bonds in DNA. The breaking of the DNA occurs at relatively random sites and the rejoining results with the transposon in a new location as well as remaining at the old site. The terminal few base pairs of the transposon are recognized by the transposases, which catalyze the transposition event, and preferences exist for homologous sequences in the target DNA.

This thesis describes transposon mutagenesis of the R-prime plasmid pRPS404 containing photosynthesis genes from R. capsulata. The genes for the RC and LH I structural genes were identified, numerous genes involved in BChl and carotenoid biosynthesis and regulatory genes affecting RC and LH I were located. In addition, complementation analysis revealed transcriptional operons including BChl and carotenoid genes suggesting coordinate control. Chapter 2 describes the replacement scheme used for replacing the wild type genes with transposon mutated genes. Chapter 3 describes the cloning of Tn5.7, the transposon used for mutagenesis, and physical mapping of restriction enzyme recognition sites in pRPS404, which were used for accurate mapping of the transposon inserts. Chapter 4 deals with the genetic-physical mapping of the

photosynthetic gene cluster on the R-prime plasmid.

CHAPTER 2:GENE REPLACEMENT SYSTEM FOR TRANSPOSON MUTAGENIZED GENES

I. INTRODUCTION

Transposon mutagenesis was utilized to determine the coding identity of the DNA outside the genetically mapped region within the R-prime. The R-prime was mutagenized in *E. coli* with Tn7 and then returned to the wild type *R. capsulata*. Reciprocal homologous recombination replaces the wild type gene with the mutagenized copy. The wild type alleles, now on the R-prime, delete *via* intramolecular recombination between the insertion elements (IS21) bracketing the prime DNA in direct repeat. This deletion reveals the mutant phenotype resulting from transposon insertion. The position of the transposon in the R-prime was mapped to the resolution of a restriction fragment.

Twenty-four different transposon mutagenized R-primes were conjugated into *R. capsulata*. Four independently repurified transconjugants were isolated from each cross. Each of the four transconjugants, "cousins", arises from a single clone of donors bearing identical Tn7 mutagenized R-primes. Cousins arising from a single donor always have identical Tn7 induced lesions but may show different phenotypes with regard to the carotenoid content which is independent of the Tn7 insertion. The R-prime bears a *crtD* point mutation that results in a green colony color due to the accumulation of hydroxyneurosporene. The *crtD* mutation recombines independently of the transposon insertion into the chromosome.

This chapter focuses more on the description and characterization of the R-prime site-directed transposon mutagenesis scheme than on the isolation of new photosynthetic mutants. All steps in the scheme were investigated by Southern hybridizations using R-factor (vector),

R-prime, and Tn7 probes. A mutagenesis model is presented that incorporates both the physical hybridization data and the genetic data.

II. RESULTS

A. Insertion of Tn7 in the R-prime pRPS404

The R-prime was mutagenized by constructing a strain which had a copy of Tn7 in the chromosome, described in Materials and Methods. The R-prime was moved into this strain by conjugation. Another conjugation event into a new background was performed, except the recipient was challenged with simultaneous antibiotic resistances including the kanamycin (Km) marker on the R-prime and the streptomycin (Sm) marker carried by Tn7. The only way the recipient could acquire both resistances was if Tn7 was inserted into the R-prime before conjugation.

The sites of insertion of Tn7 in the chromosome have been analyzed by Southern hybridization using Tn7 probes. Lichtenstein and Brenner (1981, 1982) have determined the sequence of the ends of Tn7, mapped restriction sites, and characterized transposition properties. Tn7 has asymmetric direct repeats and is 13kb in length. EcoRI cleaves the transposon once, generating 8.9 and 4.3kb fragments. The 4.3kb fragment bears all of the antibiotic resistance genes and was used in the construction of Tn5.7 described in Chapter 3. There are two internal BamHI sites generating a 0.9kb internal fragment. In mapping Tn7 insertions with these enzymes, we expect the loss of the R-prime target fragment, which is now part of two new bands. The two Tn7 probes used for Southern analysis are pVCT14, containing the entire transposon, and pVCT15, containing the 4.3kb EcoRI fragment. The pVCT15 and pVCT14 probes hybridize to one and two bands, respectively, in an EcoRI or a BamHI digest of the mutants, with the exception of the small 0.9 kb BamHI fragment which is present in all of the BamHI digestions.

In 23 out of 24 Tn7 mutagenized R-primes, the data are consistent

with the insertion of a single transposon and the lack of any detectable rearrangements. R-primes with multiple insertions have not been observed. With the exception of UAE91, there is only one missing R-prime EcoRI or BamHI band in each digest. Two new bands are generated by the Tn7 and R-prime junctions that hybridize to the pVCT14 probe as expected, Fig. 2-1. In each case, only one of the pair of fragments hybridizes with the pVCT15 probe. These data may be used to position and orient the Tn7 insertions. Since the restriction fragments involved are large and the maps are at low resolution, positioning is imprecise. Therefore, in Table 2-1, the transposon insertion data are presented specifying only the target BamHI and EcoRI fragments.

B. Chromosomal Tn7 insertion sites

When total DNA, rather than episomal DNA, is extracted from strains bearing Tn7 mutagenized R-primes, twice the expected number of hybridizing bands are observed, Fig. 2-2. Controls indicate that neither Tn7 or the vector portion of the probes used for hybridization contain homology with the E. coli chromosome. This phenomenon has been explained by Lichtenstein and Brenner. They have observed a chromosomal "hot spot" for Tn7 insertion in the E. coli chromosome at minute 82. Tn7 occupation of this preferred site in a unique orientation was shown to generate two EcoRI genomic fragments hybridizing with a Tn7 probe. Six out of the seven of the genomic EcoRI digests displayed in Fig. 2-2 possess two bands of approximately 17kb and 10.5kb, in close agreement with the previously observed bands in E. coli. When these mutagenized R-primes are crossed into R. capsulata and the genomic hybridizations are

Figure 2-1. Southern hybridization of Tn7 probes to mutagenized R-primes. pRPS404::Tn7 plasmids were digested with EcoRI or BamHI and subject to electrophoresis in 0.7% agarose. Southern analysis was performed using either the pVCT14 (entire Tn7) of pVCT15 (part of Tn7) as hybridization probes. Samples: M, molecular weight markers; R, pRPS404; a, UAE70; b, UAE78; c, UAE81; d, UAE91; e, UAE131.

Figure 2-1

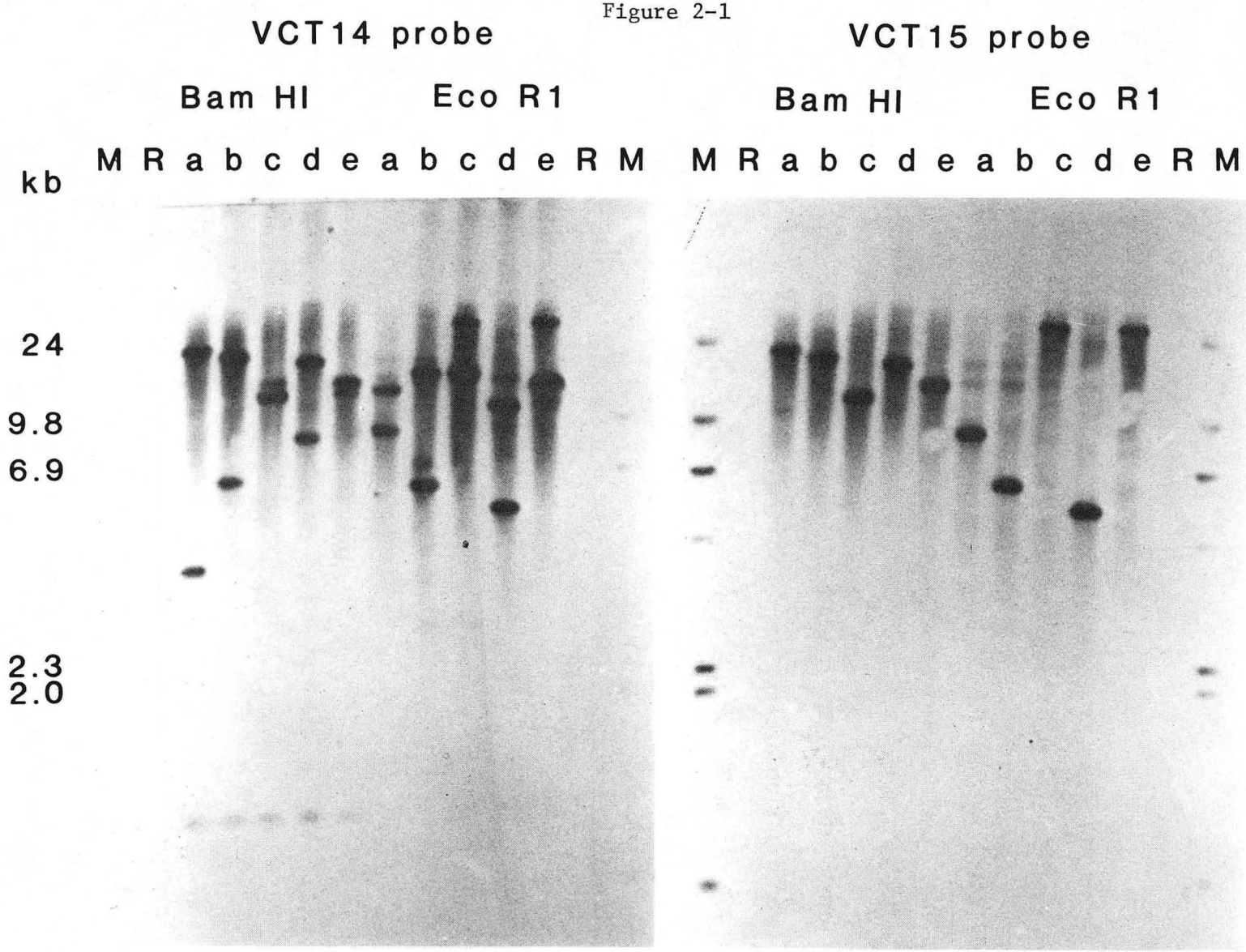

XBB 823-2783

repeated, there are still two extra bands. These bands have a constant size in seven out of seven strains, analyzed in Fig.2-2, of 10.5 and 6.7kb. Presumably, this is an example of a preferred Tn7 integration site in another chromosome. Whether the *R. capsulata* site has homology with the *E. coli* hot spot has not been determined.

Table 2-1

UAE#	BamHI	EcoRI
3	E	E
15	E	E
18	E	E
19	ND	G
22	E	E
28	E	E
33	ND	D
37	ND	G
39	D	F
67	F	F
70	C	H
78	C	H
81	C	B
87	F	F
91	C	A
100	E	E
110	NT	E
112	NT	G
115	E	E
118	NT	D
122	NT	G
131	C	B
219	E	E

The UAE strains contain pRPS404::Tn7 plasmids. The target BamHI and EcoRI restriction fragments are indicated. ND, no pertubation of the restriction fragment shown on the map in Fig. 3-3. NT, no test.

Figure 2-2. Insertion of Tn7 into a preferred site in the chromosomes of E. coli and R. capsulata. Total DNA was isolated, digested with EcoRI, electrophoresed in 0.7% agarose, and southern hybridization was performed. Samples: a, NEC0100::Tn7; b, UAE18; c, UAE19; d, UAE22; e, UAE39; f, UAE67; g, UAE70; h, UAE78; i, UAE115; j, SB1003; k, UAR18f; l, UAR19e; m, UAR22h; n, UAR39f; o, UAR67h; p, UAR70e; q, UAR78e; r, UAR115h; s, U23. E, fragments generated by Tn7 insertion into the E. coli chromosome. R, fragments generated by the insertion of Tn7 into the R. capsulata chromosome.

Figure 2-2

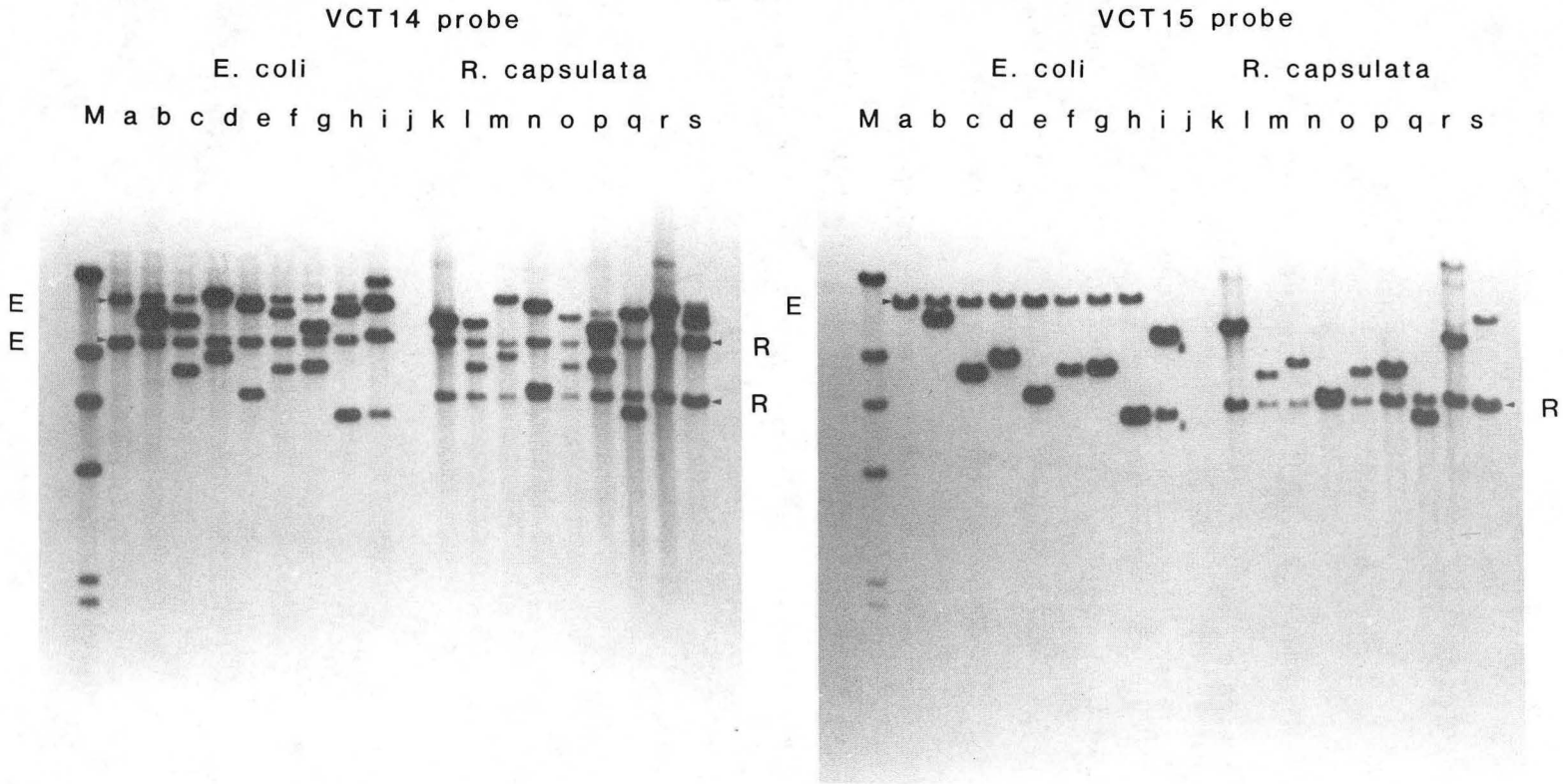

XBB 823-2776

C. Conjugation of Tn7 mutagenized R-primes into R. capsulata

Twenty-four UAE strains, bearing Tn7 insertions in the R-prime, were mated with SB1003 recipients, and selection was made for the transfer of the mutagenized R-prime into the R. capsulata background by selection for Sm^R on RCV plates. The RCV minimal plates counterselect the E. coli donors by auxotrophy. Four transconjugants from each cross were repurified independently and these are termed cousins, since they arose from a mating with a clonal donor. Different cousins are designated by a lower case letter following the strain number.

The fate of the mutagenized DNA has been investigated by comparing genomic Southern hybridizations between the E. coli donors and the R. capsulata recipients. Fig. 2-3 clearly reveals that the position of the Tn7 in R. capsulata relative to the adjacent R-prime restriction site is unchanged. Recombination events that may have incorporated the Tn7 into the chromosome have preserved the adjacent restriction sites. In addition, the cousins contain identical restriction fragments; therefore, the transfer of Tn7 into the chromosome does not perturb the surrounding DNA.

D. RecA+ dependent deletion of R. capsulata DNA mediated by IS21

The transposon lesion and the crtD gene may be crossed into the chromosome independently as long as the transposon is not in the crtD gene. Once the crtD gene has recombined into the chromosome, the crtD phenotype (green pigmentation) becomes apparent. Apparently, the wild type alleles are lost after reciprocal homologous recombination.

Figure 2-3. Comparison of Tn7 insertions in the UAE and UAR strains. Lanes are arranged to demonstrate the stability of Tn7 in the prime DNA. Lane o was mistakenly digested with BamHI, otherwise the total DNA was digested with EcoRI. Samples: a, UAE18; b, UAR18f; c, U23; d, UAE22; e, UAR22h; f, UAE39; g, UAR39f; h, UAR39h; i, UAE70; j, UAR70e; k, UAR70f; l, UAR70g; m, UAR70h; n, UAE115; o, UAR115e; p, UAR115f; q, UAR115g; r, UAR115h.

Figure 2-3

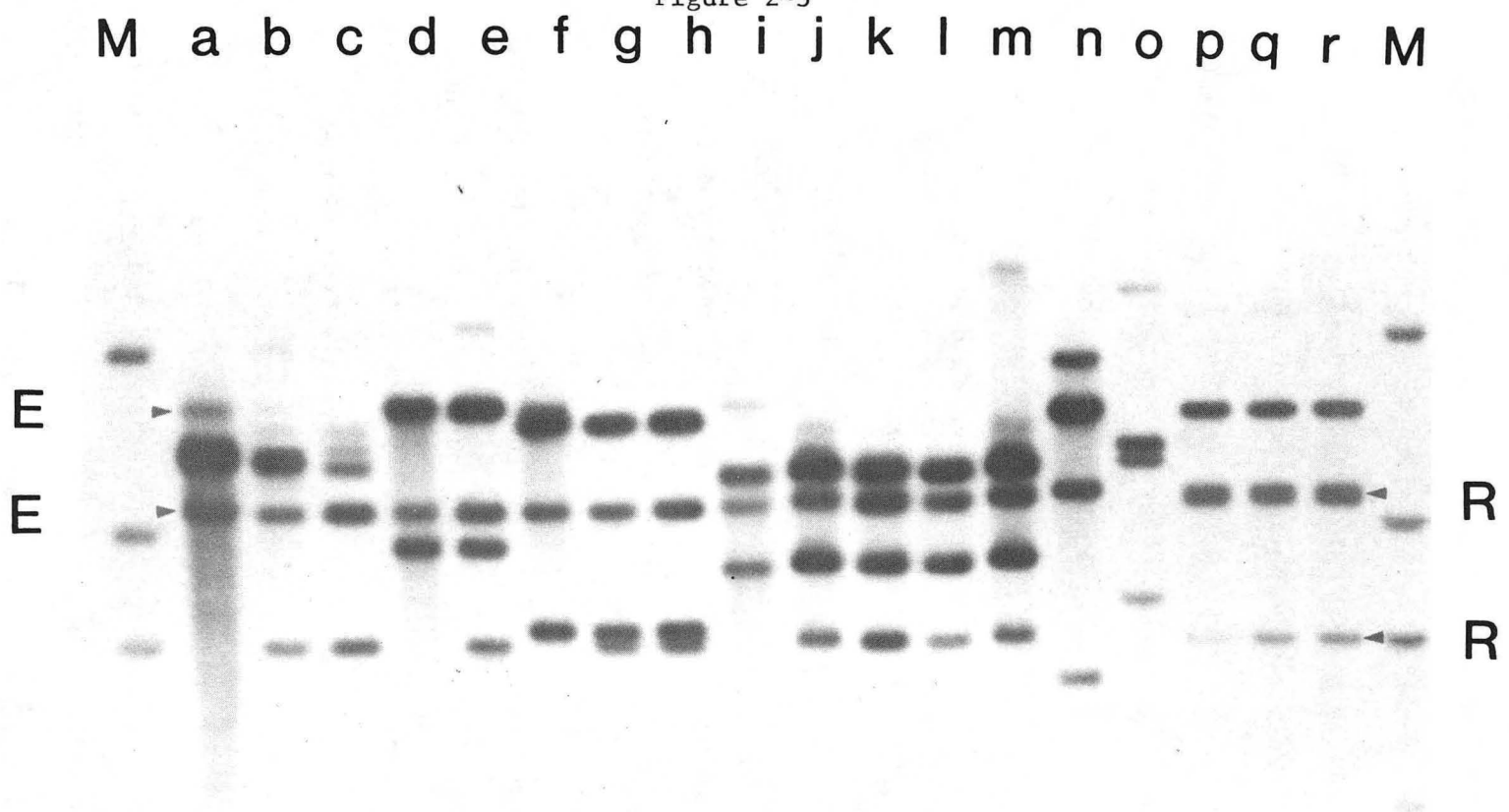

XBB 823-2777

One explanation for the loss of the wild type phenotype after recombination with the mutagenized R-prime is that the R. capsulata DNA on the plasmid has been deleted. This is not due to the deletion of the entire R-prime, since the kanamycin marker is present in green colonies. The R-prime contains two homologous IS21 elements which bracket the R. capsulata DNA. This suggests a mechanism for the deletion of R. capsulata DNA on the plasmid resulting in a loss of wild type alleles after recombination with the chromosome. Intramolecular recombination between the IS21 elements should regenerate the parent R-factor pLM2 bearing one IS21 element and a circular piece of DNA bearing the R. capsulata DNA and the other IS21 element. The pLM2 plasmid is a replicon and is maintained, unlike the second product which does not contain an origin of replication and is lost within a few generations.

To test for plasmid deletion, pRPS404 was conjugated from a recA$^-$ background (HB101) into two isogenic strains: SK2267 (recA$^-$) and SK1593 (recA$^+$). Transconjugants were selected by kanamycin and the donor was counterselected by auxotrophy on M9 medium. These strains were repurified twice. After repurification, plasmids were analyzed by restriction digestion and agarose gel electrophoresis. In Fig. 2-4 are shown the plasmids from 15 independently repurified strains in a recA$^+$ background. As can be seen, they are all in various stages of deletion. The non-stoichiometric ratios among the bands result from a mixed population of deleted R-factors and undeleted R-primes. The most intense bands map to the R-factor (EcoRI fragments C, G, and K, see Fig. 3-3). When these same samples are digested by both HindIII and SalI, Fig. 2-5, a 4.6kb fragment is generated. In similar experiments with another broad host range plasmid R68.45 (Currier and Morgan, 1982), it

Figure 2-4. Deletion of the prime sequence from pRPS404 in Rec A+ E. coli. R-primes were transferred from a recA$^-$ to a recA$^+$ background, isolated, digested with EcoRI, and electrophoresed in 0.7% agarose. Fifteen of these plasmids were analyzed, lanes a through o, and most of them have undergone specific deletion events when compared to the R-prime in lane R. The fragment names are shown on the right and those fragments which are native to the R-factor (vector) are underlined.

Figure 2-5. Deletion of the R-prime pRPS404 to the parental R-factor pLM2. The samples are the same as in Fig. 2-4 except in this case the DNA has been digested with HindIII and SalI. Lane L, pLM2 (one IS21) and lane B, pBLM2 (two IS21). Lanes a through reveal that plasmids are deleting to pLM2.

Figure 2-4

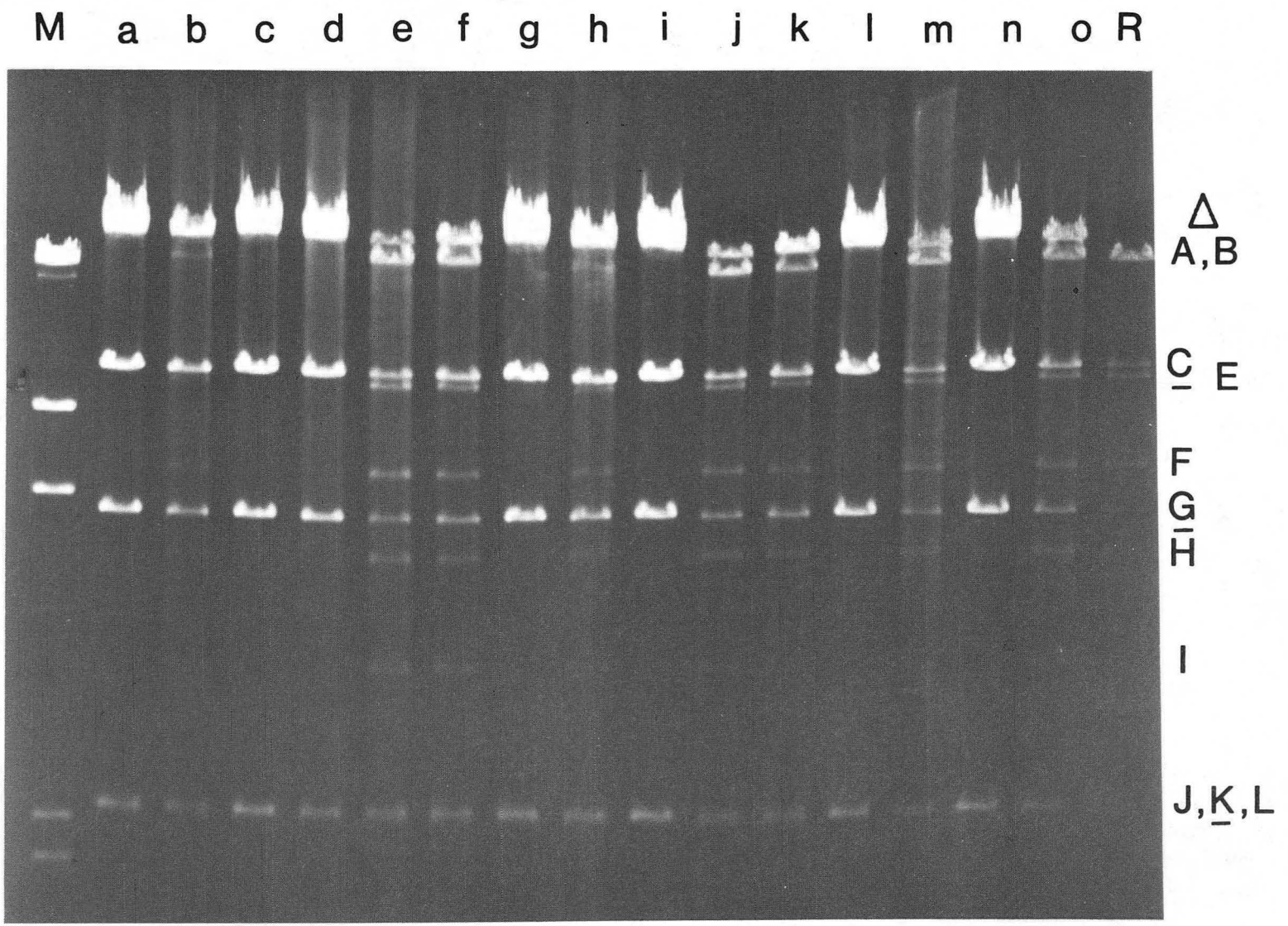

XBB 823-2780

Figure 2-5

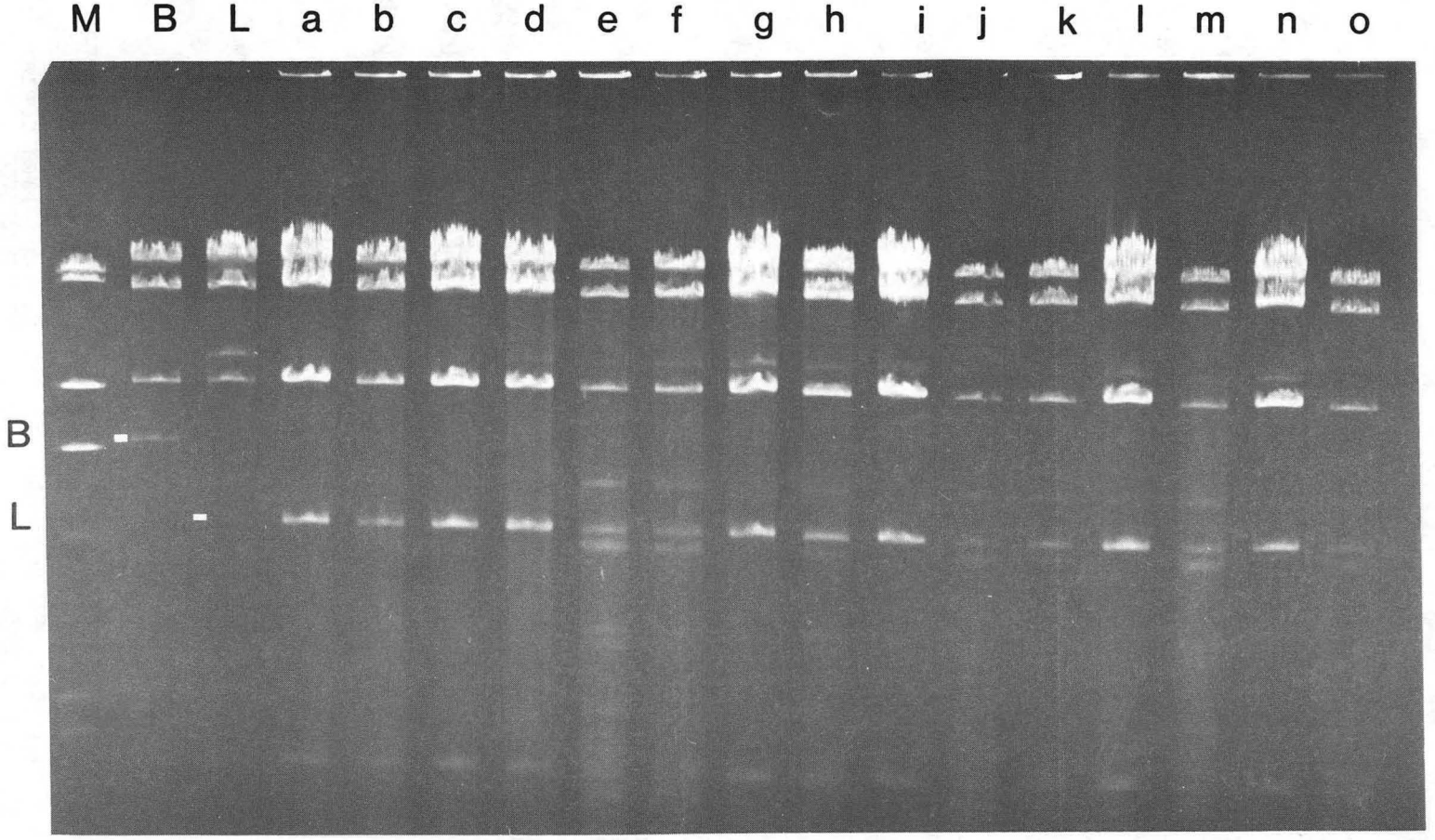

XBB 823-2781

was found that a 4.6kb fragment results from one copy of IS21 and a 6.7kb fragment is obtained from two tandem IS21 elements, as in pBLM2. All plasmids analyzed were deleting to a single copy of IS21, resulting in the generation of a 4.6kb HindIII-SalI fragment. The plasmids which had been transfered into a recA$^-$ background were analyzed in a similar fashion and 18 out of 18 plasmids analyzed were identical to the R-prime (data not shown). Therefore, it is concluded that in E. coli, deletion of pRPS404 is dependent on the RecA protein.

Deletion of pRPS404 to parental R-factors has also been observed in the homologous organism. Similar to the E. coli deletion experiments described above, the R-prime was conjugated from a RecA$^-$ background into wild type R. capsulata. Plasmid DNA was extracted and only R-factor bands were observed (data not shown). These digests are obscured by endogenous plasmids. However, when these plasmids were mobilized back into a RecA$^-$ E. coli background, the experiment in Fig. 2-5 can be repeated. Fig. 2-6 demonstrates that of the 12 plasmids isolated from R. capsulata, the characteristic HindIII-SalI fragment indicates that seven plasmids have deleted to pLM2 and five plasmids have deleted to pBLM2. The deletion events resulting in loss of R. capsulata DNA but leaving two intact IS21 elements result in plasmids which can undergo further deletions into the R-factor and are discussed in Chapter 4.

E. Analysis of Tn7 insertions into the R. capsulata chromosome

In order to characterize the Tn7 generated mutants, Southern hybridizations to total DNA from UAR strains R. capsulata containing Tn7 in the chromosome were performed. The UAR DNA was digested with

Figure 2-6. Deleted R-primes rescued from UAR strains. Thirteen PS^- UAR strains were mated with *recA*$^-$ *E. coli*, plasmid DNAs were purified, digested with *EcoRI*, and electrophoresed in 0.7% agarose, lanes a through o. Lane B, pBLM2, and lane L, pLM2. Both pLM2 and pBLM2 deletion products were observed.

Figure 2-6

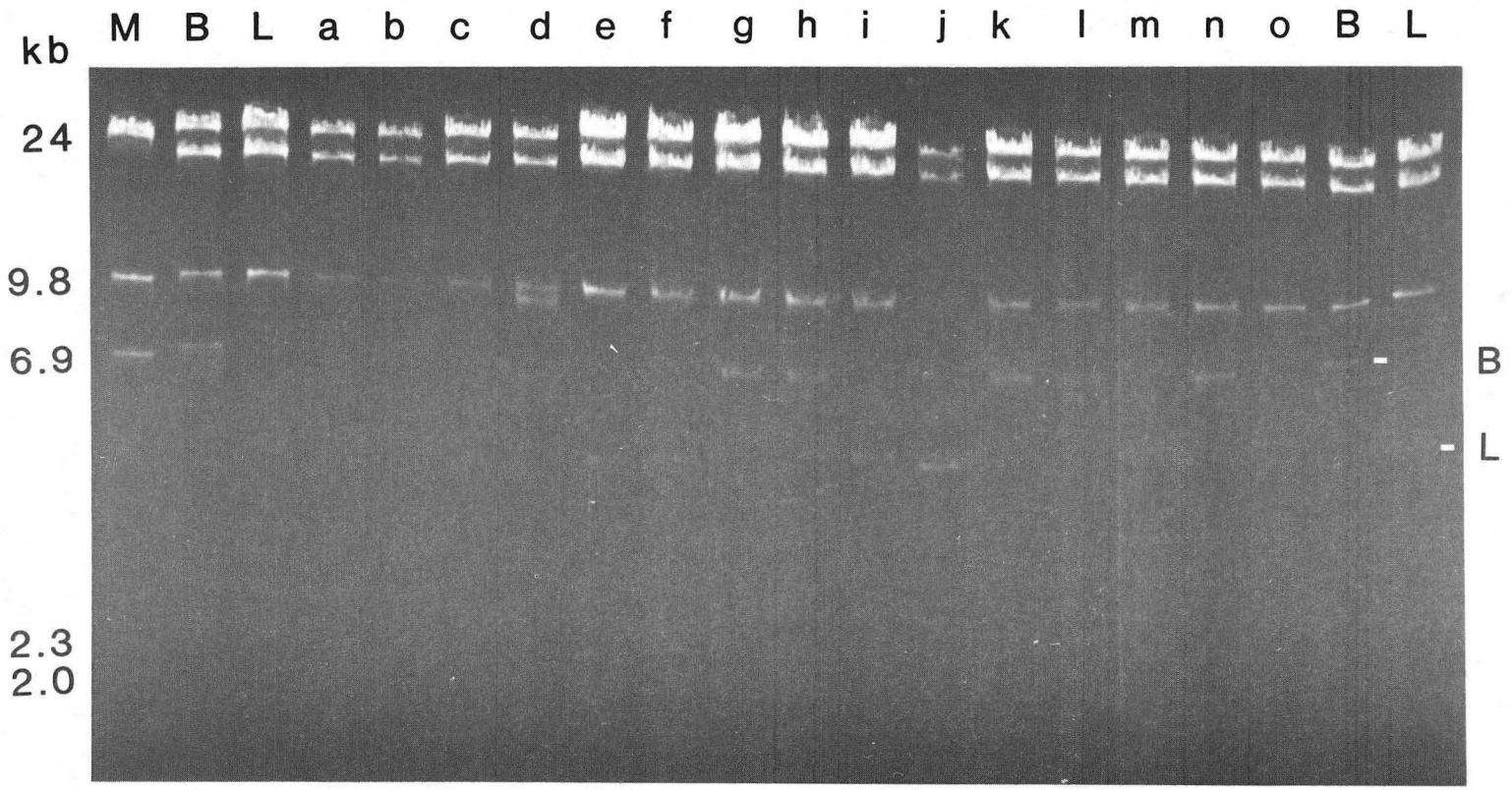

XBB 823-2778

EcoRI and BamHI and probed with a Tn7 probe and the R-prime. With the R-prime probe, the target restriction band should be missing due to the insertion of Tn7. As shown in Fig. 2-7 (left), characteristic bands are missing which correspond to the fragments identified in Table 2-1 as the Tn7 target bands, with the exception of UAR87e, lane h, which is discussed below. In the right half of Fig. 2-7, the same samples have been probed with Tn7. The EcoRI and BamHI digests of US404, lane a, reveal hybridizing bands characteristic in size of the Tn7 insertion into the E. coli preferred site at minute 82. Lane b is total DNA from SB1003 (wild type R. capsulata), which shows no cross-hybridization with the Tn7 probe. All of the UAR strains have three common BamHI bands: the upper two common bands are characteristic of the chromosomal preferred insertion site in R. capsulata and the lower common band is the internal BamHI fragment from Tn7. The two common bands in the EcoRI digest are also due to the chromosomal preferred insertion site. Other bands in each digest are characteristic of the junction fragments between the ends of Tn7 and the target restriction fragment.

The Tn7 insertion UAR87 is in the BamHI F and EcoRI F fragments, however these bands remain intact in Fig. 2-7. Since the UAR strain from which the DNA was extracted from showed no particular PSA lesion, it appeared that the Tn7 had not recombined into the chromosome. Subsequent attempts to recombine the Tn7 into the chromosome at the UAR87 location proved to be successful. The recombination event was monitored by fluoresence photography using IR sensitive 35mm film (Youvan et al., 1983). A loss of RC results in increased fluoresence from the LH complexes. Fig. 2-8 is a photograph of wild type, a known RC^- mutant, and UAR87 as colonies on a petri dish in the fluorescence mode. The

UAR87 Tn7 insertion strain specifically lacks the reaction center complex and the SDS-PAGE profile of this strain is shown in Fig. 2-9.

Figure 2-7. Analysis of Tn7 insertions in the PSA genes of R. capsulata. Total DNA was purified from UAR strains and subject to Southern analysis using either the R-prime or Tn7 as a hybridization probe. Samples: a, US404; b, SB1003 (wild type); c, UAR18f; d, UAR19e; e, UAR39f; f, UAR67h; g, UAR70e; h, UAR87e; i, UAR115h. BamHI and EcoRI fragment names are shown on the left and right respectively.

Figure 2-7

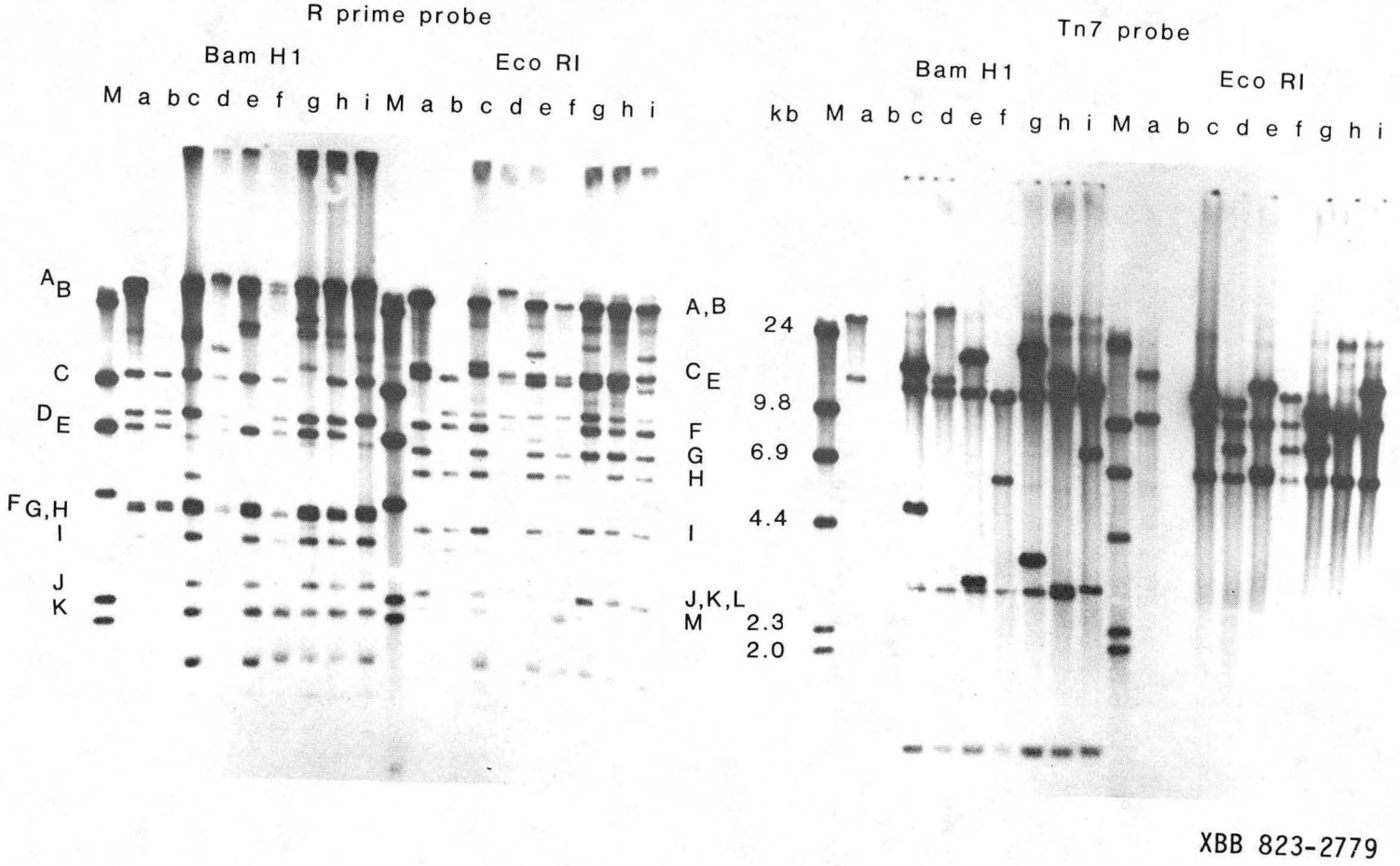

XBB 823-2779

This mutation, along with marker rescue experiments (Youvan et. al., 1983) was instrumental in the DNA sequencing strategy which led to the sequencing of the structural polypeptides for the reaction center (Youvan et al, 1984). The UAR87 Tn7 insertion is in or is transcriptionally upstream from the structural gene for the H subunit of the reaction center.

Figure 2-8. IR fluorescence photography of SB1003 (wild type), Y142 (RC^-), and UAR87 colonies streaked on a petri dish. The petri dish is irradiated with blue light, and photons emitted as fluoresence with 780nm $<\lambda>$ 900nm are imaged on the camera. Technique described in Youvan et. al., 1983)

Figure 2-9. SDS-PAGE of wild type, lane a, and UAR87, lane b. Chromatophore fractions were prepared and protein samples electrophoresed in a 9-18% acrylamide gradient gel.

Figure 2-8

Figure 2-9

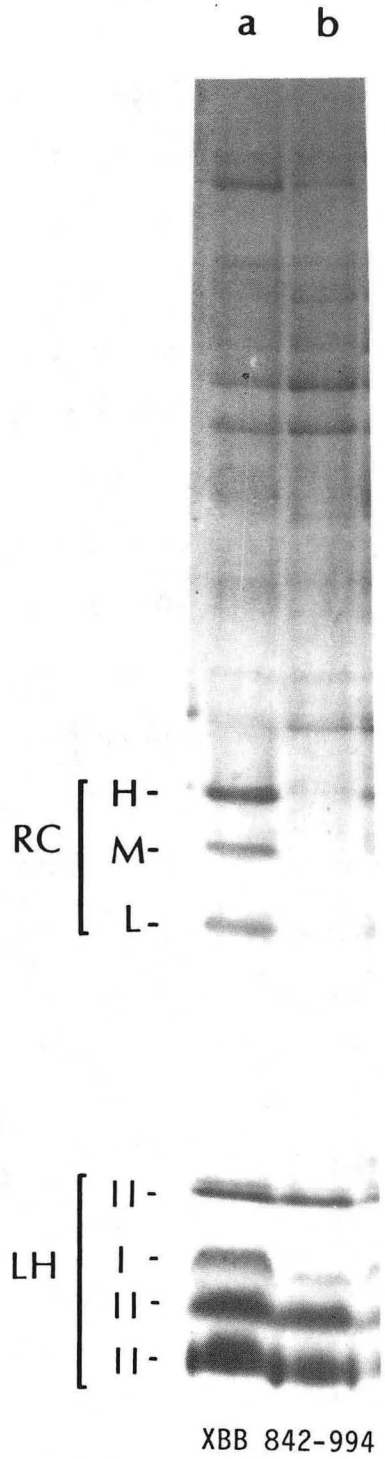

III. DISCUSSION

The scheme for site-directed transposon mutagenesis is shown in Fig. 2-10. The genetic data and physical Southern hybridization data supporting this model are presented above. Transposon Tn7 is inserted into the R-prime in a *recA*$^-$ *E. coli* and then the R-prime::Tn7 is conjugated into *R. capsulata*, where recombination may transfer the Tn7 into the chromosome. IS21 mediated intramolecular recombination on the plasmid deletes the wild type alleles. Ruvkin and Ausubel (1981) proposed a general scheme for site-directed mutagenesis using homologous recombination with transposon mutagenized plasmids. Recombined plasmids bearing wild type alleles must be excluded to reveal the mutagenized chromosomal gene. This requires a second cross in which a second, incompatable plasmid is selected. Our scheme avoids this step. In addition, the gene dosage effect of streptomycin selection aids the recombination of the transposon into the chromosome by maintaining multiple copies of R-prime::Tn7 in the cell.

Figure 2-10. A model for recombinaton and deletion of Tn7 mutagenized PSA genes. Model is described in the text.

Figure 2-10
Recombination and Deletion

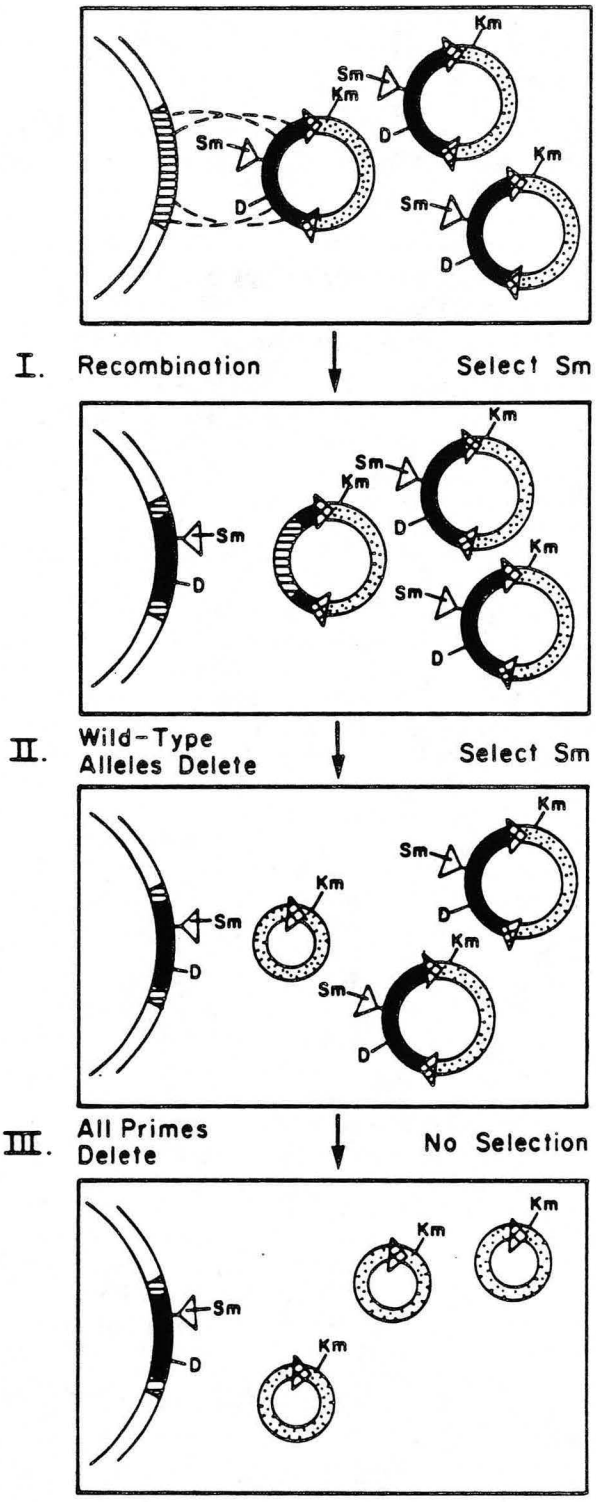

XBL 842-646

CHAPTER 3: CONSTRUCTION OF Tn5.7 AND PHYSICAL MAPPING OF pRPS404

I. INTRODUCTION

This chapter describes the construction of Tn5.7 and physical mapping of pRPS404 necessary for transposon mutagenesis. A scheme for site directed transposon mutagenesis using pRPS404 is described in Chapter 2, however, Tn7 was used in those experiments, and it was found that i) due to a hot spot in the R. capsulata chromosome, gene replacement by selection for Sm^R was not optimal and ii) because of the size of Tn7(13kb) and lack of terminal restriction recognition sites, accurate mapping was difficult.

Many broad host range cloning vectors with chromosome mobilizing ability (Cma) have recently been isolated. (Holloway, 1979) These plasmids are capable of intergeneric conjugation between E. coli and species from a wide range of gram negative genera including Klebsiella, Proteus, Pseudomonas, Rhizobium, Rhodopseudomonas, Salmonella, and Serratia. Tandem duplications of IS elements are thought to be involved in some forms of Cma (Willetts et al., 1981). In the R-prime, the R. capsulata DNA is flanked by direct repeats of IS21 which in a Rec+ background recombine, resulting in a deletion of the chromosomal DNA (Chapter 2; Youvan et al., 1982). This provides a useful means of gene replacement if selection can be maintained for a mutation.

Of the transposons available for mutagenesis, Tn5 and Tn7 have been widely used for this purpose. Tn5 is easily mapped because of convenient terminal restriction endonuclease recognition sites (Auerswald et al., 1980). Also, transposition of Tn5 is well characterized (Reznikoff, 1982; Rothstein, 1980). Tn7 is useful because of multiple antibiotic

resistances to Trimethoprim (Tp), Streptomycin (Sm), and Spectinomycin (Sp) (Lichtenstein and Brenner, 1981). Tn5 cannot be used to mutagenize many plasmids in which Cma exists because most of these are naturally Kanamycin^R (Km^R).

II. RESULTS

A. Construction of Tn5.7

In order to mutate the R-prime and accurately map the mutations, a transposon was constructed, Tn5.7, combining the antibiotic resistance factors from Tn7 and the transposition properties of Tn5. Fig.3-1 is a diagram of the construction of Tn5.7 and Fig. 3-2 shows a physical map of the transposon. Tn5.7 contains an intact IS50R from Tn5 and IS50L without the terminal BglII site. It is 7.6kb in length and has approximately a twofold lower transposition frequency than Tn5, probably because of the increased size.

This transposon was constructed to mutagenize the photosynthetic genes of R. capsulata contained on the plasmid pRPS404. Switching to mutagenesis with Tn5.7 required mapping the restriction sites for XhoI and BglII on pRPS404 since there are no internal EcoRI or BamHI sites in Tn5.7. A partial physical-genetic map has been described (Taylor et al., 1983) for pRPS404, and the entire EcoRI and BamHI map is to be published (Clark et al., 1980).

Figure 3-1. Construction of Tn5.7. pBR322::Tn5 was digested with BglII and ligated to a Sau3A partial digest of pRS5. pRS5 contains a ColE1 origin of replication and the tmp^R, sm^R, and spc^R genes from Tn7. (These genes provide resistances to trimethoprim, streptomycin, and spectinomycin, respectively.

Figure 3-2. Physical map of Tn5.7. Heavy lines represent IS50 elements from Tn5. The 4.6kb fragment is from Tn7.

Cloning of Transposon Tn5.7

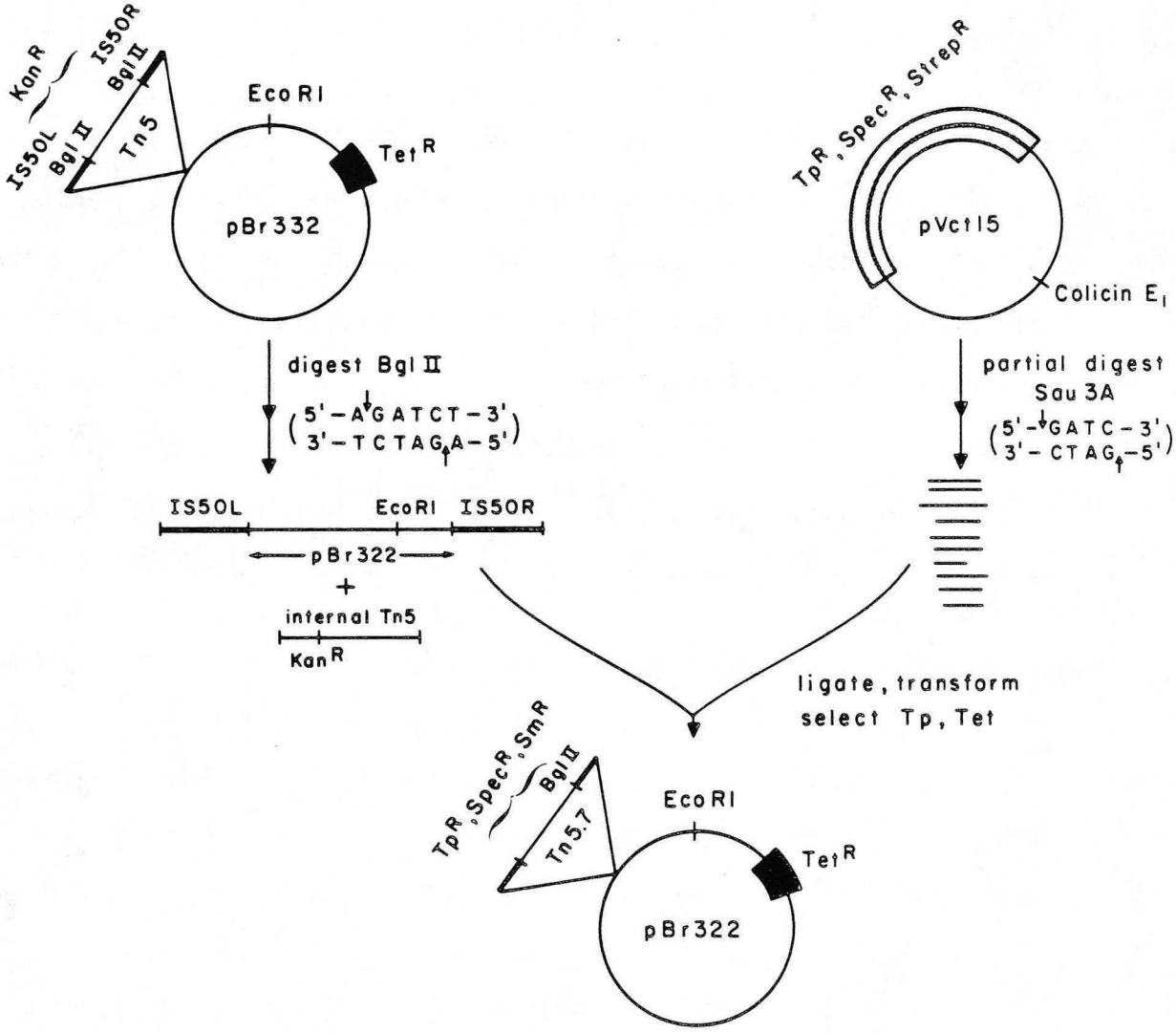

XBL 830-8344

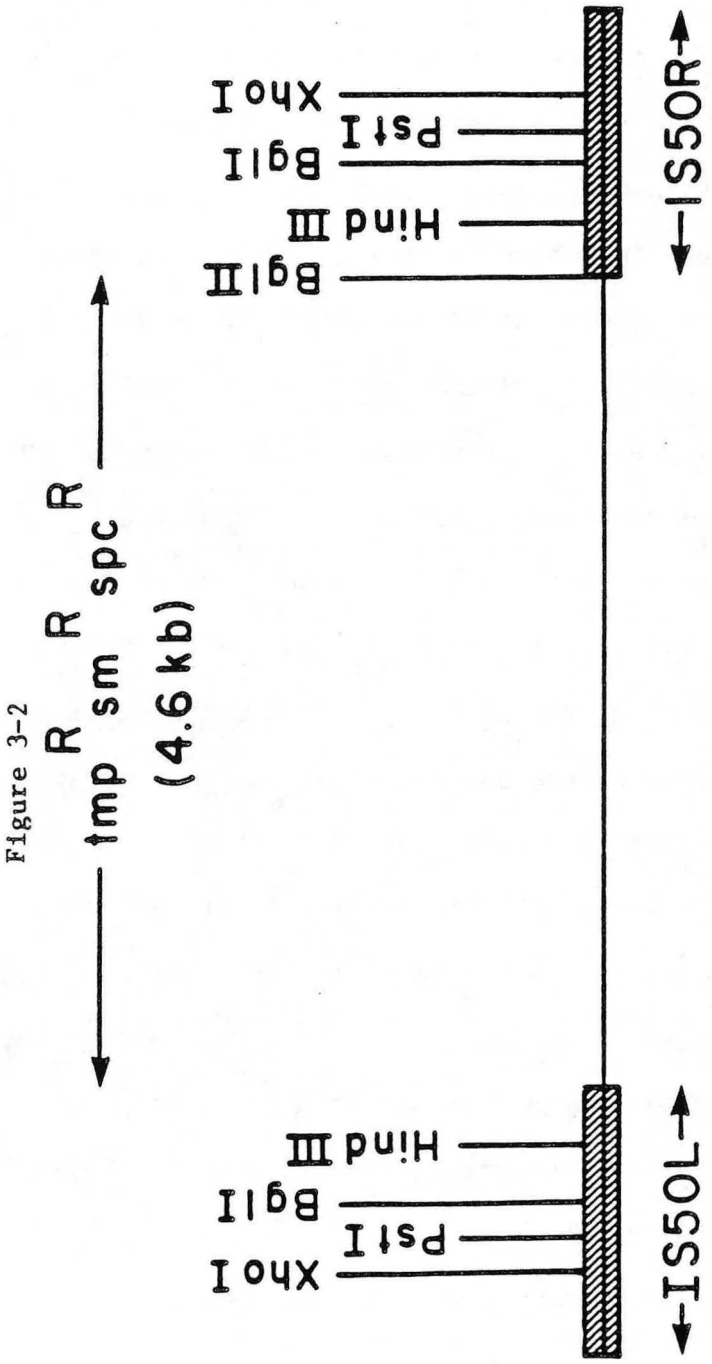

Figure 3-2

B. Physical Mapping of pRPS404

The physical map of the R-prime, pRPS404, is shown in Fig. 3-3. The XhoI, BglII, SstI, and KpnI restriction enzyme recognition sites were mapped initially by combining a series of single and double digests with end labelling using reverse transcriptase, examples of which are shown in Figs. 3-4 and 3-5. The molecular weights of the labelled fragments are given in Tables 3-1, 3-2, and 3-3. These experiments, in conjunction with previously published restriction maps of RP1 (De Picker et al., 1979) and the BamHI and EcoRI map of pRPS404, allowed the placement of most of the BglII fragments and the larger of the XhoI fragments.

From the restriction map for EcoRI and BamHI (Clark et al., 1980) and from Tables 3-1, 3-2, and 3-3, the preliminary BglII sites could be placed relative to the EcoRI and BamHI fragments. Fig 3-4. shows an assignment of the EcoRI-BglII and BamHI-BglII junction fragments from Table 3-1. By the pattern of which BamHI or EcoRI fragments have internal BglII sites, Table 3-3, the BglII D, E, and F fragments can be tentatively placed. The fragments left are fragments A, B, and C. Fragments A and B can be placed from the restriction map of RP1. This leaves the BglII fragment C. This must extend into the EcoRI F fragment since there is an internal BglII site there. Fig. 3-5 shows an assignment of junction fragments from the BglII C and neighboring BamHI and EcoRI sites.

From Tables 3-4 and 3-5, the XhoI J fragment probably spans the EcoRI O, BamHI O and L fragments since it has an internal BglII site (region [1] in Fig. 3-6). XhoI I spans the BamHI D fragment to the XhoI J junction (region [2] in Fig.3-6) since it has no BglII site and since the only other possibility is the XhoI H which does have an internal

Figure 3-3. Physical map of pRPS404. Arrows indicate IS21 elements which bracket the R. capsulata DNA from 22 to 68kb on the above map. The Tn5.7 insertions are named for their position in kb on this map.

Figure 3-4. Restriction mapping of pRPS404 by single and double digests combined with end labelling. Plasmid DNA was digested with the restriction enzymes indicated, end labelled with ^{32}P using reverse transcriptase, digested a second time where indicated, and electrophoresed in 0.7% agarose. For example, BglII*/BamHI indicates that the plasmid was first cut with BglII, end labelled, and re-cut with BamHI. This kind of experiment can determine the junction fragment sizes between two restriction sites.

Figure 3-5. Same as Fig. 3-4 except electrophoresis is in 3.5% acrylamide, 1% agarose. Resolves low molecular weight fragments.

Figure 3-3

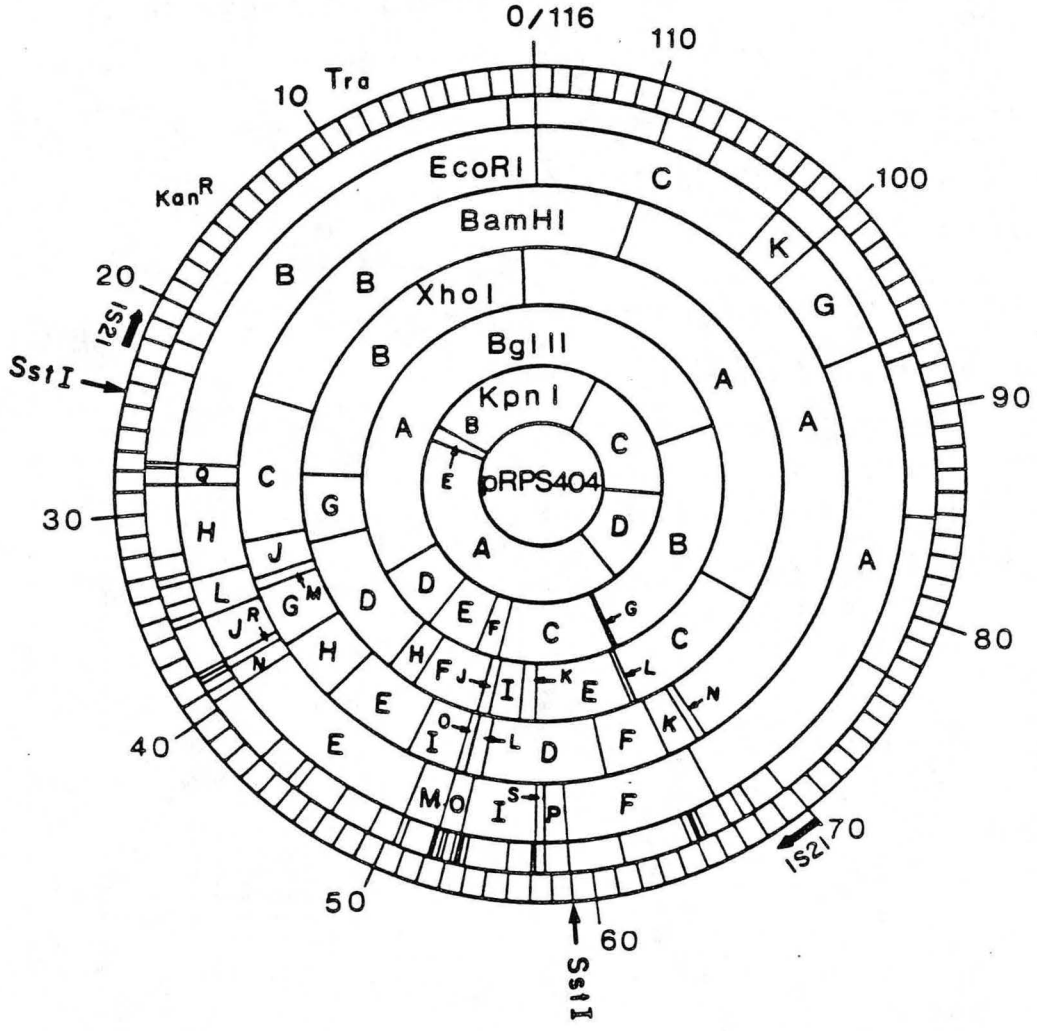
0/116
110
10
Tra
100
EcoRI
KanR
BamHI
20
IS21
XhoI
SstI
BglII
90
KpnI
30
pRPS404
80
40
IS21
70
50
60
SstII

Figure 3-4
Mapping Bgl II Restriction Enzyme on pRPS404

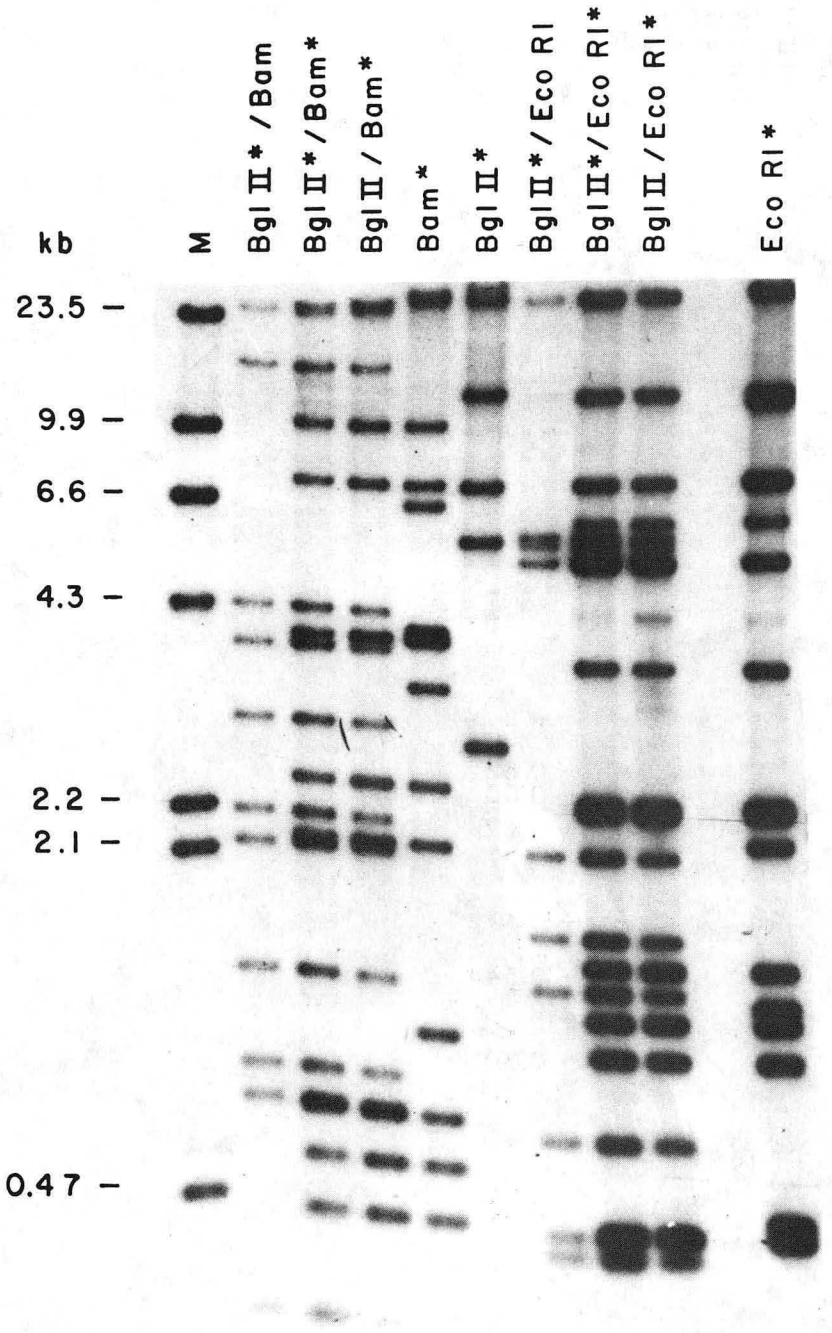

XBB 820-10692A

Figure 3-5

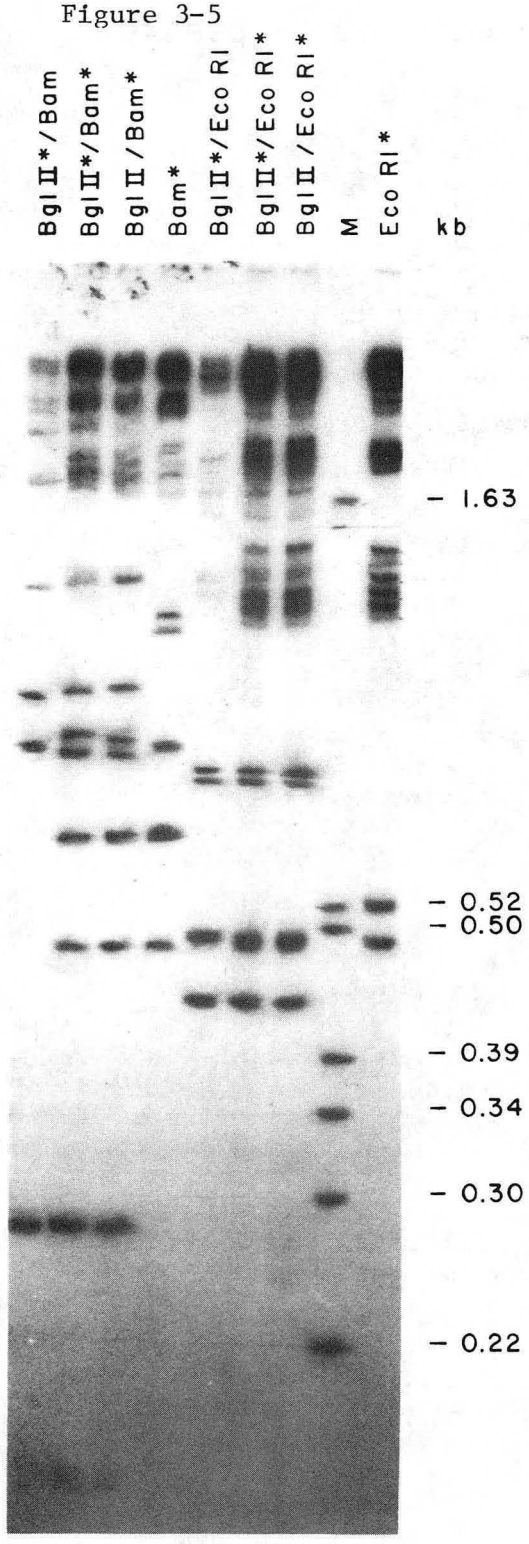

XBB 820-10691A

BglII site. XhoI H spans the BglII E-D junction (region [3] in Fig. 3-6). Since it has no internal EcoRI or BamHI site but does have an internal BglII site. This leaves a 5-6kb junction which fits XhoI "F" (region [4] in Fig. 3-6). BamHI D was isolated by preparative gel electrophoresis and re-cut with XhoI. This liberated the XhoI K fragment and 2kb fragment which is part of XhoI I (regions [5] and [2] in Fig. 3-6, respectively).

Since the BamHI J and EcoRI Q have internal XhoI sites, the only possibility is that XhoI G spans the BamHI C, J, and EcoRI Q and H. (shown in Fig. 3-7).

From the map of RP1, the XhoI C is tentatively located. Also, the XhoI C and D fragments co-migrate upon gel electrophoresis as determined from end labeling experiments.

Following the tentative map positions described above, insertions of Tn5.7 confirmed the overlapping fragments and the sizes of the XhoI and BglII Tn5.7-pRPS404 junction fragments, Table 3-6, helped refine the XhoI positions relative to the BamHI, EcoRI, and BglII positions.

Table 3-1

Fragment sizes of pRPS404 digested with BamHI, EcoRI, BglII, and XhoI. All sizes are in kilobase pairs of DNA.

BamHI	kb	EcoRI	kb	BglII	kb	XhoI	kb
A	∿30	A	∿29	A	∿60	A	∿37
B	∿29	B	∿27	B	∿25	B	∿28
C	9.8	C	11.5	C	12.8	C,D	13.5
D	7.0	E	10.7	D	7.5	E	7.5
E	6.4	F	6.9	E	6.0	F	5.8
F	4.0	G	5.6	F	2.6	G	5.2
G,H	3.9	H	5.1	G	0.27	H	2.6
I	3.2	I	3.5			I	2.1
J	2.2	J,K,L	2.3			J	1.55
K	2.09	M	2.10			K	1.42
L	1.96	N	1.50			L	0.10
M	0.87	O	1.42				
N	0.61	P	1.35				
O	0.56	Q	1.29				
		R	0.52				
		S	0.48				

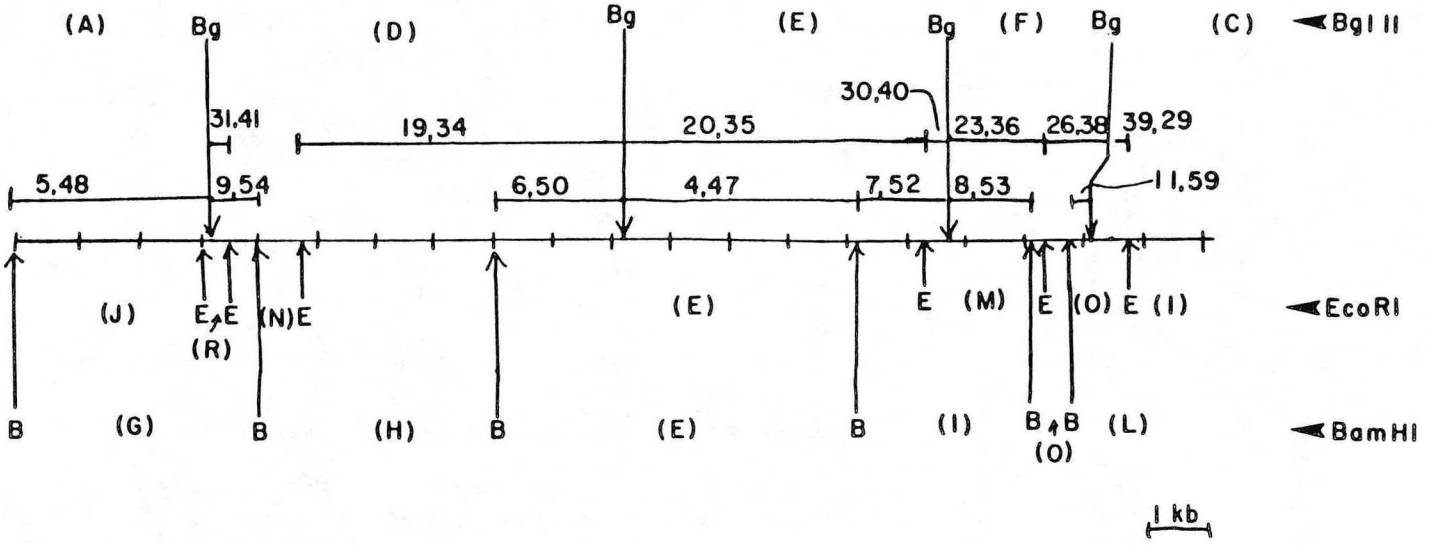

Fig. 3-6 A partial restriction map of pRPS404 indicating assignment of junction fragments generated from end labelling experiments. The letters in parenthesis indicate the letter name (Table 3-1) of intact fragments generated by digestion with enzymes BglII, EcoRI, and BamHI. The numbers refer to junction fragments described in Table

Table 3-2

Double digests of end labeled pRPS404. The * indicates the digest which was labeled prior to the second cleavage. These fragments were compared to a lane in which both restriction enzyme sites were labeled in a double digest. The fragments designated by () refer to an intact fragment generated by the enzyme which was labeled. The # refers to the numbered junction fragments identified in Figs. 3-6 and 3-7.

*BglII/BamHI	#	*EcoRI/BglII	#	*BglII/EcoRI	#	*BamHI/BglII	#
∿25	1	∿25	13	∿25	32	∿24	
16	2	∿23	14	5.5	33	∿21(B)	
4.1	3	11.5(C)	15	5.3	34	16	42
3.8	4	6.7	16	5.1	35	9.8(C)	43
2.8	5	5.8(G)	17	2.05	36	6.8(D)	44
2.20	6	5.5	18	1.72	37	4.1	45
2.09	7	5.3	19	1.42	38	3.9(H)	46
1.86	8	(doublet)5.2(H)	20	0.80	39	3.8	47
1.30	9	3.5	21	(doublet)0.48	40,41	2.8	48
0.70	10	(triplet)2.2(J,K,L)	22			2.4(J)	49
0.28	11	2.05	23			2.2	50
0.17	12	1.72	24			2.15(K)	51
		1.50(N)	25			2.09	52
		1.42	26			1.86	53
		1.35(P)	27			1.30	54
		1.29(Q)	28			(doublet)0.70(M)	55,56
		0.80	29			0.64(N)	57
		(doublet)0.48	30,31			0.57(O)	58
						0.28	59
						0.17	60

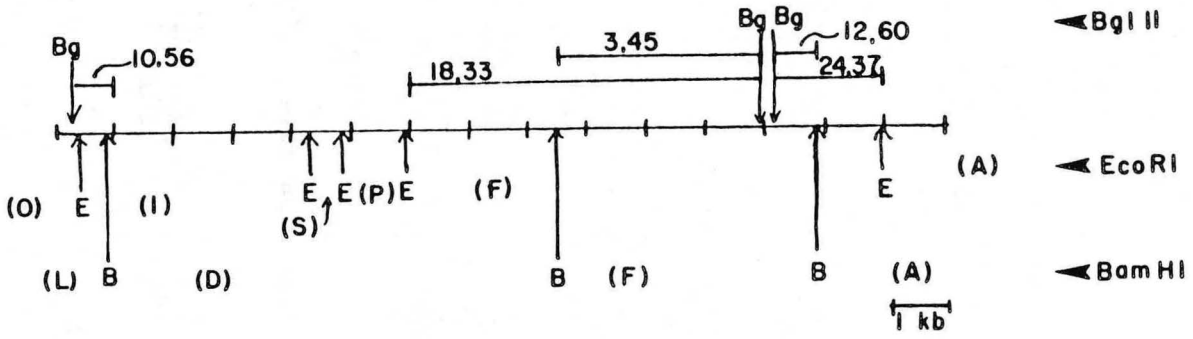

Fig. 3-7 A partial restriction map of pRPS404 indicating assignment of junction fragments generated from end labelling experiments. The letters in parenthesis indicate the letter name (Table3-1) of intact fragments generated by digestion with enzymes BglII, EcoRI, and BamHI. The numbers refer to junction fragments from Table 3-2.

Table 3-3

BamHI and EcoRI fragments which have internal BglII sites.

BamHI	EcoRI
A	A
E	E
F	F
G	M
I	O
L	R

Table 3-4

BamHI, EcoRI, and BglII fragments which have internal XhoI sites.

BamHI	EcoRI	BglII
A	A	A
B	C	B
C	E	C
D	F	D
E	H	E
F	I	F
J	O	
L	Q	
O		

Table 3-5

Partial summary of XhoI fragments relative to internal EcoRI, BamHI, and BglII sites.

	Internal		
XhoI fragment	EcoRI	BamHI	BglII
E	+	+	−
F	+	+	+
G	+	+	−
H	−	−	+
I	−	+	−
J	+	+	+
K	−	−	−

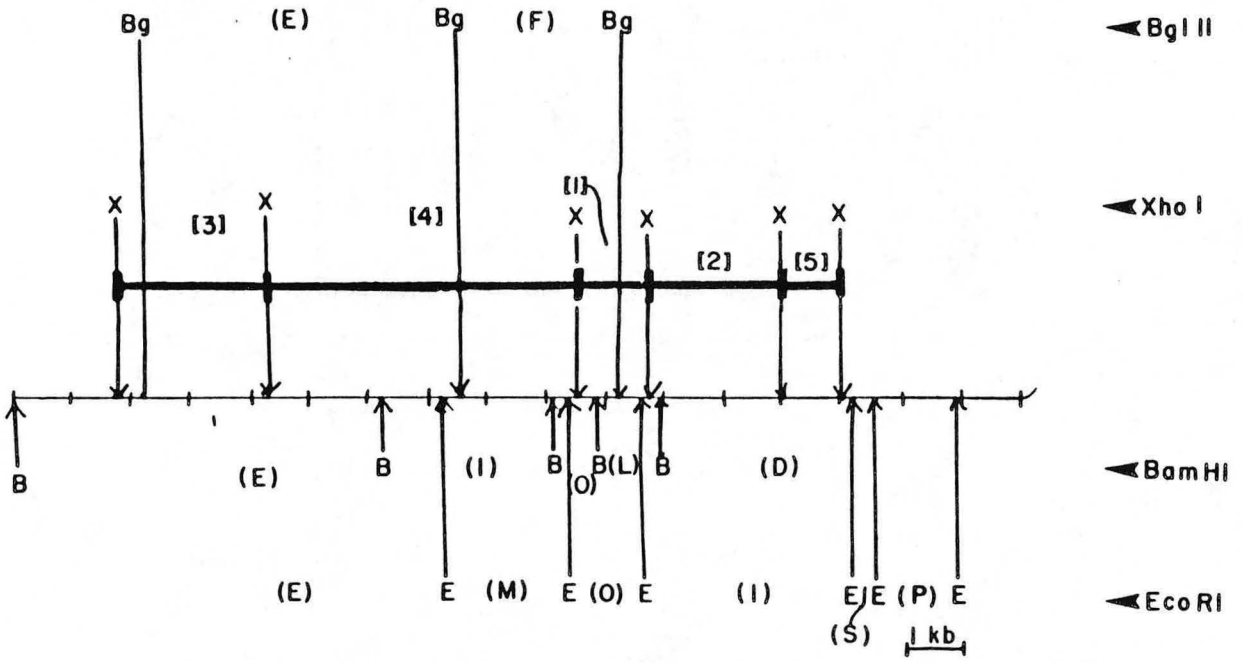

Fig. 3-8. A partial restriction map of pRPS404. The letters in parenthesis indicate the letter name (Table 3-1) of intact fragments generated by digestion with BglII, BamHI, and EcoRI. The numbers in brackets refer to the XhoI fragments marked in heavy lines which are discussed in the text in numerical order.

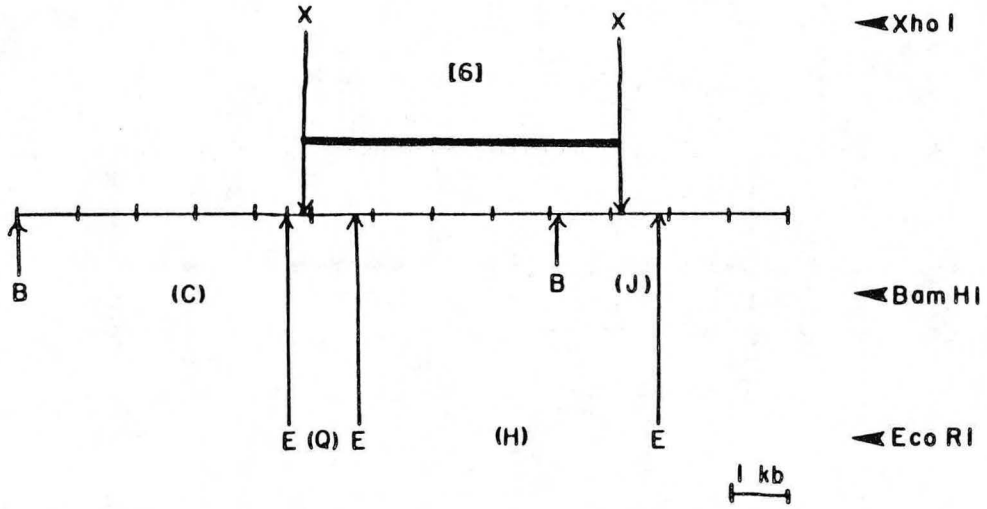

Fig. 3-9. A partial restriction map of pRPS404. The letters indicate the letter name (Table 3-1) of intact fragments generated by digestion with BamHI and EcoRI. The number in the bracket refers to a XhoI fragment marked in a heavy line and discussed in the text.

Table 3-6

Tn 5.7 Insertions in pRPS404, KZE strains are E. coli Neco 100[pRPS404::Tn 5.7]. B= Bam H1, E= Eco R1, Bg= Bgl II, X= Xho I Fragment sizes are in kilobase pairs of DNA. X1 and X2 are new fragments produced when the individual pRPS404::Tn5.7 DNA is cut with Xho I, resulting from Tn5.7 insertions. Bg1 and Bg2 are the corresponding new Bgl II fragment sizes.

KZE (Tn5.7#)	B	E	Bg	X	X1	X2	Bg1	Bg2
3G7	C	H	A	G	4.4	1.8	14.40	
3H2	I	M	F	F	5.3	1.2	3.1	7.2
3H3	J	L	A	D		.9	10.4	
1A2	G	J	A	D	8.7	4.4	2.8	
3A1	I	E	E	F	4.1	2.6	6.0	
3A3	F	F	C	E	7.8		15.7	2.2
IA1	K	F	B	C	1.17		23.5	1.9
IA4	C	H	A	G	4.7	1.6	27.4	10.7
IA7	E	E	D	D	11.4	2.2	11.3	3.5
8B8	C	H	A	G	5.6	.8	11.7	
8H10	D	P	C	E	0.9		10.4	9.0
8H12	C	H	A	G	4.0	2.3	25.8	9.9
8A1	M	L	A	D	11.4	1.7	10.1	
8A8	I	M	F	F	3.8	2.6	9.1	1.5
8A9	F	F	C	E	4.65	3.39	13.3	5.0
8B1	F	F	C	E	6.93	1.82	11.4	7.5
8B3	H	E	D	D	8.5	5.1	8.4	6.3
8B4	D	F	C	E	5.8	3.1	11.9	6.9
8D6	C	H	A	G	3.4		13.9	
8D7	H	E	D	D	10.0	3.5	10.1	4.9
8D9	L	I	C	J	1.7		12.8	6.9
8E6	C	B	A	B	3.17		14.8	
8E9	C	B	A	B	2.22		13.6	
8E11	C	B	A	B	3.36		14.7	
8E12	E	E	D	D	12.1	2.0	8.2	7.2
8F1	I	M	F	F	5.6	1.1	7.9	2.7
8F2	J	H	A	D	0.64		11.2	
8F6	J	L	A	D	12.8		5.7	
8G2	C	Q	A	G	6.0		15.9	
8G3	C	H	A	G	3.6		10.2	
8G5	I	E	E	F	3.3	3.1	7.0	6.8
8G9	D	I	C	I	1.8		16.3	
8G10	C	H	A	G	4.8	1.4	15.2	
8G12	D	F	C	E	2.9	5.6	11.5	8.35
9A4	I	M	F	F	4.1	2.2	8.8	1.9
9A6	E	E	D	D	12.6	.5	13.5	1.8
9A9	C	H	A	G	3.3	2.7	14.32	
9A11	H	E	D	D	8.4	4.8	11.4	4.1
9A12	H	E	D	D	9.1	4.2	10.8	4.7
9B4	N	A	B	C	9.6	3.5	4.6	
9B7	F	F	C	E	7.47	1.75	8.0	
9B9	F	F	C	E	7.07	2.24	16.5	3.6

Table 3-6 (continued)

KZE (Tn5.7#)	B	E	Bg	X	X1	X2	Bg1	Bg2
9C1	K	F	B	C	1.09		1.9	
9C4	C	H	A	G	3.9	2.1	13.9	
9C6	D	F	C	E	3.0	5.6	13.4	7.3
9C7	C	H	A	G	3.8	2.2	13.5	
9C8	C	H	A	G	4.5	1.5	11.2	
9C10	E	E	E	F	5.9	.8	9.5	4.0
9D1	C	B	A	B	2.24		18.2	
9D5	E	E	E	H	2.8	0.8	8.4	5.2
9D10	G	J	A	D	9.0	4.2	2.8	
9D11	C	B	A	B	3.09		19.5	
9E3	O	O	F	J	1.8		6.9	
9E6	C	B	A	B	2.22		19.6	
9E11	D	I	C	I	1.9		12.5	8.7
9F2	D	P	C	E	7.4	1.5	12.1	9.2
9F4	H	E	D	D	5.5		8.6	7.0
9F6	F	F	C	E	7.58	1.76	8.0	
9F12	G	J	A	D	9.8	3.7	3.4	
9G5	D	I	C	K	1.2	1.0	11.1	10.1
9G6	C	B	A	B	3.44			

C. Isolation of Tn5.7 Insertions into pRPS404

Transposition of Tn5.7 onto pRPS404 was accomplished via the following scheme. i) Tn5.7 was inserted into phage λ and lysogenized into the E. coli chromosome.(courtesy J. Yin) ii) pRPS404 was conjugated into this strain and transconjugants were independently repurified and grown up to 10ml in liquid culture. This insured that subsequent analysis would be performed on insertions resulting from independent transpositions. iii) The pRPS404::Tn5.7 plasmids were selected for in another conjugation event with simultaneous selection for Sp^R and Km^R. By switching antibiotics during repurification to Km and Tp, spontaneous Sp^R mutants were eliminated. The plasmids were isolated (Birnboim and Doly, 1979) and analyzed by restriction endonuclease digestion.

The combination of transposon mutagenesis using Tn5.7 and the availability of broad host range cloning vectors with Cma should facilitate genetic-physical mapping in a wide range of bacterial genera.

CHAPTER 4: GENETIC PHYSICAL MAPPING USING Tn5.7

I. INTRODUCTION

In this chapter the genetic-physical map of the photosynthesis region is extended by the use of transposon Tn5.7 mutagenesis and complementation analysis with various pRPS404::Tn5.7 plasmids. In Chapter 2, a gene replacement system was described utilizing the inherent instability of the R-prime in a recombination proficient background. The construction of Tn5.7 and physical mapping of the insertions into the R-prime was described in Chapter 3. The gene dosage effect of streptomycin(Sm) resistance, provided by Tn5.7, and the instability of the R-prime have been utilized to isolate mutations in previously undescribed genetic loci effecting the differentiation of intracytoplasmic photosynthetic structures. We have isolated 60 independent insertions of Tn5.7 into pRPS404, 31 of which have recombined into the chromosome of R. capsulata. Southern analysis of the R. capsulata mutants confirms the location of the transposon to be identical to the insertion site in the R-prime in E. coli. Phenotypic characterization of photosynthetic mutants by determining capability for photosynthetic growth (PS+/-), absorption spectroscopy, and SDS-PAGE of subcellular chromatophores identified new phenotypic classes including regulatory mutations affecting RC as well as previously unidentified loci involved with bacteriochlorophyl and carotenoid biosynthesis. Complementation analysis has tentatively identified transcriptional operons for certain photopigment genes.

II. RESULTS AND DISCUSSION

A. Tn5.7 Mutagenesis and Gene Replacement

To identify photosynthesis genes located on the R-prime plasmid pRPS404, 45 insertions of Tn5.7 were isolated as described in Chapter 3. The location of the transposon was determined by restriction enzyme digests of various pRPS404::Tn5.7 plasmids using XhoI and BglII. The transposon insertions were named by their distance in kb counter-clockwise from the EcoRI restriction site at 0kb on pRPS404, (Fig. 3-3). These transposon containing plasmids were conjugated from *E. coli* into *R. capsulata* by selection for the transposon mediated resistance to Sm. The R-prime has been shown to be unstable in Rec+ strains, Chapter 2. Therefore, stable resistance to Sm can arise from either recombination events between the chromosome and the plasmid placing the transposon in the chromosome and the wild type gene on the plasmid or a transposition into the chromosome. Once the transposon is in the chromosome, the wild type gene is lost since there is no longer any selection pressure for maintenance of an intact plasmid.

In order to confirm that the mutant phenotypes observed were due to homologous recombination of the fragment which contains the transposon into the chromosome, the DNA of various mutant strains was examined by Southern hybridization technique. DNA isolated from each strain was digested with BamHI or EcoRI and probed with ^{32}P-labelled pRPS404 or a Tn5.7 probe, pRS5 (Lichtenstein and Brenner, 1981). Fig. 4-1 shows an example of a genomic Southern analysis of Tn5.7 generated mutants of *R. capsulata*. The bands which hybridize to the pRPS404 probe are a combination of native *R. capsulata* genomic DNA fragments and remnants of

deleted R-primes which are homologous to the vector portion of pRPS404. It has been found that deletion events involving the R-prime occur via intramolecular recombination between the IS21 elements but that additional deletion events occur extending into the Km^R gene and into *sex*, the locus involved with surface exclusion in RP1 type plasmids (Chapter 1; Hedges et al.,1974). Similar phenomena have been observed with spontaneous deletions of R68.45, a related plasmid, in *Pseudomonas aeruginosa* (Haas and Reiss, 1983) and *Erwinia carotorora* (Currier and Morgan, 1982). Deletions of the Km^R gene were found as well as deletions of the transfer region, *tra*. If gene replacement has gone to completion, then the Tn5.7 target restriction fragment should be missing from the hybridization pattern and be replaced by a hybrid band with the molecular weight of the transposon plus the original fragment, since Tn5.7 has no internal *BamHI* or *EcoRI* sites. As is illustrated in Fig. 4-1, when compared to the hybridization pattern from wild type, mutant strains lack only one fragment which corresponds to the fragment mutated by Tn5.7. In addition, there are new bands which either hybridize to the transposon probe or to the vector probe and were confirmed by separate Southern analysis. These bands resulted from partial deletions of pRPS404 extending into various regions of the R factor. As seen in Table 4-1, most hybrid bands have a molecular weight equal to the original band plus the transposon (7.6kb). An exception is insertion 64.4 shown in Fig. 4-1o, which results in a hybrid fragment with a molecular weight 2kb greater than expected. This insertion maps within *rxcB*. The mutant is PS^+ and therefore suggests that a rearrangement has taken place which allows expression of *rxcB*.

Figure 4-1. Southern analysis of of Tn5.7 insertions into photosynthesis genes of R. capsulata. Total DNA prepared from R. capsulata strains that received different pRPS404::Tn5.7 plasmids were subject to digestion with BamHI, lanes a thru l, or EcoRI, lanes m thru r, electrophoresed on a 0.7% agarose gel, and transfered bidirectionally to nitrocellulose. Shown in this figure, one filter was hybridized to pRPS404, labelled by nick-translation. Lanes marked M refer to end labeled λ/HindIII fragments, with molecular weights (kb) 21, 9.4, 6.6, 4.4, 2.3, and 2.0. Letters A to L on the left and A to M on the right refer to BamHI and EcoRI restriction fragments from pRPS404, respectively. Open triangles to the left of a lane indicate a band which hybridized to pRS5, a Tn5.7 probe (data not shown) and are analyzed in Table 2. Open circles also to the left of a lane indicate the target band into which a Tn5.7 insertion has occurred. Lanes listed below refer to Tn5.7 insertion name; strains can be cross referenced from Table 1. Lane a, rxcAΩ26.3; b, bchEΩ51.0; c,Ω46.9; d, Ω47.4; e, Ω51.7; f, Ω55.1; g, bchJΩ49.2; h, bchAK28.0; i, bchKΩ56.7; j, bchHΩ58.5; k, Ω58.0; l and m, SB1003 (wild type); n, Ω65.7; o, Ω64.4; p, F1696Ω63.6; q, F1696Ω63.5; r, Ω53.5B. The fragments joining R. capsulata DNA from pRPS404 and the chromosome are >30kb for BamHI and are 8.5 and 3.4kb for EcoRI digests.

Figure 4-1

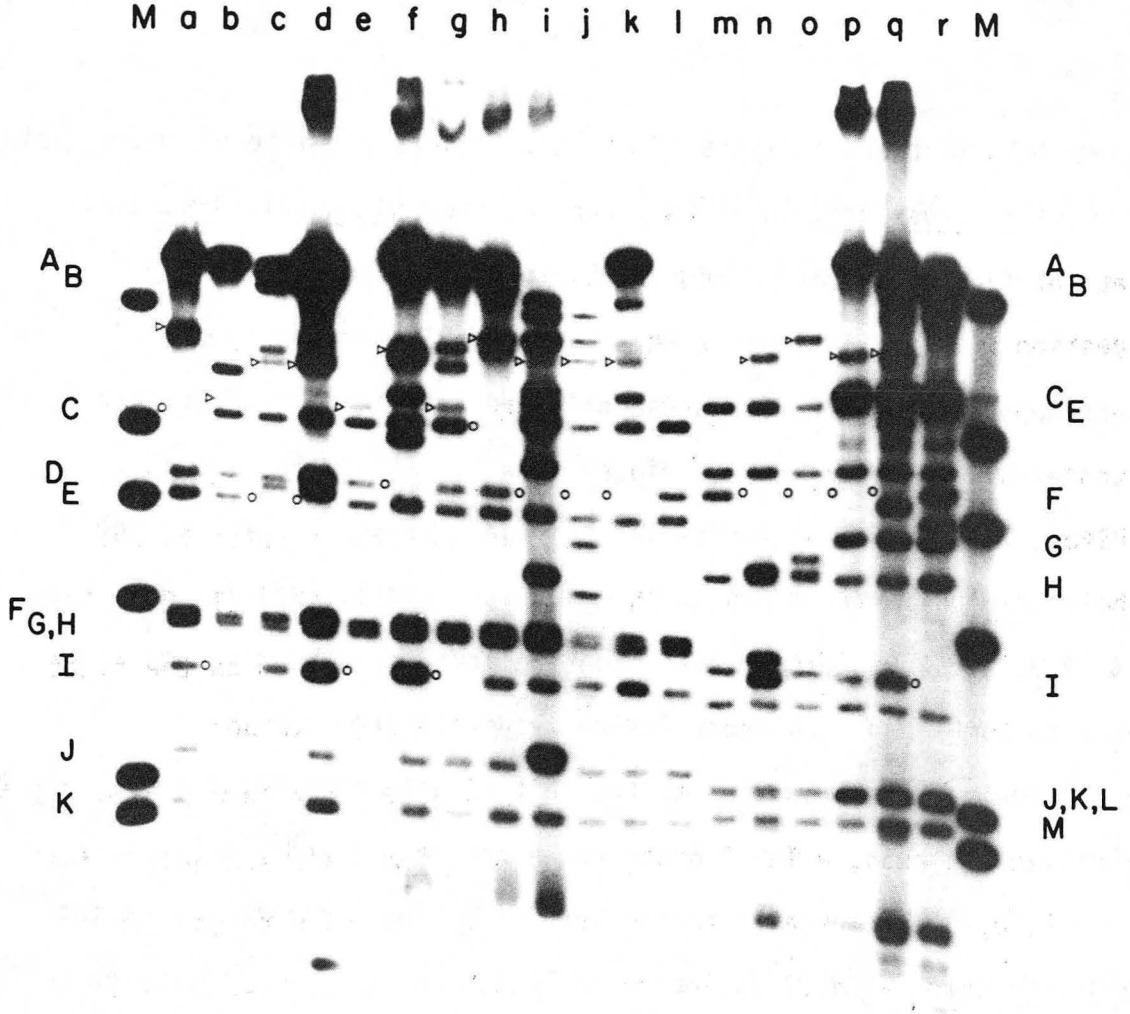

XBB 830-10648

Table 4-1. Molecular Weights of Tn5.7 Hybrid Restriction Fragments

Tn5.7 # MW(kb)	Mutated Fragment		MW(kb)	Expected MW(kb)	Actual
	BamHI	EcoRI			
26.3	C		10.0	17.6	17.8
51.0	I		3.5	11.0	10.8
46.9	E		6.6	14.2	13.9
47.4	E		6.6	14.2	13.9
55.1	D		3.5	11.0	10.7
49.2	I		7.3	14.9	14.5
28.0	C		10.0	17.6	17.8
56.7	D		7.1	14.7	14.6
58.5	D		7.1	14.7	14.5
58.0	D		7.1	14.7	14.5
65.7		F	7.9	15.5	15.3
64.4		F	7.9	15.5	17.6
63.6		F	7.9	15.5	15.4
63.5		F	7.9	15.5	15.4
53.5B		I	3.6	11.2	11.5

B. Phenotypic Characterization of Tn5.7 Generated Mutants

Once pRPS404::Tn5.7 plasmids were conjugated into R. capsulata, many transconjugants showed abnormal pigmentation or fluoresence (Youvan et al., 1983) after one or two repurifications on Sm. These phenotypes were observed as sectors in colonies, visible only as the wild type alleles were deleted. Analysis of mutant phenotypes included determination of capability for photosynthetic growth, PS+/-, visible absorption spectroscopy of chromatophore fractions, and SDS-PAGE. PS+/- phenotypes are listed in Materials and Methods I. Absorption spectra of photosynthetic membrane fractions are mostly indicative of LHI and LHII since reaction centers are a minor component. The LHI complex absorbs maximally at 870nm and LHII absorbs at 800 and 850nm (Lien, 1973). Carotenoids absorb between 400-500nm (Scolnik, 1980). Bchl absorption peaks common to all complexes are at 590 and 375nm (Jensen et al., 1964). Fig. 4-2 is an absorption spectrum of wild type R. capsulata, SB1003, and two mutants resulting from insertions 28.0, KZR8G2, and 39.8, KZR9F4. Insertion 28.0 results in a bchA phenotype, which is accumulation of 2-devinyl,2-hydroxyethyl chlorophyllide a and chlorophyllide a, both Bchl precursors which absorb at around 665nm (Biel and Marrs, 1983). When mature Bchl is not made, the polypeptides of the various complexes never appear in the membrane fraction. As can be seen in Fig. 4-2, insertion 28.0, strain KZR8G2, results in a lack of absorption peaks attributable to LHI and LHII. Previously unidentified bch genes found in this study are bchI, bchJ, bchK, bchL. The bchL gene, localized from sequence analysis of the BamHI F fragment has an open reading frame extending for 77 amino acids, is

Figure 4-2. IR-Visible absorption spectroscopy of R. capsulata strains. Chromatophore fractions from KZR8G2, containing Tn5.7 insertion 28.0; KZR9F4, containing Tn5.7 insertion 39.8; and SB1003, wild type; isolated from cells cultured in RCV liquid plus DMSO, pyruvate, and glucose according to Materials and Methods and subject to absorption spectroscopy.

Figure 4-2

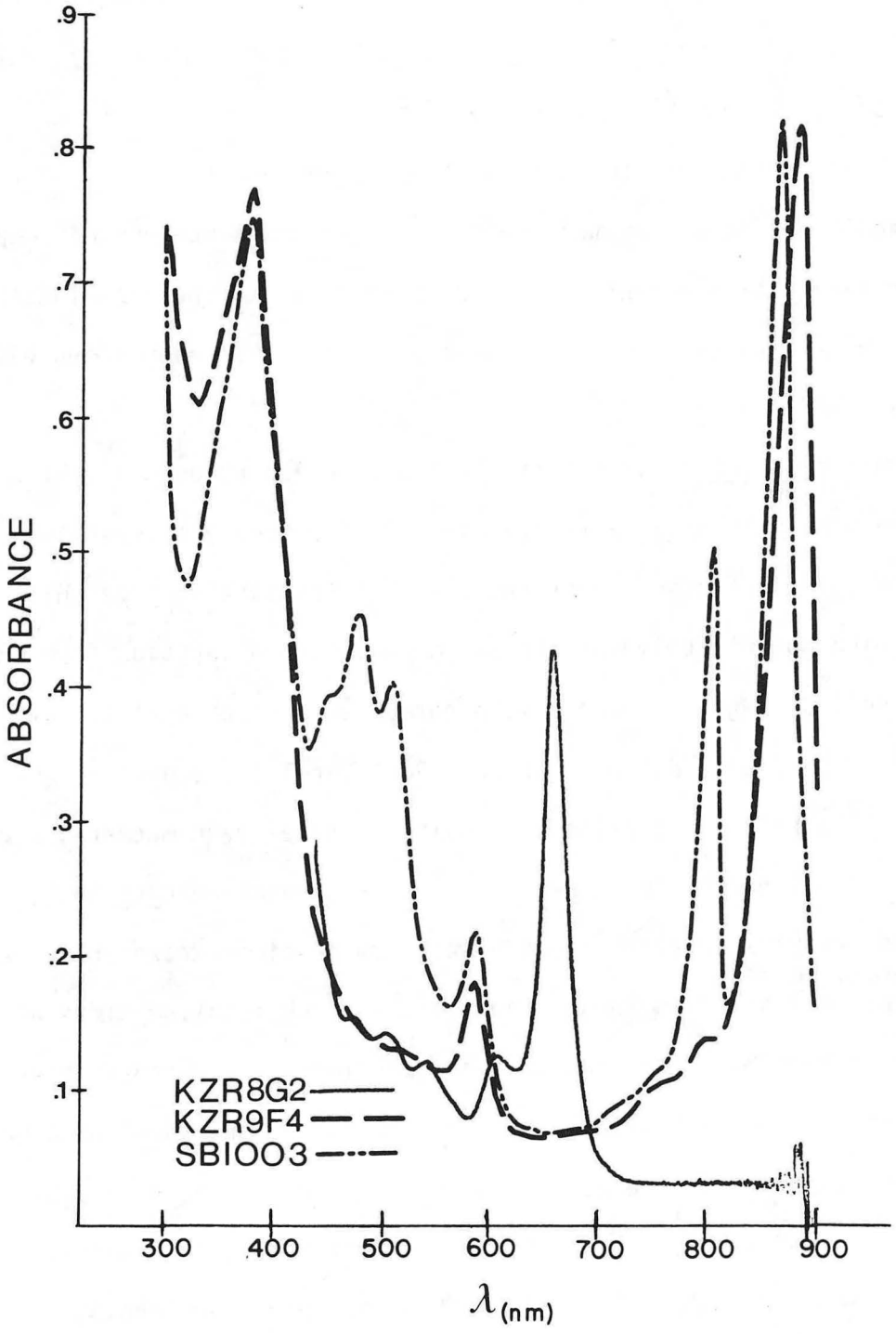

XBL 8312-4815

identified by insertion 61.6, and is transcribed from left to right in Fig. 4-6. It has not been determined what compounds are accumulated by these mutants, if any, but the absorption maxima in methanol extracts are listed in appendix I. Many of the Bchl mutants accumulate more than one compound. Possibly the Bchl biosynthetic enzymes exist in a complex. If one of the enzymes is lacking, then maybe the complex is destabilized, other enzymes are deactivated and a variety of compounds accumulate. These mutants should be helpful in further elucidation of the Bchl biosynthetic pathway, part of which is already known (Biel and Marrs, 1983).

Mutation crtIΩ39.8 results in a blue-green phenotype, which is predominantly associated with a block in carotenoid biosynthesis at an earily stage but also demonstrates a pleiotropic effect on LHII; the Bchl binding LHII polypeptides are made but no absorption from LHII is observed. Blue-green mutants make normal amounts of Bchl and are PS^+ (Yen and Marrs, 1976). Only the non-Bchl binding (Cogdell and Crofts, 1978) 14kd LHII polypeptide is missing in blue-green mutants, Figs. 4-3 and 4-4f, g, and h. As is seen in Fig. 4-2, mutation crtIΩ39.8, strain KZR9F4, results in an absorption spectrum devoid of carotenoid and LHII absorption peaks even though the 8 and 10kd LHII polypeptides are present. Possibly, the 14kd LHII polypeptide is involved with Bchl insertion into the LHII complex. Alternatively, the carotenoid may be needed to stabilize the Bchl. The crtI and crtJ genes identified by insertions of Tn5.7 all are blocked in earily stages of carotenoid biosynthesis and accumulate no visible-absorbing carotenoids.

Insertions of Tn5.7 into the structural genes of the RC

Figure 4-3. SDS-PAGE of blue green mutants. Chromatophore fractions were electrophoresed in a 9-18% acrylamide gel. Samples: a, crtIΩ39.8; b, crtB4; c, Ω53.5B; d, crtEΩ34.6; e, crtJΩ53.5A; f, Ω51.7; g, crtE6; h, wild type SB1003. The carotenoid biosynthesis mutants crtK, crtB, crtE, and crtI accumulate no visible absorbing carotenoids.

Figure 4-4. SDS-PAGE of Tn5.7 generated mutants. Chromatophore fractions were electrophoresed in a 9 to 18% acrylamide gradient gel according to Materials and Methods and stained with coomassie blue. Bands marked RC refer to the H, 28kd; M, 24kd; and L, 21kd, subunits of the reaction center. The LHII 14, 10 and 8kd polypeptides and LHI 12kd polypeptide are indicated. Tn5.7 induced mutants are shown in lane a, rxcAΩ26.3; b, F1696Ω63.5; c, F1696Ω63.6; d, F1696Ω64.4; e, rxcDΩ65.7; f, crtJΩ53.5A; g, crtEΩ34.6; h, crtIΩ39.8. Wild type, SB1003, is shown in lane i. Molecular weight standards are shown in lane M.

Figure 4-3

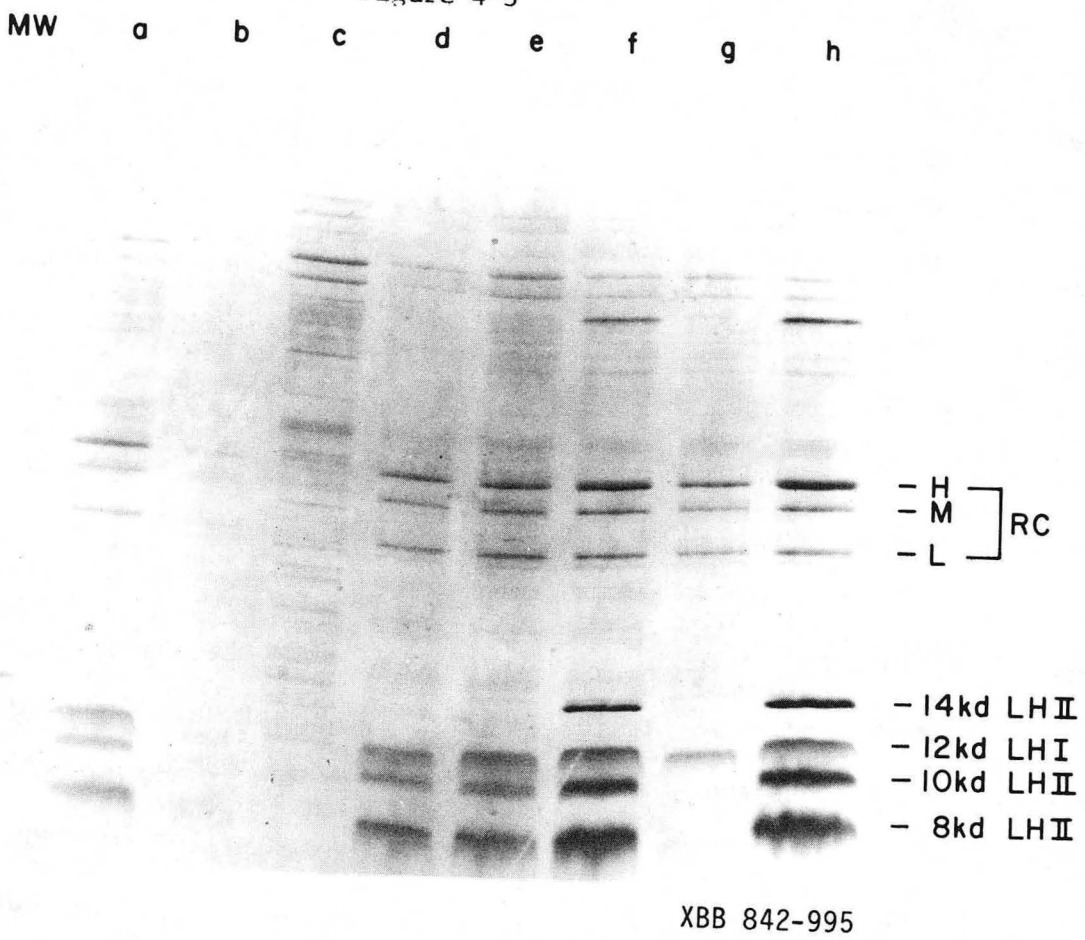

XBB 842-995

Figure 4-4

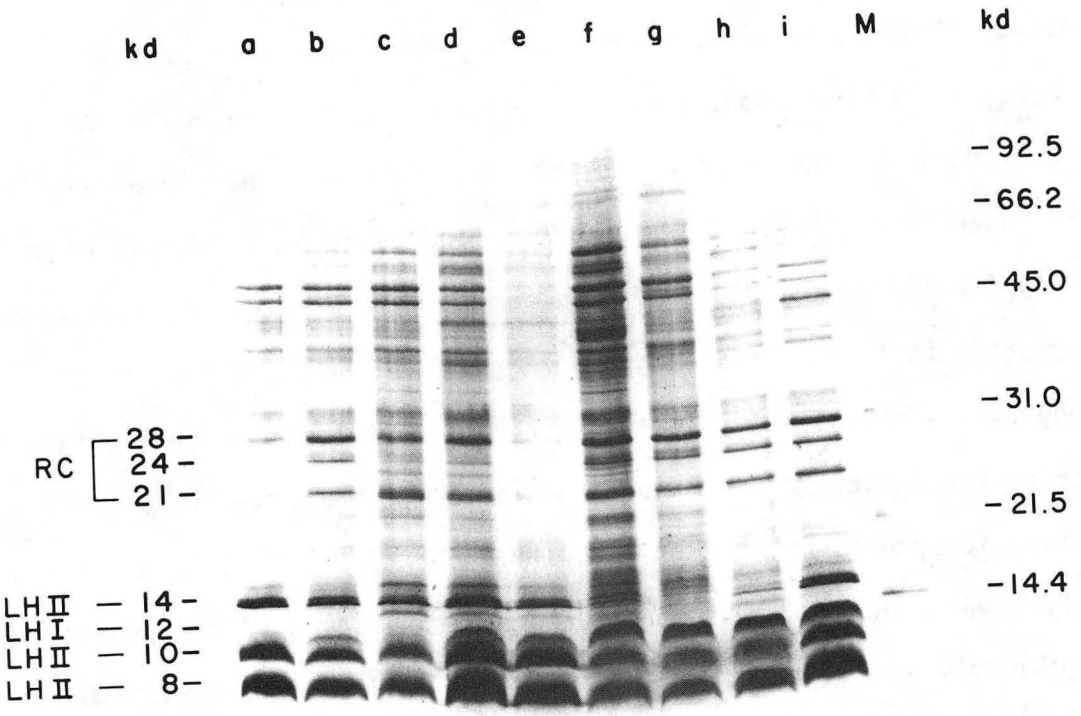

XBB 830-10647

subunits have been isolated. RC mutations are pleiotropic in that, if one subunit of the RC is not made, none of the subunits is integrated into the membrane. The SDS-PAGE profiles of mutants rxcAΩ26.3, F1696Ω63.5, F1696Ω63.6, F1696Ω64.4, and rxcDΩ65.7 are shown in Fig. 4-4a, b, c, d, and e, respectively. Insertion 26.3 is located in the structural gene for the M subunit of the RC, rxcA, and therefore results in a RC^- phenotype. F1696, has been identified as an open reading frame extending for 477 amino acids and ending just before rxcB. The direction transcription is from left to right in Fig. 4-7. The three insertions in this region all effect LHI, Fig. 4-4b, c, and d, but differ both with respect to the amount of RC incorporated into the membrane fractions and capability for photosynthetic growth. The F1696Ω63.5 mutant shows only a slightly lower amount of RC incorporated as compared to wild type and grows at normal rates photosynthetically. The F1696Ω63.6 and F1696Ω64.4 mutants have barely detectable levels of RC as judged by SDS-PAGE, repeated at least three times with different chromatophore preparations, and grow at about 50% of the wild type rate photosynthetically. The function of F1696 has not been determined. The transcriptional organization of this region is discussed below.

The rxcDΩ65.7 mutation is regulatory since the insertion is not in any of the structural genes for the RC. It is pleiotropic since the RC as well as a 44kd heme staining polypeptide are absent from the membrane. C-type cytochromes are detected in SDS-PAGE profiles because they have a covalently attached heme group which can be stained by 3,3',5,5'-tetra methyl benzidine-H_2O_2 (Hoyer-Hansen, 1980). Fig. 4-5 shows an SDS-PAGE profile of SB1003, grown under various conditions, and two PS^- RC^- mutants, rxcAΩ26.3 and rxcDΩ65.7. Fig. 4-5A shows the

Figure 4-5. Comparison of heme content in chromatophore fractions isolated from RC mutants. SDS-PAGE was performed as in Fig. 4-4. Panel A shows the gel after heme staining using 3,3',5,5'-tetramethyl benzidine and panel B shows the same gel after staining with coomassie blue. Lane 1, SB1003 grown in the dark micro-aerophilically in the presence of DMSO; 2, SB1003 grown photosynthetically; 3, SB1003 grown aerobically; 4, SB1003, same as lane 1 but boiled for 5 minutes before loading; 5, rxcD 65.7; 6, rxcA 26.3; 7, cytochrome c' (courtesy R. Salemne); 8, horse heart cytochrome c; M, molecular weight markers.

Figure 4-5

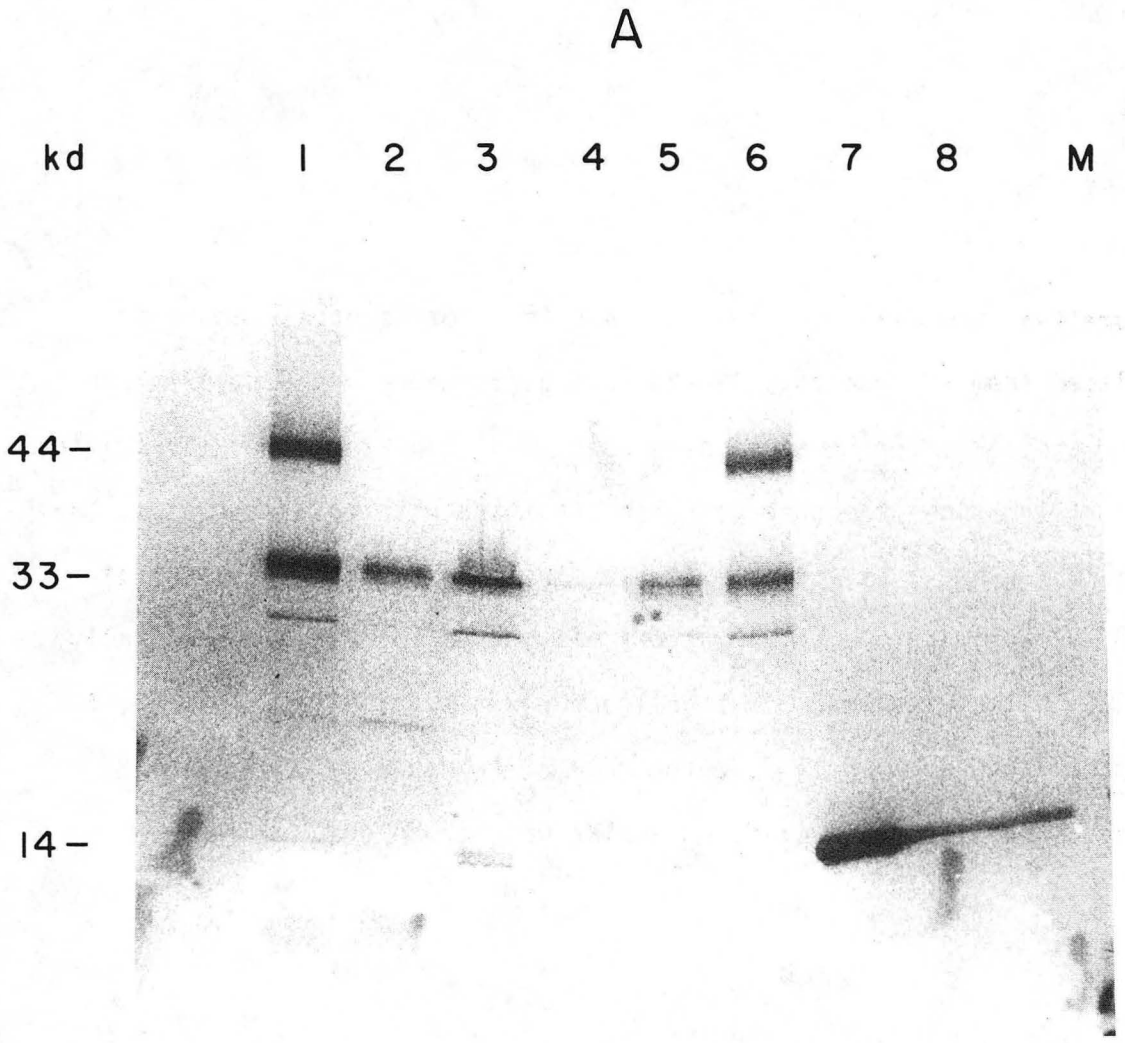

Figure 4-5

B

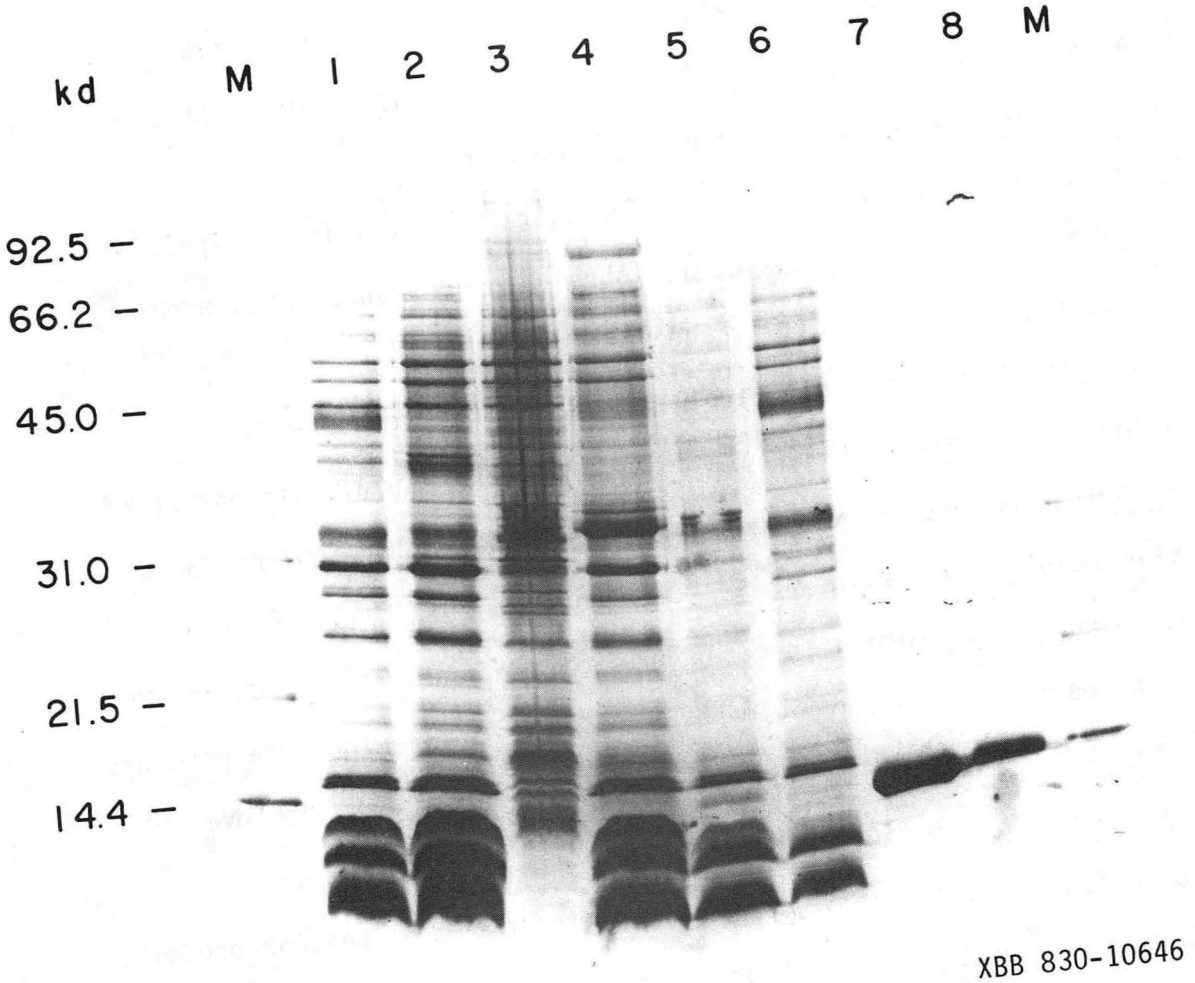

heme-stained bands, and Fig. 4-5B shows the gel after staining with Coomassie Blue. The 44kd band is induced in wild type only during dark micro-aerophilic growth with DMSO. However, this particular band is missing from the rxcDΩ65.7 mutant when grown with DMSO. The absence of this c-type cytochrome is not observed in RC structural gene mutations such as caused by insertion rxcAΩ26.3, Fig. 4-5 lane 6. The 33 and 24kd heme staining polypeptides are probably part of the ubiquinone-cytochrome b-c_1 complex. The 14kd heme staining polypeptide is probably cytochrome c_2, which is loosely bound (Zannoni and Marrs, 1981) and therefore is easily washed off.

The 44kd heme staining polypeptide is only expressed under anaerobic conditions in the presence of DMSO. The pleiotropic nature of the rxcDΩ65.7 mutant is reminiscent of mutations in fnr, coding for a positive regulatory element in E. coli (Shaw et al., 1983). It is a general regulatory protein that responds to the redox status of the cell and is necessary for the expression of a number of anaerobic respiratory systems. It is not known whether the RxcD protein acts at the level of transcription. If the block of RC synthesis is at the level of transcription, then possibly the RxcD protein resembles the Fnr protein. If the block is post-transcriptional, then the RxcD protein may be involved in the insertion of RC and the 44kd heme staining protein into the membrane. Further studies on the nature of the rxcDΩ65.7 mutation are in progress.

Certain insertions never result in abnormal colony sectors, even after many repurifications. Three of these strains, resulting from insertions 46.9, 47.4, and 51.7, appear to have a wild type photosynthetic apparatus. As shown in Fig. 4-1c, d, and e, the

recombination and deletion steps have gone to completion with these insertions.

C. Complementation Analysis by Various pRPS404::Tn5.7 Plasmids

Complementation of carotenoid, Bchl, and RC mutations with pRPS404::Tn5.7 plasmids was accomplished as described in Materials and Methods. Briefly, complementation of Bchl and RC mutations were determined by capacity for photosynthetic growth and carotenoid mutations by inspection for colored carotenoid production. Point mutations were tested simply by conjugation of a pRPS404::Tn5.7 plasmid into the R. capsulata strain with selection for either Sm^R or Sp^R. Certain KZR strains became Km^S due to a deletion into the Km^R gene and into sex so these strains could be tested for complementation by selecting for Km^R in conjugation events with pRPS404::Tn5.7 plasmids. However, the majority of KZR strains remained Km^R after the R-prime had deleted. In order to test these Tn5.7 induced mutations by complementation, the remains of the R-prime were eliminated by mobilizing in an incompatible plasmid, pLAFR1 (Friedman et al., 1982), which is a derivative of pRK290 and is a member of the incompatibility group P-1, and is tetracycline (Tet) resistant. The efficiency of transfer into strains which were Km^R was about two orders of magnitude lower than transfer into wild type R. capsulata. Some KZR strains were not capable of receiving pLAFR1 at all. This surface exclusion of pLAFR1 by the deleted R-prime suggests that sex on RP1, RP4, RK2, and R68 is near the Km^R gene. Tn7 mutagenesis of RP4 suggests the location of sex to be in a 13kb region containing the Km^R gene. The KZR strains which did receive pLAFR1 became Km^S after three repurifications on Tet, as

Table 4-2

Complementation Analysis with pRPS404::Tn5.7 Plasmids

pRPS404::Tn5.7 insertions at (kb)	rxcA142	bchC1007	crtE6	crtE526	crtB4	crtB551	crtA301	bchD1008	bchD561	bchG527	bchE604	bchF1003	bchH650	bchKΩ56.7	rxcDΔ65.7	crtEΩ34.6	bchIΩ41.6	bchLΔ61.6
26.3	-	+																
28.0	+	-																
30.3		-																
31.2		-																
31.4		-														+		
33.3		+	+	+												+		
33.4			+	+												+		
33.7			+	+												+		
33.8			-	-												-		
34.6			-	-														
36.4			+	+	+	+										+		
36.8			+	+	+	+										+		
39.8					+	+	+									+		
40.2					+	+	+	+								+		
41.0							-	+									+	
41.6							+	+	+									
43.1							+	-	-	+							-	
43.2							+	-	-	+							-	
44.6								+	+	+								
46.9										+							+	
47.4										+	+							
49.2										+	+						+	
50.8											-	+						
51.0											-	+	+					
51.7											+	+						
51.9											+	+						
53.5A											+	+						
53.5B											+	+		+				
55.0											+	+		+				
55.1											+	-		+				
56.7												+	+					+
58.0												+	+					
58.5											+	+	-	-				
59.7													-	-				
59.8													-	-				
60.0													+	+				
61.6													+	+	+			
63.5															+			+
63.6															-			+
65.6															-			
65.7															-			
67.9															+			

A positive complementation is +, a negative complementation is -, and a space means the experiment was not done.

Figure 4-6. Genetic-physical map of the photosynthetic gene cluster contained on pRPS404. The numbers on the physical map refer to kb moving counter-clockwise from the EcoRI site at 0 kb on pRPS404. X and B refer to XhoI and BglII restriction sites which were used to position Tn5.7 insertions. The numbers listed at the ends of vertical lines are the locations of insertions used in this study, +/- 200bp. The genetic map is shown above. Vertical ticks refer to insertions, either in the locus indicated or upstream. The boundaries for the loci, indicated by full vertical lines, were determined by DNA sequencing (Youvan et al., submitted), dark shading; previously published loci determined from gene transfer agent crosses (Yen and Marrs, 1976), light shading; or Tn5.7 mutagenesis and complementation analysis, no shading. The arrows above postulate direction and extent of transcription for some photosynthesis genes.

Figure 4-6

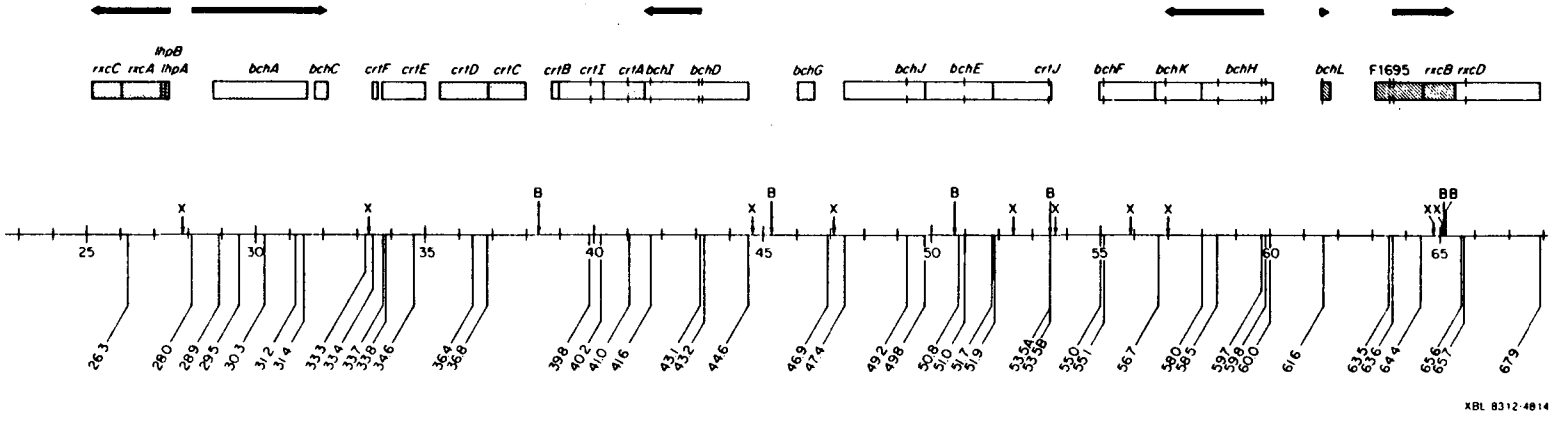
rxcC rxcA lhpB lhpA
bchA bchC
crtF crtE crtD crtC
crtB crtI crtA bchI bchD
bchG
bchJ bchE crtJ
bchF bchK bchH
bchL
F1695 rxcB rxcD
X B
25 30 35 40 45 50 55 60 65
26.3 28.0 28.9 29.5 30.3 31.2 31.4 33.3 33.4 33.7 33.8 34.6 36.4 36.8 39.8 40.2 41.0 41.6 43.1 43.2 44.6 46.9 47.4 49.2 49.8 50.8 51.0 51.7 51.9 53.5A 53.5B 55.0 55.1 56.7 58.0 58.5 59.7 59.8 60.0 61.6 63.5 63.6 64.4 65.6 65.7 67.9
XBL 8312-4814

would be expected since the RP1 type plasmids have a low copy number. Once these strains became Km^S, they could be tested for complementation by pRPS404::Tn5.7 plasmids. This conjugation event occurred at high frequency suggesting that in the construction of pRK290 (Ditta et al., 1980), sex was deleted. Table 4-2 lists the results of the complementation experiments. The crtC and crtD genes, which when mutated result in green pigmentation, could not be tested for complementation by the pRPS404::Tn5.7 plasmids because the R-prime carries a point mutation in crtD. The complementation experiments identified crtI, bchI, bchK, bchJ, and bchL as distinct genetic loci.

D. The Genetic-Physical Map

Fig. 4-6 is a genetic-physical map of the photosynthesis genes located on the R-prime. The map was constructed from previously published maps of this region (Biel et al., 1983), DNA sequence analysis of regions between 23.0 and 27.8kb and between 61.5 and 65.5kb (Youvan et al, submitted), and from mutagenesis and complementation analysis with pRPS404::Tn5.7 plasmids in this study. The rxcA, rxcB, rxcC lhpA, lhpB, and bchL genes, coding for the M, L, and H subunits of the RC, the LHI polypeptides, and a polypeptide involved in Bchl synthesis, respectively, are contained in the sequenced region.

Insertion 28.0 results in a bchA phenotype and does not complement bchC point mutants but does complement rxcA mutations. Mutations in bchC result in accumulation of 2-desacetyl-2-hydroxyethyl bacteriochlorophyllide a, which is an intermediate further along in the Bchl metabolic pathway than accumulated by bchA mutants (Biel and Marrs, 1983). Therefore, if bchA and bchC were on the same operon a polar

mutation upstream from both genes would result in a bchA phenotype. Recently, marker rescue crosses indicated that both bchA and bchC mutations could be complemented by a sub-clone of the R-prime containing the EcoRI-H fragment (Taylor et al., 1983), which extends from 28.7 to 34.6kb on the map shown in Fig. 4-6. In that study it was not determined whether the complementation observed for EcoRI subclones was due to transcription initiated from the insert DNA or the vector DNA. These data are consistent with the interpretation that the promoter for the bchA and bchC genes is located upstream from Tn5.7 insertion 28.0, bchA and bchC are located on EcoRI fragment H, and that transcription proceeds upstream from insertion 28.0 through bchA to bchC.

Complementation of crtE mutants shows that crtE is not complemented by insertions 33.8 and 34.6. Since both crtFΩ33.7, and crtDΩ36.4, do complement crtE mutants, transcriptional operons including crtFcrtE and crtDcrtE can be ruled out. Tn5.7 insertion 39.8 results in a blue-green phenotype and complements two separate point mutations in crtB, which also result in a blue-green phenotype. Therefore, the simplest interpretation is that insertion 39.8 identifies a new gene, crtI. This gene is not transcribed from crtA because polar insertions in crtA have the phenotype of crtA mutants which accumulate demethylspheroidene and spheroidene (Scolnik et al., 1980). These compounds are further along in the carotenoid biosynthetic pathway than compounds accumulated by crtI mutants. The crtA gene appears to be in a transcription unit separate from both crtI and bchI since it is complemented by insertions crtIΩ39.8 and bchIΩ41.6 but not by crtAΩ41.0.

The bchI gene is identified by insertion 41.6. The bchIΩ41.6

Figure 4-7. Agarose gel electrophoresis of pRPS404::Tn5.7 plasmids. Plasmids were purified from E. coli strains according to Materials and Methods, digested with restriction enzymes BglII, lanes a thru h, or XhoI, lanes i thru o, and electrophoresed in a 0.7% agarose gel so that the order of Tn5.7 insertions between 50.8kb and 55.1kb on pRPS404 could be determined to +/-50bp. Letters A thru K on the right refer to fragments of the plasmid after digestion with XhoI, the 6.6kb internal Tn5.7 band is indicated. Lane M refers to molecular weight markers, indicated on the left. Plasmids shown with Tn5.7 insertions are lane a and i, 55.1; b and j, 55.0; c and k, 53.5B; d and l, 53.5A; e and m; 51.7; f, 51.9; g and n, 51.0; h and o, 50.8.

Figure 4-7

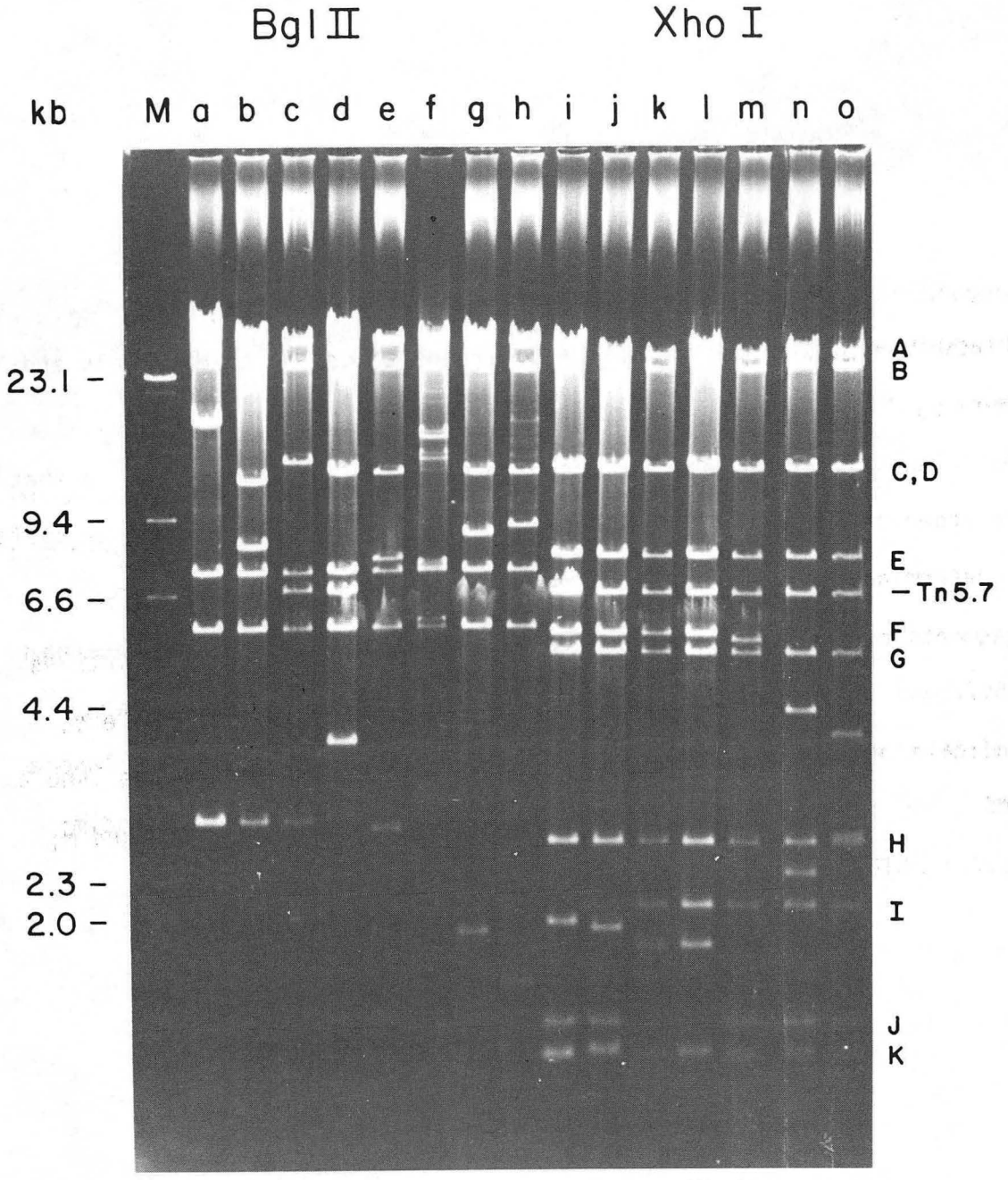

XBB 830-10644

complements two point mutations in bchD yet results in a Bchl$^-$ phenotype. Complementation analysis indicates that bchD and bchI are in the same operon, with transcription in that order (see Table 4-2). The bchJ gene is identified by insertion 49.2, is located on the BamHI I fragment, and is not on an operon with any of the Bchl genes tested. Insertions 53.5A and 53.5B appear to be insertions at the same site, as judged by ararose gel electrophoresis which has about a 50bp resolution in the <2kb range, Fig. 4-7. However, the two insertions are in the opposite orientation. Insertion 53.5A results in a blue-green phenotype and 53.5B is Bchl$^-$. It is unlikely that the orientation of insertion is the cause of the two phenotypes because the terminal portions of Tn5.7 are identical for 1500bp at the ends. Probably the two insertions differ by less that 50bp and are in two distinct genes. Both insertions resulted in abnormal phenotypes after the recombination of the transposon into the chromosome but before deletion of the wild type allele on the plasmid (data not shown) indicating that this region might serve some regulatory functions and cannot be complemented in trans. The Bchl$^-$ phenotype of the 53.5B insertion mutant could not be complemented by any of the pRPS404::Tn5.7 plasmids tested even after it had been shown to have recombined and deleted the wild type EcoRI I fragment. Therefore, it is omitted from the genetic map in Fig. 4-6 as a bch locus.

Insertion bchFΩ55.1 is the only pRPS404::Tn5.7 plasmid which did not complement point mutations in bchF and so bchF is not in the same operon as bchK and bchH. The bchLΩ56.7 mutant, is not complemented by insertions in bchH, but bchH point mutants are complemented by bchKΩ56.7. Therefore, it seems that the two genes are transcribed

together in the order bchH bchK, shown in Fig. 4-6.

In the region to the left of rxcD in Fig. 4-6 there is a division in phenotypes and complementation groups around 63.5kb. Inspection of this region for consensus promoter sequences from enteric bacteria (Hawley and McClure, 1983) show no significant homologies. It has not been determined what an oxygen regulated promoter consists of in R. capsulata. A comparison of the 5' DNA sequence for the M subunit gene from R. spheroides (Williams et al, 1983); R. capsulata lhpA, F1696, and the region around 63.5kb revealed sequence homologies shown in Fig. 4-8.

Figure 7. Comparison of DNA sequences between R. spheroides and R. capsulata. Regions located 5' to the R. spheroides M subunit of the RC gene are compared with R. capsulata 5' region to lhpA, 5' to the F1696 open reading frame, and the region around 63.5kb (+/- 200bp) in the BamHI F fragment, where insertions of Tn5.7 indicate the beginning of a transcriptional unit. The A of the ATG codon starting translation is numbered +1. Regions upstream have negative numbers. The region around 63.5kb is identified as 1921bp from the BamHI site at around 61.6kb on pRPS404.

Figure 4-8

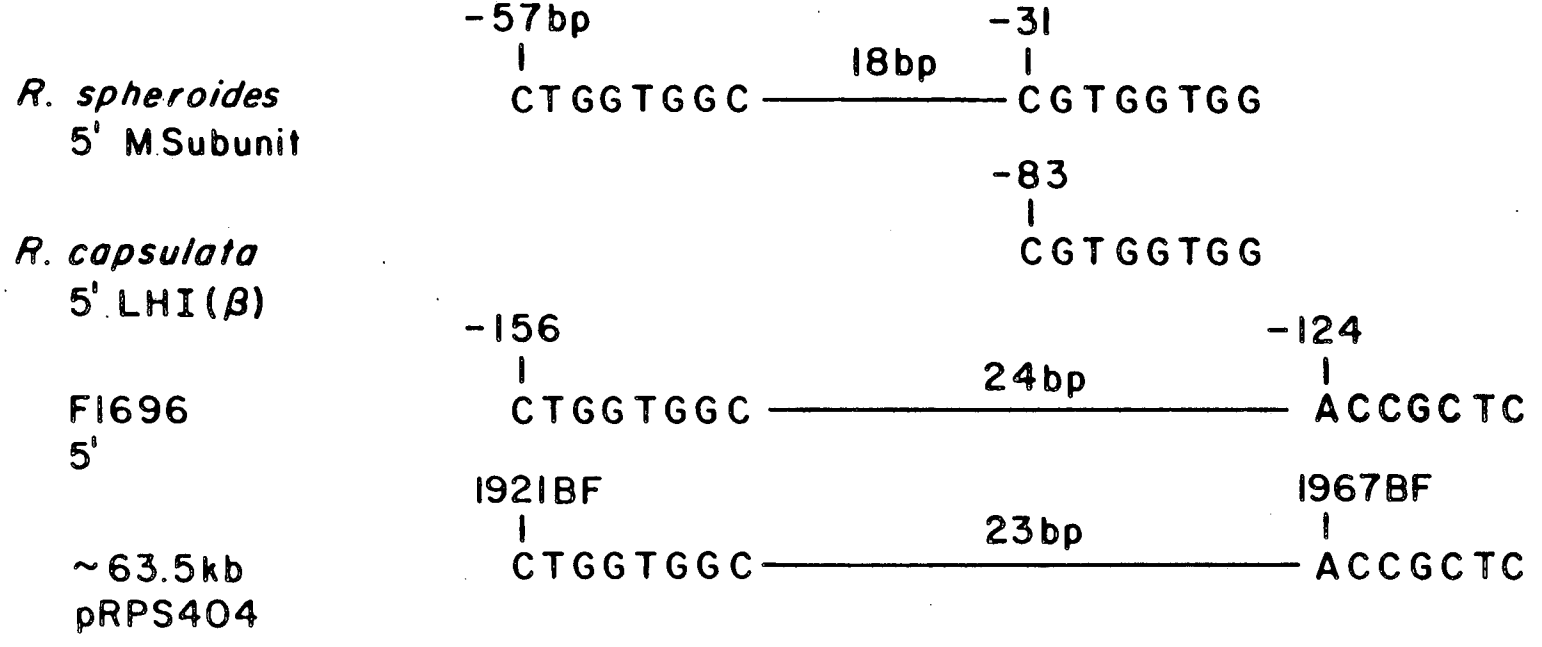
-57bp
-31
18bp
R. spheroides
5' M.Subunit
CTGGTGGC
CGTGGTGG
-83
CGTGGTGG
R. capsulata
5' LHI(β)
-156
-124
24bp
F1696
5'
CTGGTGGC
ACCGCTC
1921BF
1967BF
23bp
~63.5kb
pRPS404
CTGGTGGC
ACCGCTC

The function of this conserved region is not known but it might be involved in some aspect of promoter recognition. One model consistent with the data is that the reduced RC incorporation by F1696Ω63.6 and F1696Ω64.4 is due to polar inactivation of the rxcB gene and that this gene has two promoters, one which is between insertions 63.5 and 63.6 and another just before rxcB.

Transposon Tn5.7 mutagenesis of a photosynthetic gene cluster from R. capsulata has provided a number of mutations which may aid in the understanding of both bacterial and higher plant photosynthesis. The target DNA sequence may be subcloned by direct selection for the Tn5.7 antibiotic resistance markers. Recently found homologies between R. capsulata and the 32kd thylakoid membrane protein (Hearst and Sauer, in press) suggest that through heterologous hybridizations, higher plant photosynthesis genes may be cloned using bacterial sequences. Mutations in the Bchl biosynthetic genes provide a number of intermediates which may help in elucidating the biosynthetic pathway for Bchl and chlorophyll biosynthesis. A regulatory mutation affecting RC as well as a 44kd heme staining polypeptide has been identified and may provide clues to the regulatory interactions necessary for the differentiation of photosynthetic membranes. Complementation analysis has led to the postulation of transcriptional units containing both Bchl and carotenoid biosynthesis genes, suggesting a coordinate control for the biosynthesis of Bchl and carotenoids.

CHAPTER 5: SUMMARY AND CONCLUSIONS

The genetic analysis of photosynthesis genes has been greatly extended by the use of transposon mutagenesis of a photosynthetic gene cluster. This kind of analysis goes hand in hand with the work of Biel and Marrs (1983), on the identification of oxygen regulated genes; with the work of Taylor et al., (1983), in similar genetic mapping of the same region; and Yen and Marrs (1976), in gene transfer agent mediated mapping. The transposon mutagenesis work with Tn5.7 is distinguished by the number of genes identified and the increased resolution of the mapping procedure. In the case of Biel and Marrs, their resolution was hampered by the size of their transposon, 50kb. The work of Taylor was restricted to the length of the DNA fragments used which varied from 4-10kb. The gene transfer agent paved the way for isolation of the pRPS404 plasmid but was limited by the inability to distinguish two closely spaced genetic loci which resulted in the same phenotype when mutated.

Transposon mutagenesis described in this thesis provides a framework upon which future experiments can be based. An even higher resolution genetic map may be obtained by performing such experiments as mapping of RNA transcripts to conclusively determine promoter sequences, studying the regulatory interactions between Tn5.7 generated mutants at the RNA level, and identifying genes by in vitro transcription-translation systems.

One of the more intriging results from this study is the isolation of a regulatory mutation effecting reaction centers and a 44kd heme staining protein. Further analysis of this mutation may shed light on

regulatory interactions in photosynthesis. Preliminary experiments performed on photosynthetic revertants of the original mutation indicate an inverse relationship between the degree of photosynthetic competence and the ability to utilize DMSO and TMAO as terminal electron acceptors. This suggests a multiple domain protein interaction where one domain may be mutated, escaping from a control function but altering the function of another domain i.e., utilization of DMSO. This interaction could be envisioned as arising from a regulatory protein which interacts with DNA or another protein to couple the synthesis of reaction centers and the 44kd heme protein. These results need to be analyzed in more detail, both at the RNA level and at the DMSO reduction level.

Due to the high degree of homology between R. capsulata and R. spheroides reaction centers, it may be possible to extend the genetic physical mapping of related species by heterologous hybridizations using genes identified in R. capsulata.

Transposon mutagenesis has provided a higher resolution of the photosynthesis genes located on the plasmid pRPS404.

CHAPTER 6: MATERIALS AND METHODS

I. Bacterial Strains

KZE strains are *E. coli* containing a library of pRPS404::Tn5.7 plasmids which are named for the insertion site in pRPS404 numbering counter-clockwise from the EcoRI site at 0kb. KZR strains are *R. capsulata* containing Tn5.7 in the chromosome. The Tn5.7 insertion name in pRPS404 has been conserved for the sake of clarity. An example of this nomenclature is as follows: *rxcD*::65.7 means that the insertion of Tn5.7 at 65.7kb in pRPS404 is either in or is transcriptionally upstream from *rxcD*.

The phenotypes listed for the KZR strains are as follows: The absence of structural polypeptides is indicated where applicable in reference to RC, LHI, or LHII. Bacteriochlorophyll mutations are either $Bchl^-$, no precursors detected, or a number is listed after P, indicating the absorption maxima of the Bchl precursor in methanol extracts. The *R. capsulata* strains used in this study other than KZR strains have references sited which describe the nomenclature used for Bchl precursors. UAR#1 strains are the repurified transconjugants from the corresponding UAR# merozygotes resulting from crosses between a particular UAE# donor and SB1003 recipients. The lower case letter after the number designates a particular, independently repurified transconjugant. A set of independently repurified transconjugants arising from the same donor and bearing the same strain number are termed cousins.

Table 5-1

Genotype	Phenotype, Comments, and References
E. coli	
NEC0100 *leu⁻ thr⁻ thi⁻ trp⁻ recA⁻ lacY⁻*	Rif^R, Youvan, et al., 1982
NEC0125 *leu⁻ thr⁻ thi⁻ trp⁻ recA⁻ lacY⁻*	Nl^R, Youvan, et. al., 1982
NEC0125($\lambda b_{515} b_{519} c_{I857} nin5 S_7$::Tn5.7)	this work
KZ404 *ibid*, [pRPS404]	this work
SK1592 *gal⁻ thi⁻ hsdM⁺ hsdR⁻*	S. Kushner
SK2267 SK1592, *recA⁻*	N. Panopoulos
NEC0100::Tn7 (@82 min.)	Youvan et. al., 1982
BEC404 HB101[pRPS404]	B. Marrs
US404 NEC0100::Tn7[pRPS404]	Youvan et. al., 1982
UAE# Library of NEC0125[pRPS404::Tn7]	Youvan et. al., 1982
HB101 *pro⁻ leu⁻ thr⁻ lacY⁻ hsdM⁻ hsdR⁻ recA⁻*	Sm^R, S. Cohen
NEC0205 HB101[pLAFR1]	Friedman et al., 1982
NEC0200 HB101[pRK2013]	Ditta et al., 1980
KZE8E9 NEC0100[pRPS404 Ω(26.3kb::Tn5.7)]	this work
KZE8G2 NEC0100[pRPS404 Ω(28.0kb::Tn5.7)]	this work
KZEIA4 NEC0100[pRPS404 Ω(28.9kb::Tn5.7)]	this work
KZE8H12 NEC0100[pRPS404 Ω(29.5kb::Tn5.7)]	this work
KZE8D6 NEC0100[pRPS404 Ω(30.3kb::Tn5.7)]	this work
KZE9C4 NEC0100[pRPS404 Ω(31.2kb::Tn5.7)]	this work
KZE3G7 NEC0100[pRPS404 Ω(31.4kb::Tn5.7)]	this work
KZE8B8 NEC0100[pRPS404 Ω(33.3kb::Tn5.7)]	this work
KZE8F2 NEC0100[pRPS404 Ω(33.4kb::Tn5.7)]	this work
KZE3H3 NEC0100[pRPS404 Ω(33.7kb::Tn5.7)]	this work
KZE8F6 NEC0100[pRPS404 Ω(33.8kb::Tn5.7)]	this work

KZE8A1	NEC0100[pRPS404Ω(34.6kb::Tn5.7)]	this work
KZE9F12	NEC0100[pRPS404Ω(36.4kb::Tn5.7)]	this work
KZE9D10	NEC0100[pRPS404Ω(36.8kb::Tn5.7)]	this work
KZE9F4	NEC0100[pRPS404Ω(39.8kb::Tn5.7)]	this work
KZE8B3	NEC0100[pRPS404Ω(40.2kb::Tn5.7)]	this work
KZE9A12	NEC0100[pRPS404Ω(41.0kb::Tn5.7)]	this work
KZE8D7	NEC0100[pRPS404Ω(41.6kb::Tn5.7)]	this work
KZEIA7	NEC0100[pRPS404Ω(43.1kb::Tn5.7)]	this work
KZE8E12	NEC0100[pRPS404Ω(43.2kb::Tn5.7)]	this work
KZE9A6	NEC0100[pRPS404Ω(44.6kb::Tn5.7)]	this work
KZE9D5	NEC0100[pRPS404Ω(46.9kb::Tn5.7)]	this work
KZE9C10	NEC0100[pRPS404Ω(47.4kb::Tn5.7)]	this work
KZE3A1	NEC0100[pRPS404Ω(49.2kb::Tn5.7)]	this work
KZE8G5	NEC0100[pRPS404Ω(49.8kb::Tn5.7)]	this work
KZR8A8	NEC0100[pRPS404Ω(50.8kb::Tn5.7)]	this work
KZR9A4	NEC0100[pRPS404Ω(51.0kb::Tn5.7)]	this work
KZE8F1	NEC0100[pRPS404Ω(51.7kb::Tn5.7)]	this work
KZE3H2	NEC0100[pRPS404Ω(51.9kb::Tn5.7)]	this work
KZE9E3	NEC0100[pRPS404Ω(53.5Akb::Tn5.7)]	this work
KZE8D9	NEC0100[pRPS404Ω(53.5Bkb::Tn5.7)]	this work
KZE9E11	NEC0100[pRPS404Ω(55.0kb::Tn5.7)]	this work
KZE8G9	NEC0100[pRPS404Ω(55.1kb::Tn5.7)]	this work
KZE9G5	NEC0100[pRPS404Ω(56.7kb::Tn5.7)]	this work
KZE8H10	NEC0100[pRPS404Ω(58.0kb::Tn5.7)]	this work
KZE9F2	NEC0100[pRPS404Ω(58.5kb::Tn5.7)]	this work
KZE8G12	NEC0100[pRPS404Ω(59.7kb::Tn5.7)]	this work
KZE8B4	NEC0100[pRPS404Ω(59.8kb::Tn5.7)]	this work

KZE9C6	NEC0100[pRPS404 Ω(60.0kb::Tn5.7)]	this work
KZE8A9	NEC0100[pRPS404 Ω(61.6kb::Tn5.7)]	this work
KZE8B1	NEC0100[pRPS404 Ω(63.5kb::Tn5.7)]	this work
KZE9F6	NEC0100[pRPS404 Ω(63.6kb::Tn5.7)]	this work
KZE3A3	NEC0100[pRPS404 Ω(64.4kb::Tn5.7)]	this work
KZE9C1	NEC0100[pRPS404 Ω(65.6kb::Tn5.7)]	this work
KZEIA1	NEC0100[pRPS404 Ω(65.7kb::Tn5.7)]	this work
KZE9B4	NEC0100[pRPS404 Ω(67.9kb::Tn5.7)]	this work

Rcapsulata

KZR8E9	rxcA Ω(26.3::Tn5.7) rif-10	PS^-, RC^-, LHI^{red}, Sm^R, Sp^R, Km^R, this work
KZR8G2	bchA Ω(28.0::Tn5.7) rif-10	PS^-, P670, Sm^R, Sp^R, Km^R, this work
KZRIA4	bchA Ω(28.9::Tn5.7) rif-10	PS^-, P670, Sm^R, Sp^R, Km^R, this work
KZR8H12	bchA Ω(29.5::Tn5.7) rif-10	PS^-, P670, Sm^R, Sp^R, Km^R, this work
KZR8D6	bchA Ω(30.3::Tn5.7) rif-10	PS^-, P670, Sm^R, Sp^R, Km^R, this work
KZR9C4	bchA Ω(31.2::Tn5.7) rif-10	PS^-, P670, Sm^R, Sp^R, Km^R, this work
KZR3G7	bchA Ω(31.4::Tn5.7) rif-10	PS^-, P670, Sm^R, Sp^R, Km^R, this work
KZR8A1	crtE Ω(34.6::Tn5.7) rif-10	PS^+, blue-green, Sm^R, Sp^R, Km^R, this work

KZR9F4	crtIΩ(39.8::Tn5.7)rif-10	PS^+, blue-green, Sm^R, Sp^R, Km^R, this work
KZR9A12	crtAΩ(41.0::Tn5.7)rif-10	PS^+, yellow, Sm^R, Sp^R, Km^R, this work
KZR8D7	bchIΩ(41.6::Tn5.7)rif-10	PS^-, trace P590, Sm^R, Sp^R, Km^R, this work
KZRIA7	bchDΩ(43.1::Tn5.7)rif-10	PS^-, $Bchl^-$, Sm^R, Sp^R, Km^R, this work
KZR8E12	bchDΩ(43.2::Tn5.7)rif-10	PS^-, $Bchl^-$, Sm^R, Sp^R, Km^R, this work
KZR9D5	Ω(46.9::Tn5.7)rif-10	PS^+, Sm^R, Sp^R, Km^R, this work
KZR9C10	Ω(47.4::Tn5.7)rif-10	PS^+, Sm^R, Sp^R, Km^R, this work
KZR3A1	bchJΩ(49.2::Tn5.7)rif-10	PS^-, P750, P630, P580, P530, Sm^R, Sp^R, Km^R, this work
KZR3A1	bchJΩ(49.2::Tn5.7)rif-10	PS^-, P750, P630, P580, P530, Sm^R, Sp^R, Km^R, this work
KZR9A4	bchEΩ(51.0::Tn5.7)rif-10	PS^-, P620, P570, P538, Sm^R, Sp^R, Km^R, this work
KZR8F1	Ω(51.7::Tn5.7)rif-10	PS^+, Sm^R, Sp^R, Km^R, this work
KRZ9E3	crtKΩ(53.5A::Tn5.7)rif-10	PS^+, blue-green, Sm^R, Sp^R, Km^R, this work
KZR8D9	Ω(53.5B::Tn5.7)rif-10	$Bchl^-$, Sm^R, Sp^R, KmR, this work

KZR8G9	bchFΩ(55.1::Tn5.7)rif-10	PS^-, P630, P590, P570, P520, Sm^R, Sp^R, Km^R, this work
KZR9G5	bchKΩ(56.7::Tn5.7)rif-10	PS^-, $Bchl^-$, Sm^R, Sp^R Km^R, this work
KZR8H10	bchlΩ(58.0::Tn5.7)rif-10	$PS^{red}Bchl^{red}$, Sm^R, Sp^R, Km^S, this work
KZR9F2	bchHΩ(58.5::Tn5.7)rif-10	PS^-, P630, Sm^-, Sp^R, Km^R, this work
KZR8G12	bchHΩ(59.7::Tn5.7)rif-10	PS^-, $Bchl^-$, Sm^R, Sp^R, Km^R, this work
KZR8A9	bchLΩ(61.6::Tn5.7)rif-10	PS^-, P630, P590, P570, Sm^R, Sp^R, Km^R, this work
KZR8B1	F1696Ω(63.5::Tn5.7)rif-10	PS^+, LHI^{red}, Sm^R, Sp^R, Km^R, this work
KZR9F6	F1696Ω(63.6::Tn5.7)rif-10	PS^{red}, RC^{red}, LHI^{red}, Sm^R, Sp^R, Km^R, this work
KZR3A3	F1696Ω(64.4::Tn5.7)rif-10	PS^{red}, RC^{red}, LHI^{red}, Sm^R, Sp^R, Km^R, this work
KZRIA1	rxcDΩ(65.7::Tn5.7)rif-10	PS^-, RC^-, LHI^{red}, Sm^R, Sm^R, Km^S, this work
UAR#	Library of SB1003[pRPS404::Tn7]	Youvan et. al., 1982
SB1003	rif-10	Marrs, 1981
Y142	rxcA142 str-2	PS^-, RC^-, LHI^-, Sm^R, Marrs, 1982
BPY38	bchA538crtF129	PS^-, P670, Scolnik, 1980
MB1007	bchC1007	PS^-, P710, Taylor, 1983
BW604	crtE6	PS^+, blue-green,

		Yen & Marrs, 1983
BPY26	crtE526crtF129	PS^+, blue-green, B. Marrs
W4	crtB4	PS^+, blue-green, Yen and Marrs, 1976
BPY51	crtB551	PS^+, blue-green, B. Marrs
B301	crtA301rif-10	PS^+, yellow, Yen and Marrs, 1976
MB1008	bchD1008	PS^-, trace Bchl, Taylor et al., 1983
BPY61	bchD561crtF129	PS^-, trace Bchl, Scolnik, et al., 1980
BPY27	bchG527crtF129	PS^-, P760, Marrs, 1981
BRP4	bchE604crtF129hsd-1str-2	PS^-, P590, Sm^R, Taylor et al., 1983
MB1003	bchF1003	PS^-, P730, Taylor et al., 1983
BRP50	bchH650crtF129hsd-1str-2	PS^-, $Bchl^-$, Sm^R Taylor

II. Media and Cultivation

E. coli strains were grown on L medium or M9 (Mantiatis, et al., 1982). *R. capsulata* strains were grown on plates chemoheterotrophically on PYE medium or minimal RCV medium (Yen and Marrs, 1977), or in liquid in RCV supplemented with 50mM dimethyl sulfoxide, 0.6% (w/v) dextrose, and 0.5% (w/v) sodium pyruvate (Yen and Marrs, 1977). Photosynthetic growth defective (PS^-) mutants were screened by streaking replica PYE plates. One plate was incubated aerobically in the dark (permissive for (PS^-) and the duplicate plate was incubated under photosynthetic conditions, with both PS+/- controls, in an anaerobic jar (BBL GasPak) within a temperature controlled light-box ($3mW/cm^2$). Antibiotics were used at the following concentrations (μg/ml): kanamycin 15, streptomycin 10, spectinomycin 10, tetracycline 15.

III. Selection for Tn5.7 Insertions into pRPS404

In order to isolate insertions of Tn5.7 into pRPS404, the following scheme was used. Tn5.7 was inserted into the chromosome by transposition to phage lambda followed by lysogenization (J. P. Yin). This strain, Neco125($\lambda b5_{15}b_{519}C_{I857}nin_5S_7$::Tn5.7) was used as a recipient of pRPS404 in a mating event. Each of the transconjugants, KZ404 series, were handled separately from this point to ensure independent transposition events. The KZ404 strains were grown up to 10ml. Each of these was then mated with NECO100. Selection was for Km, Sp, and rifampicin. Repurification was on Km, Sp, and rifampicin.

IV. Conjugal Matings

pRPS404::Tn5.7 plasmids were congujated in spots on PYE agar plates between *E. coli* donors and *R. capsulata* recipients at 32°C. A 1:10 ratio of donor:recipient was used, the donors being in mid-log phase. The spots were incubated overnight. For the KZR library construction, the transconjugants were selected on RCV containing Sm (5 day incubations). After two repurifications on this media, repurification continued on PYE containing Sp (3 day incubations). Most KZR strains went through about ten repurifications on this media to ensure that phenotypic analysis was not performed on merodiploids. For complementation analysis of *R. capsulata* point mutants and transposon generated mutants by pRPS404::Tn5.7 plasmids, transconjugant selection was on RCV containing 10µg/ml kanamycin. For conjugation of pLAFR1 into KZR strains, triparental matings were performed with pRK2013, pLAFR1, and KZR recipients as described above for pRPS404 transfers. Selection of transconjugants was performed on RCV containing Tet. The efficiency of transfer was variable from 0- 10^{-5}. After two repurifications on RCV 10ug/ml tetracycline, and an additional repurification on PYE Tet, all strains which received pLAFR1 became Km^S.

V. Complementation Analysis

R. capsulata mutants were tested for complementation by various pRPS404::Tn5.7 plasmids by performing conjugations as described above. Complementation of blue-green mutants was tested simply by observation of colony pigmentation of transconjugants. For $Bchl^-$ mutants, a colony

from each merodiploid strain was resuspended in liquid RCV media and serially diluted to 10^{-7}, then spotted on replica RCV plates containing 10µg/ml Km. One set was incubated aerobically in the dark and one set was grown photosynthetically. A positive complementation resulted in a difference of 10^1 to 10^2 colonies between the PS^+ plate and the PS^- plate. A negative complementation resulted in a difference between 10^4 to 10^6 colonies between the two plates. The bchA mutations were difficult to complement by any pRPS404::Tn5.7 plasmids, i.e., there was no clear designation between positive or negative complementation and therefore they are not included in the results.

VI. Nucleic Acid Isolation and Analysis

Plasmid DNA was isolated essentially as described (Birnboim and Doly, 1979). Total DNA was isolated as described (Marmur, 1961) but with an isopropanol precipitation included. DNA samples were digested with restriction enzymes according to Bethesda Research Laboratories. Agarose gels, 0.7%, transfer of DNA to nitrocellulose, Nick-translation of pRPS404, and hybridization was performed as described (Maniatis et al, 1975). End labelling using reverse transcriptase was done according to Bethesda Research Lab.

VII. Absorption Spectroscopy and SDS-PAGE

Chromatophores were isolated as described (Youvan et al, 1983). Absorption spectroscopy was performed on a cleared cell lysate on a Varian 2300 spectrophotometer. Bacteriochlorophyll precursor absorption

maxima were determined in methanol extracts of whole cell pellets 1ml CH_3OH/g cells. SDS-PAGE performed on twice washed chromatophores as described (Youvan et al, 1983). Staining for heme containing polypeptides was performed as described (Hoyer-Hansen, 1980).

VIII. DNA Homology Searches

Searches for DNA homology between R. capsulata and R. spheroides were done using a high speed homology matrix program (Pustell and Kafatos, 1982).

REFERENCES

Auserwald, E. A., Ludwig, G., Schaller, H. (1980). In "Cold Spring Harbor Symposium on Quantative Biology". 45, 107-113.

Beatty, T. J. and Gest. H. (1981). Biosynthetic and bioenergetic functions of citric acid cycle reactions of R. capsulata. J. Bacteriol. 148, 584-593.

Barth, P. T., Grinter, N. J., Bradley, D. E. (1978). Conjugal transfer system of RP4: Analysis by Tn7 insertions. J. Bacteriol. 133, 43-52.

Biel, A., and Marrs, B. L. (1983). Transcriptional regulation of several genes for bacteriochlorophyll biosynthesis in Rhodopseudomonas capsulata in response to oxygen. J. Bacteriol. 156, 686-694.

Birnboim, H. C., and Doly, J. (1979). A rapid alkaline extraction procedure for screening recombinant plasmid DNA. Nucl. Acids Res. 7, 1513-1523.

Bose, H. and Gest, H. (1962). Electron transport systems of purple bacteria. Nature. 195, 1168-1171.

Broglie, R. M., Hunter, N., Delepelaire, P., Niederman, R. A., Chua, N. H., Clayton, R. K. (1980). Isolation and characterization of the pigment protein complexes of R. spheroides by lithium dodecyl sulfate PAGE. Proc. Natl. Acad. Sci. 77, 87-91.

Buchanan, B. B., and Evans, M. C. W. (1969). Photoreduction of ferredoxin and its use in $NAD(P)^+$ reduction by a subcellular preparation from the photosynthetic bacterium Chlorobium thiosulfatophilum. Biochim. Biophys. Acta. 180, 123-129.

Burton, G., Jordon, P. M., Mackenzie, N. E., Fagerness, P. E., Scott, A. I. (1981). Control of porphyrin biosynthesis in R. spheroides and

Propionibacterium shermanii. Biochem. J. *194*, 627-631.

Chance, B. C., Hollunger, G. (1960). Energy linked reduction of mitochondrial pyridine nucleotides. Nature. *185*, 666-672.

Chen, J. Miller, G. W., Takemoto, J. Y. (1981). Biosynthesis of ALA in *R. spheroides*. Arch. Biochem. Biophys. *208*, 221-228.

Clark, G., Taylor, D. P., Cohen, S. N., Marrs, B. L. (1981). 81st Annual Meeting of the American Society of Microbiologists. Abstract #H50.

Clement-Metral, J. D. (1981). Control of *R. spheroides* Y ALA-synthetase by reduced thioredoxin. In "Photosynthesis V", G. Akoyunoglou ed. Balaban Int. Science Serv., Philadelphia, PA. 695-700.

Cogdell, R., and Crofts, A. (1978). Analysis of the pigment content of an antenna pigment-protein complex from *R. spheroides.* Biochim. Biophys. Acta. *502*, 409-416.

Cogdell, R., Parson, W. W., Kerr, M. A. (1976). The type, amount, location, and energy tranfer properties of the carotenoid in the reaction center from *R. spheroides*. Biochim. Biophys. Acta. *430*, 83-93.

Cox, J. C., Madigan, M. T., Favinger, J. L., Guest, H. (1980). Redox mechanisms in "oxidant-dependent" hexose fermentation by *R. capsulata*. Arch. Biochem. Biophys. *204*, 10-17.

Cogdell, R. J. and Crofts, A. R. (1978). Analysis of the pigment content of an antenna pigment-protein complex from three strains of *R. spheroides*. Biochim. Biophys. Acta. 502, 409-416.

Cramer, W. A., Crofts, A. R. (1982). In "Photosynthesis I: Energy Conversion by Plants and Bacteria", Govindjee, ed. Academic Press, San Francisco. 427-433.

Currier, T. C., and Morgan, M. K. (1982). Direct DNA Repeat in plasmid

R68.45 is associated with deletion formation and concomitant loss of chromosome mobilizing ability. J. Bacteriol. 150, 251-259.

Dailey, H. A. (1982). Purification and characterization of membrane bound ferrochelatase from R. spheroides. J. Biol. Chem. 257, 14714-14718.

DePicker, A., Van Montagu, M., Schell, J. (1979). In "DNA Insertion Elements, Plasmids, and Episomes", Cold Spring Harbor Laboratory, Cold Spring Harbor, New York. 678-679.

Dickerson, R. E. (1980). Cytochrome c and the evolution of energy metabolism. Sci. Amer. 242, 137-153.

Ditta, G., Stanfield, S., Corbin, D., Helenski, D. R. (1980). Broad host range DNA cloning system for gram-negative bacteria: Construction of a gene bank of Rhizobium meliloti. Proc. Natl. Acad. Sci. 77, 7347-7351.

Feher, G. and Okamura, M. Y. (1978). In" The Photosynthetic Bacteria" Clayton, R. K. and Sistrom, W. R., ed. Plenum Press, NY. 349-382.

Feick, R. G., and Drews, G. (1978). Isolation and characterization of light harvesting bacteriochlorophyll-protein complexes from R. capsulata. Biochim. Biophys. Acta. 501, 499-512.

Feick, R., and Drews, G. (1979). Ztschr. Naturforsch. 34c, 196-198.

Folkers, K., Shunk, C. H., Linn, B. O., Robinson, F. M., Skeggs, H. R. (1959). Biosynthesis of terpenes and sterols. CIBA Found. Symp. p.118.

Fox, G. E. (1980). The phylogeny of prokaryotes. Science. 209, 457-463.

Friedman, A. M., Long, S. R., Brown, S. E., Buikema, W. J., and Ausubel, F. M. (1982). Construction of a broad host range cosmid cloning vector and its use in the genetic analysis of Rhizobium meliloti.

Gene. 18, 289-296.

Haas, D., Reiss, G. (1983). Spontaneous deletions of the chromosome-mobilizing plasmid R68.45 in Pseudomonas aeruginosa PAO. Plasmid. 9, 42-52.

Hallenbeck, P. C., Jouanneau, Y., Vignais, P. M. (1982). Purification and molecular properties of a soluble ferredoxin from R. capsulata. Biochim. Biophys. Acta. 681, 168-176.

Hawley. D. K., and McClure,, N. K. (1983). Compilation and analysis of E. coli promoter DNA sequences. Nucl. Acid Res. 11, 2237-2250.

Hearst, J. E., and Sauer, K. Protein homologies between portions of the L and M subunits of reaction centers of R. capsulata and the Q_B-protein of chloroplast thylakoid membranes: A proposed relation to quinone binding sites. Zeifschrift für Naturforschung. In press.

Hedges, R. N., Cresswell, J. M., Jacob, A. E. (1976). A non-transmissible variant of RP4 suitable as a cloning vehicle for genetic engineering. FEBS Lett. 61, 186-188.

Hollaway, B. W. (1979). Plasmids that mobilize the bacterial chromosome. Plasmid. 2, 1-19.

Horio, T., Yamashita, J. (1963). Biochim. Biophys. Acta. 37-43.

Hoyer-Hansen, G. (1980). Identification of Haem-proteins in thylakoid polypeptide patterns of barley. Carlsberg Res. Commun. 45, 167-176.

Jacobs, N. J., Jacobs, J. M. (1981). Protophorinogen oxidation in R. spheroides, a step in heme and bacteriochlorophyll biosynthesis. Arch. Biochem. Biophys. 211, 305-311.

Jensen, A., Aasmundrud, O., Eimhjellen, K. E. (1964). Chlorophylls of photosynthetic bacteria. Biochim. Biophys. Acta. 88, 466-479.

Johansson, B. C., and Gest, H. (1976). Inorganic nitrogen assimilation by the photosynthetic bacterium R. capsulata. J. Bacteriol. 128, 683-688.

Jones, O. T. G., and Sanders, V. A. (1972). Energy linked electron transfer reactions in R. viridis. Biochim Biophys. Acta. 275, 427-436.

Kaplan, S., and Arntzen, C. J. (1982). In "Photosynthesis I: Energy Conversion by Plants and Bacteria", ibid. Chapter 3.

Klein, O., Porra, R. J. (1982). Z. Physiol. Chem. 363, 551-562.

Klemme, J. H., Schlegel, H. G. (1967). Photoreduktion von pyridinnucleotide durch chromophoren aus R. capsulata mit molekularen. Arch. Mikrobiol. 59, 185-196.

Krinsky, N. I. (1978). Philos. Trans. Roy. Soc. Lond. Ser. B. Biol. Sci. 284, 581-590.

Lascelles, J. (1978). In "The Photosynthetic Bacteria", ibid 795-808.

Lehninger, A. L. 1978. "Biochemistry", Worth Publishers. p. 446.

Lichtenstein, C. and Brenner, S. (1981). Site specific properties of Tn7 Transposition in the E. coli chromosome. Mol. Gen. Genet. 183, 380-387.

Lien, S., Gest, H. and San Pietro, A. (1973). Regulation of Chlorophyll synthesis in photosynthetic bacteria. J. Bioenerget. 4, 423-434.

Lundquist, R. C., Close, T. J., Kado, C. I. (1984) Genetic complementation of Agrobacterium tumefaciens Ti plasmid mutants in the virulence region. Mol. Gen. Genet. 193, 1-7.

Madigan, M. T., Cox, J. C., Gest, H. (1980). Physiology of dark fermentative growth of R. capsulata. J. Bacteriol. 142, 908-915.

Madigan, M. T. and Gest, H. (1978). Growth of a photosynthetic

bacterium anaerobically in darkness, supported by "oxidant-dependent" sugar fermentation. Arch. Micribiol. 117, 119-122.

Madigan, M. T., and Gest, H. (1979). Growth of the photosynthetic bacteria R. capsulata chemoautotrophically in darkness with H_2 as the energy source. J. Bacteriol. 137, 524-530.

Mantiatis, T., Frisch, E. F., Sambrook, J. (1982). In "Molecular Cloning". Cold Spring Harbor Laboratory, NY.

Mantiatis, T., Jeffery, A., and Kleid, D. G. (1975). Nucleotide sequence of the rightward operator of Phage λ Proc. Natl. Acad. Sci. 72, 1184-1188.

Marmur, J. (1961). A procedure for isolating DNA from micro-organisms. J. Mol Biol. 3, 208-218.

Marrs, B. (1974). Genetic recombination in R. capsulata. Proc. Natl. Acad. Sci. 71, 971-973.

Marrs, B. (1981). Mobilization of the genes for photosynthesis from Rhodopseudomonas capsulata by a promiscuous plasmid. J. Bacteriol. 146, 1003-1012.

Marrs, B. (1982) Genetics and molecular biology in "The Anoxygenic Phototrophic Bacteria". J. Omerod ed. Blackwell Scientific Publication, Oxford.

Nelsen, A. M., and Sojka, G. A. (1979). Photoheterotrophic utilization of acetate by wild type and an acetate-adapted mutant of R. capsulata. Arch. Microbiol. 120, 39-42.

Neith, K. F., Drews, G., Feick, R. G.(1975). Arch. Microbiol. 105, 43-45.

Neuberger, A., Turner, J. M. (1963). Biochim. Biophys. Acta. 67,

342-345.

Okamura, M. Y., Feher, G., and Nelson, N. (1982). In," Photosynthesis I: Energy Conversion by Plants and Bacteria", ibid. Chapter 5.

Omerod, J. G., and Gest, H. (1962). Symposia on metabolism of inorganic compounds. IV. Hydrogen photosynthesis and alternative metabolic pathways in photosynthetic bacteria. Bacteriol. Rev. 26, 51-66.

Pandian, S., Saengchjan, S., Raman, T. S. (1981). An alternative pathway for the biosynthesis of isoprenoid compounds in photosynthetic bacteria. Biochem. J. 196, 675-681.

Pustell, J., and Kafatos, F. C. (1982). A high speed, high capacity homology matrix: zooming through SV40 and polyoma. Nucl. Acid Res. 10, 4765-4782.

Rebeiz, C. A., and Lascelles, J. (1982). In "Photosynthesis I: Energy Conversion by Plants and Bacteria", ibid. Chapter 15.

Reznikoff, W. S. (1982). Tn5 transposition and its regulation. Cell. 31, 307-308.

Rothstein, S. J., Jorgensen, R. A., Yin, J. C. P., Yong-DI, Johnson, R. C., Reznikoff, W. S. (1980). In "Cold Spring Harbor Symposia on Quantitative Biology" Vol. 45

Ruvkun, G. B., Sundaresan, V., Ausubel, F. M. (1982). Directed Tn5 mutagenesis and complementation analysis of R. meliloti symbiotic nitrogen fixation genes. Cell. 29, 551-559.

Ruvkun, G. B., and Ausubel, F. M. (1981). A general method for site-directed mutagenesis in prokaryotes. Nature. 289, 85-89.

Schmidt, K. (1978). In "The Photosynthetic Bacteria", ibid. Chapter 39.

Schultz, J. E., and Weaver, P. F. (1982). Fermentation and anaerobic

respiration by Rhodospirillum rubrum and Rhodopseudomonas capsulata. J. Bacteriol. 149, 181-190.

Scolnik, P. A., Walker, M. A., Marrs, B. L. (1980). Biosynthesis of carotenoids derived from neurosporene in R. capsulata. J. Biol. Chem. 255, 2427-2432.

Seehra, J. S., Jordan, P. M., Akhtar, M. (1983). Anaerobic and aerobic coproporphyrinogen III oxidases of R. spheroides. Biochem. J. 209, 709-718.

Shaw, D. J., Rice, D. W., and Guest, J. R. (1983). Homology between CAP and Fnr, a regulator of anaerobic respiration in Escheria coli. J. Mol. Biol. 166, 241-247.

Slovin, J. P., and Tobin, E. M. (1982). Synthesis and turnover of the light harvesting chl a/b protein in Lemna gibba grown with intermittent red light: possible translational control. Planta. 154, 465-472.

Smith, L., and Pinder, E. (1978). In "The Photosynthetic Bacteria", ibid. Chapter 33.

Smith, S. E., and Summers, M. D. (1980). Anal. Biochem. 109, 123-129.

Taylor, D. P., Cohen, S. N., Clark, W. G., and Marrs, B. M. (1983) Alignment of genetic and restriction maps of the photosynthesis region of the Rhodopseudomonas capsulata chromosome by a conjugation-mediated marker rescue technique. J. Bacteriol. 154, 580-590.

Weaver, P. F., Wall, J. D., Gest, H. (1975). Characterization of R. capsulata. Arch. Microbiol. 105, 207-216.

Webster, G., Cogdell, R., Lindsay, J. (1980) FEBS Lett. 111, 391-394.

Willetts, N. S., Crowther, C., Holloway, B. W. (1981). The insertion

sequence IS21 of R68.45 and the molecular basis for mobilization of the bacterial chromosome. Plasmid. 6, 30-52.

Williams, J. C., Steiner, L. A., Ogden, R. C., Simon, M. L., and Feher, G. (1983). Primary structure of the M subunit of the reaction center from Rhodopseudomonas spheroides. Proc. Natl. Acad. Sci. 80, 6505-6509.

Wilson, D. F., Dutton, P. L., Erecinska, M. (1974). Ann. Rev. Biophys. Bioenerg. 3, 203-230.

Wood, P. M. (1981). The redox potential for dimethyl sulphoxide reduction to dimethyl sulphide. FEBS Lett. 124, 11-14.

Yakunin, A. F., Gogotov, I. N. (1983). Properties and regulation of synthesis of two ferredoxins from R. capsulata. 725, 298-308.

Yen, H.-C. and B. Marrs. (1976). Map of genes for carotenoid and bacteriochlorophyll biosynthesis in Rhodopseudomonas capsulata. J. Bacteriol. 126, 619-629.

Yen, H.-C. and B. Marrs. (1977). Growth of Rhodopseudomonas capsulata under anaerobic dark conditions with dimethylsulfoxide. Arch. Biochem. Biophys. 181, 411-418.

Youvan, D. C., Elder, J. T., Sandlin, D.E., Zsebo, K.M., Alder, D. P., Panopoulos, N. J., Marrs, B. L., and Hearst, J. E. (1982). R-prime site- directed transposon mutagenesis of the photosynthetic apparatus in Rhodopseudomonas capsulata. J. Mol. Biol. 162, 17-41.

Youvan, D. C., Hearst, J. E., and Marrs, B. L. (1983). Isolation and characterization of enhanced fluorescence mutants of Rhodopseudomonas capsulata. J. Bacteriol. 154, 748-755.

Youvan, D. C., Bylina, E., Alberti, M., Begusch, H., and Hearst, J. E. Sequence of the reaction center genes from Rhodopseudomonas

capsulata. Submitted, Cell.

Zannoni, D., Baccarini-Melandri, C., Melandri, B. A., Evans, E. H., Prince, R. C., Crofts, A. R. (1974). Energy transduction in photosynthetic bacteria: the nature of cyt c oxidase in the respiratory chain of R. capsulata. FEBS Lett. 48, 152-155.

Zannoni, D., and Marrs, B. L. (1981). Redox chain and energy transduction in R. capsulata cells grown anaerobically in the dark and DMSO. Biochim. Biophys. Acta. 637, 96-106.

Zannoni, D., Jasper, P., Marrs, B. (1978). Arch. Biochem. Biophys. 191, 625-631.

Zsebo, K. M., Wu, F., and Hearst, J. E. Physical mapping and Tn5.7 mutagenesis of pRPS404 containing photosynthesis genes from Rhodopseudomonas capsulata. Plasmid, in press.

Appendix: Absorption Spectra of R. capsulata generated mutants

The following spectra were recorded from either chromatophore fractions or methanol extracts of a 10ml culture cell pellet. All strains were grown in RCV^{+} according to Materials and Methods.

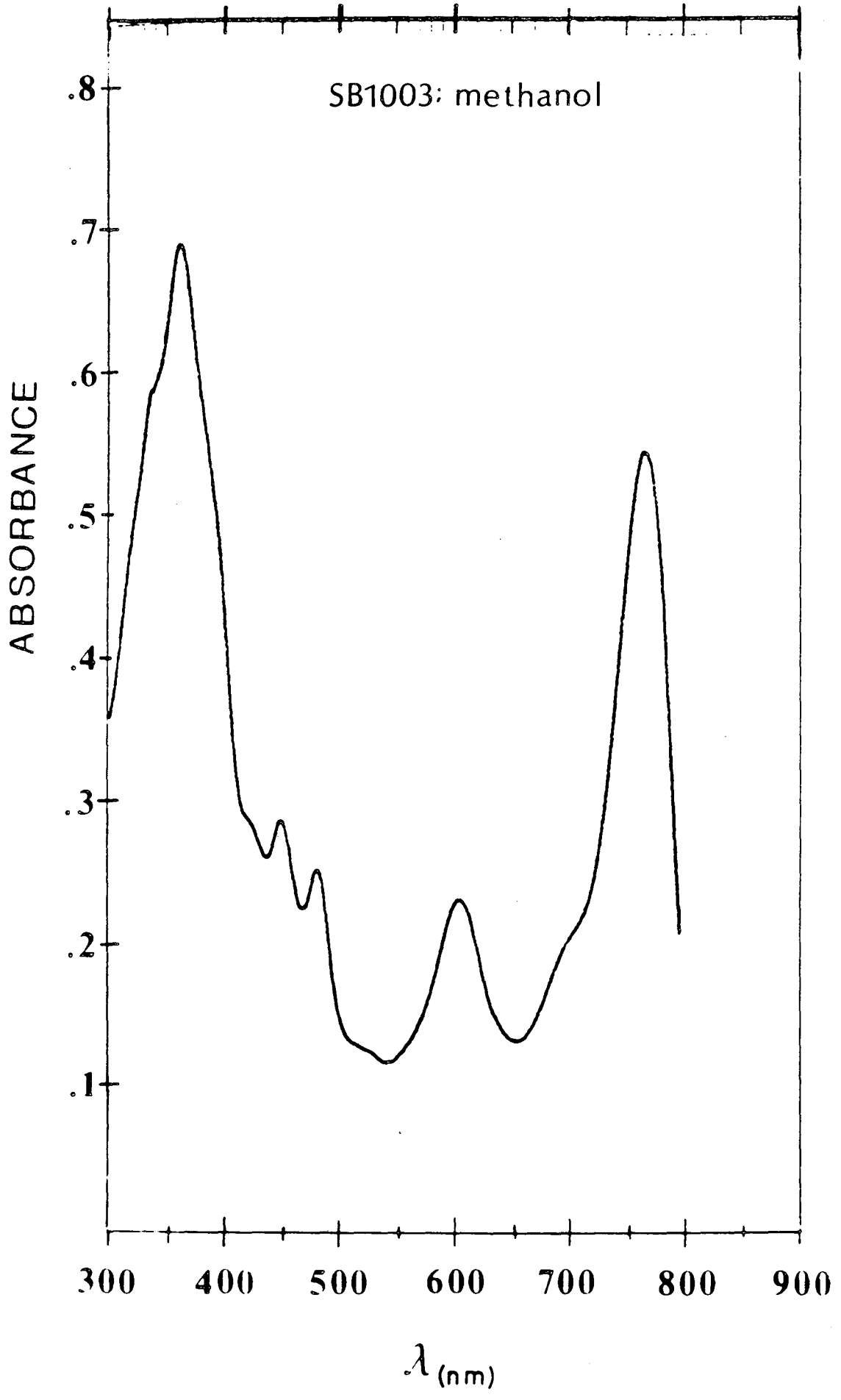
SB1003: methanol
ABSORBANCE
.8
.7
.6
.5
.4
.3
.2
.1
300
400
500
600
700
800
900
λ (nm)

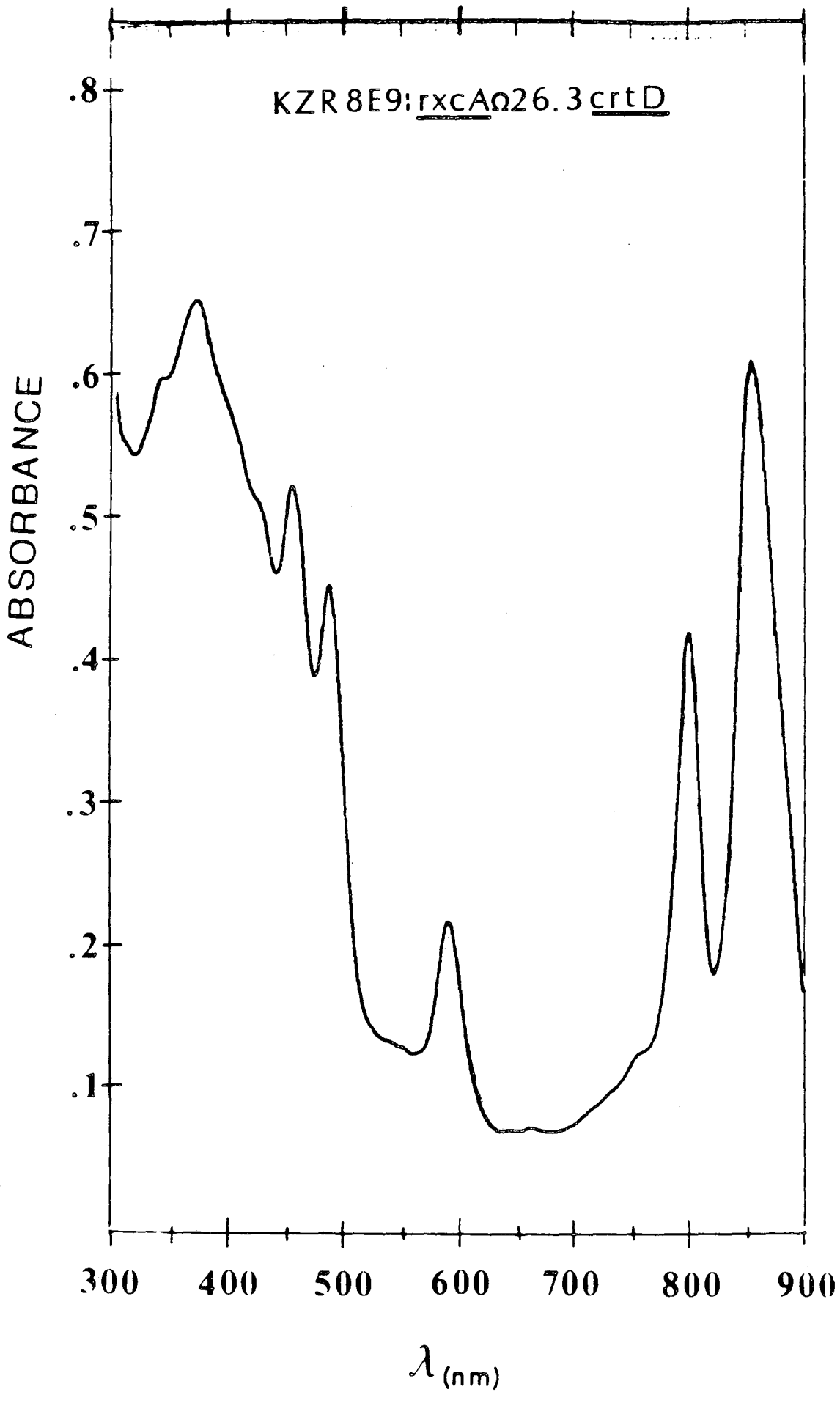
KZR8E9:rxcAΩ26.3crtD
ABSORBANCE
.8
.7
.6
.5
.4
.3
.2
.1
300
400
500
600
700
800
900
λ (nm)

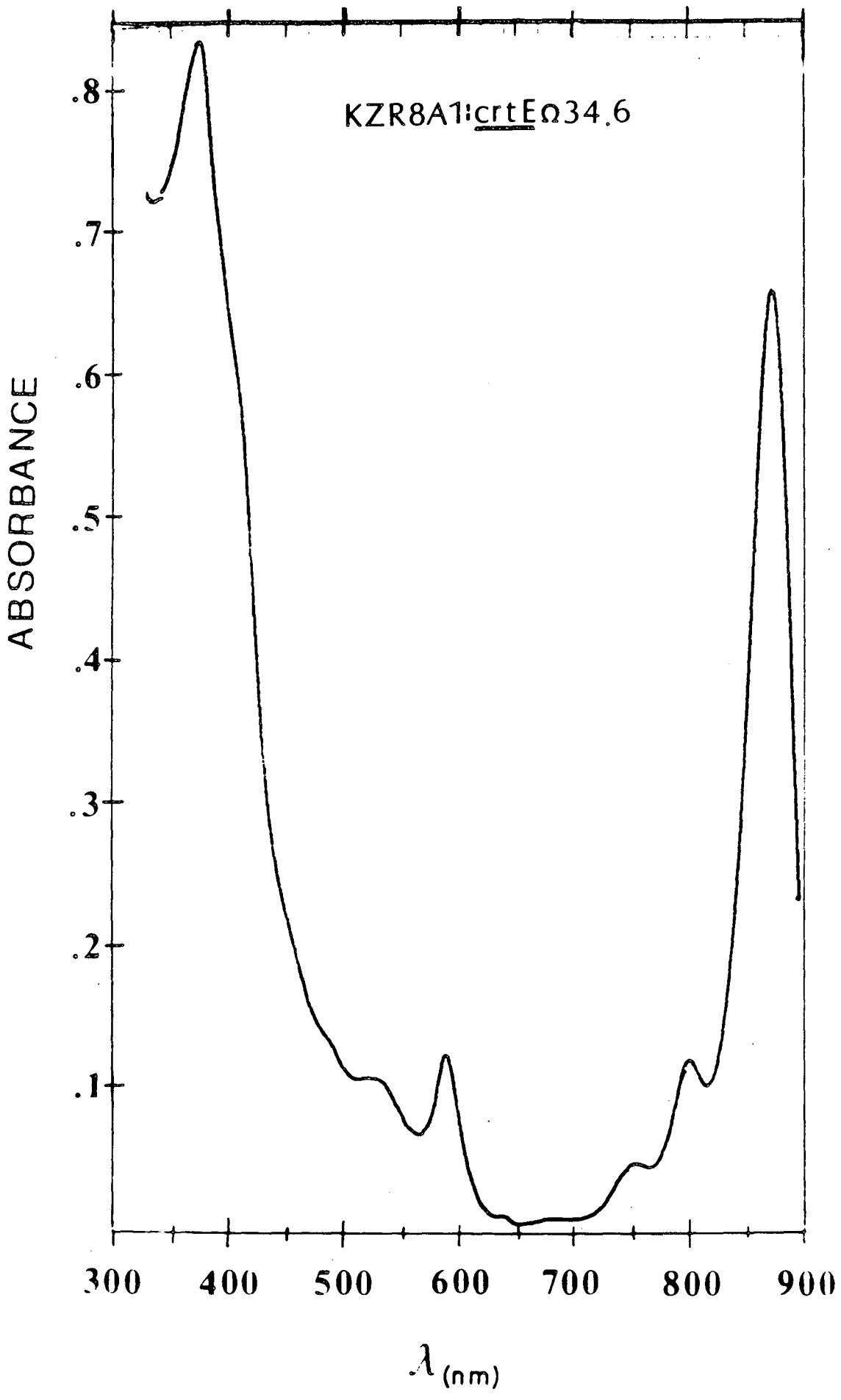
KZR8A1:crtEΩ34.6
ABSORBANCE
.8
.7
.6
.5
.4
.3
.2
.1
300
400
500
600
700
800
900
λ (nm)

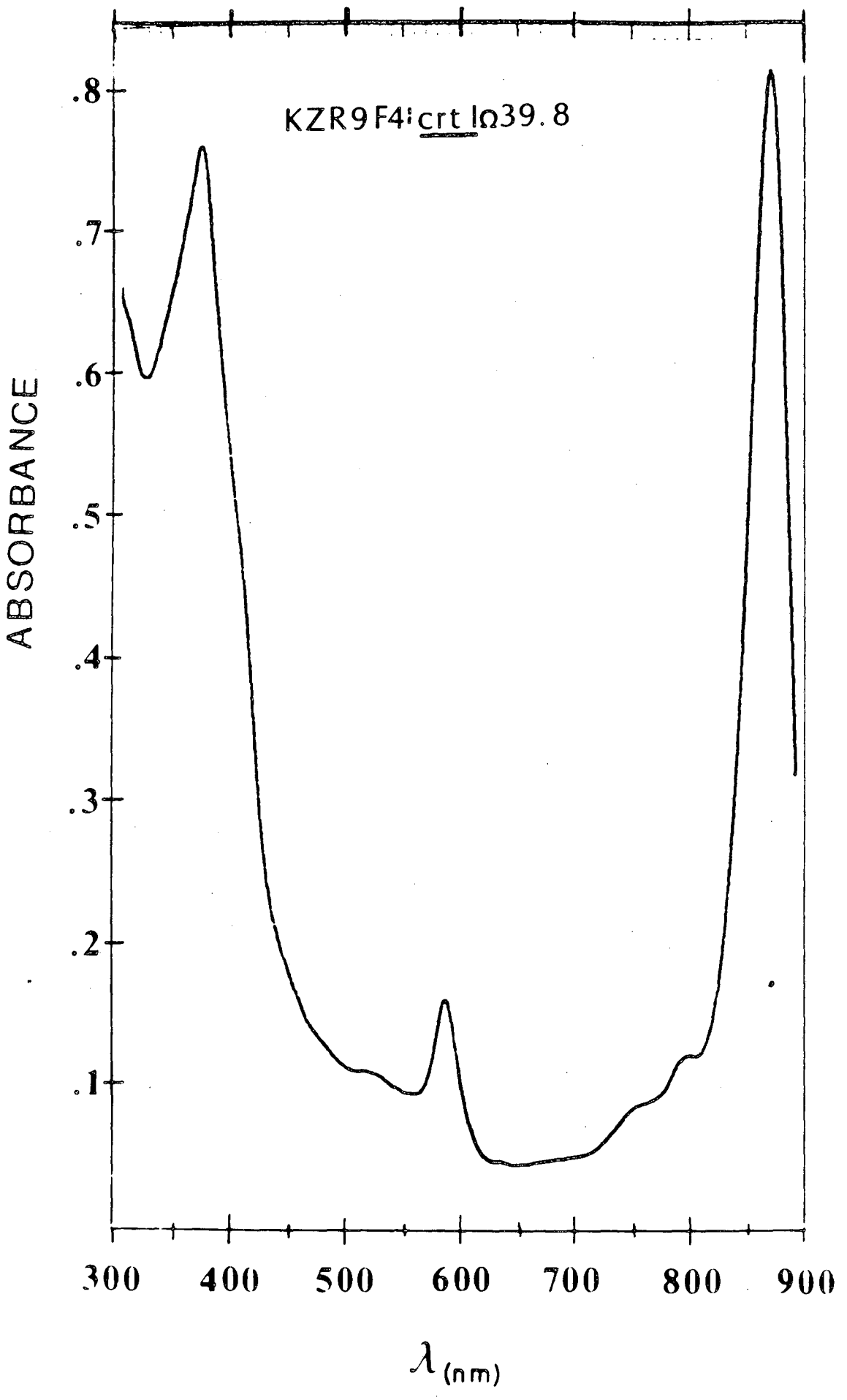
KZR9F4icrt lΩ39.8
ABSORBANCE
.8
.7
.6
.5
.4
.3
.2
.1
300
400
500
600
700
800
900
λ (nm)

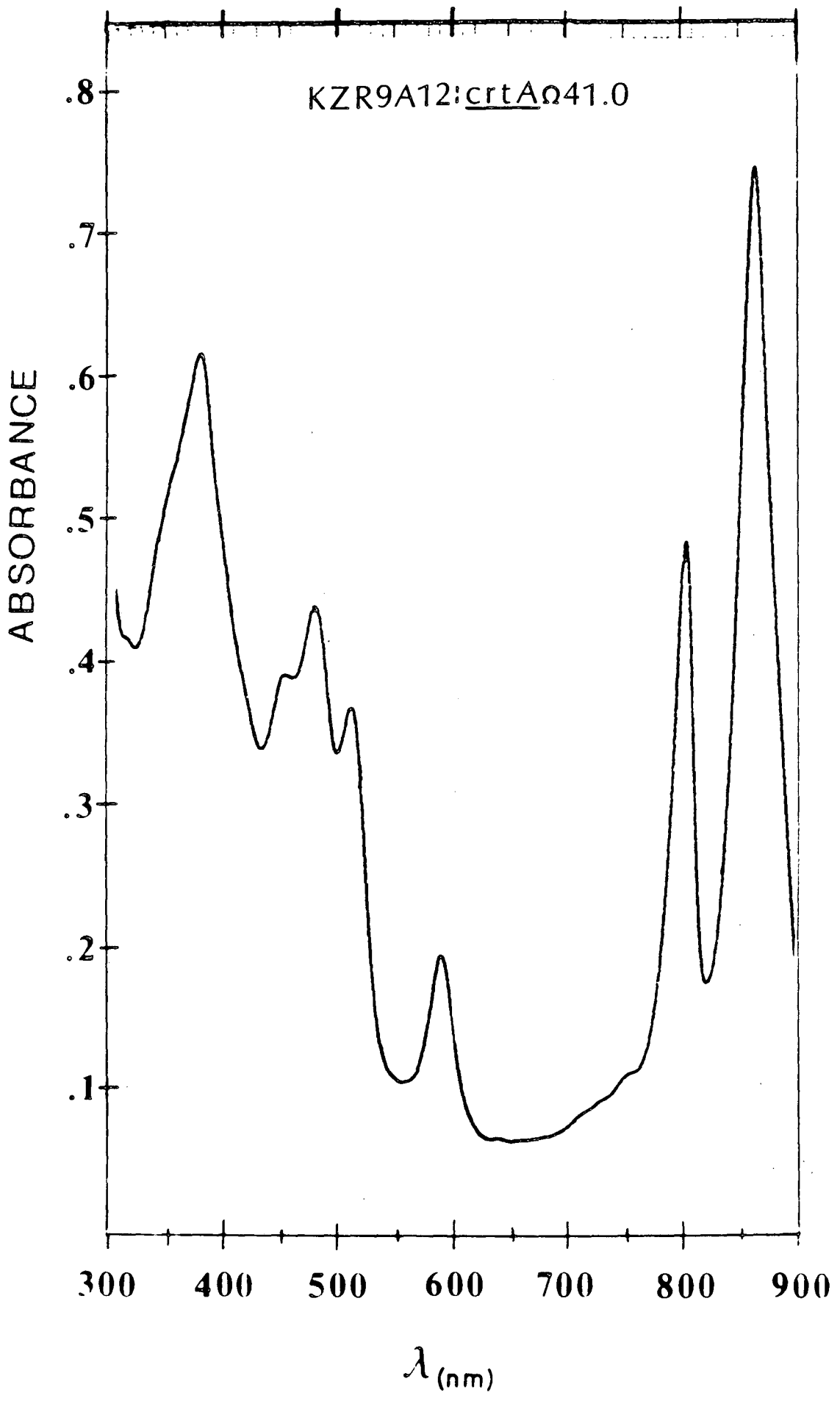
KZR9A12:crtAΩ41.0
ABSORBANCE
.8
.7
.6
.5
.4
.3
.2
.1
300
400
500
600
700
800
900
λ (nm)

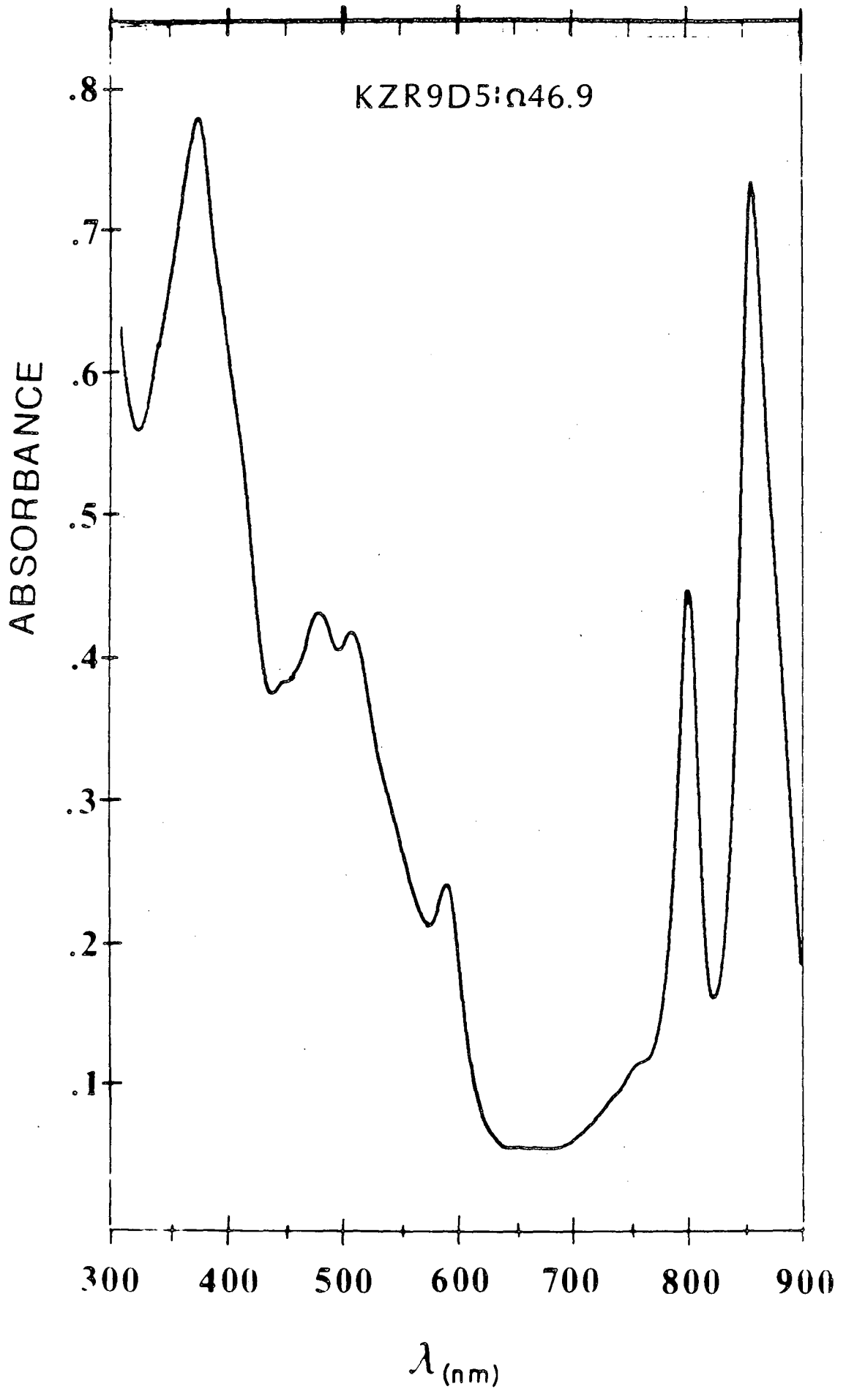
KZR9D5:Ω46.9
ABSORBANCE
.8
.7
.6
.5
.4
.3
.2
.1
300
400
500
600
700
800
900
λ (nm)

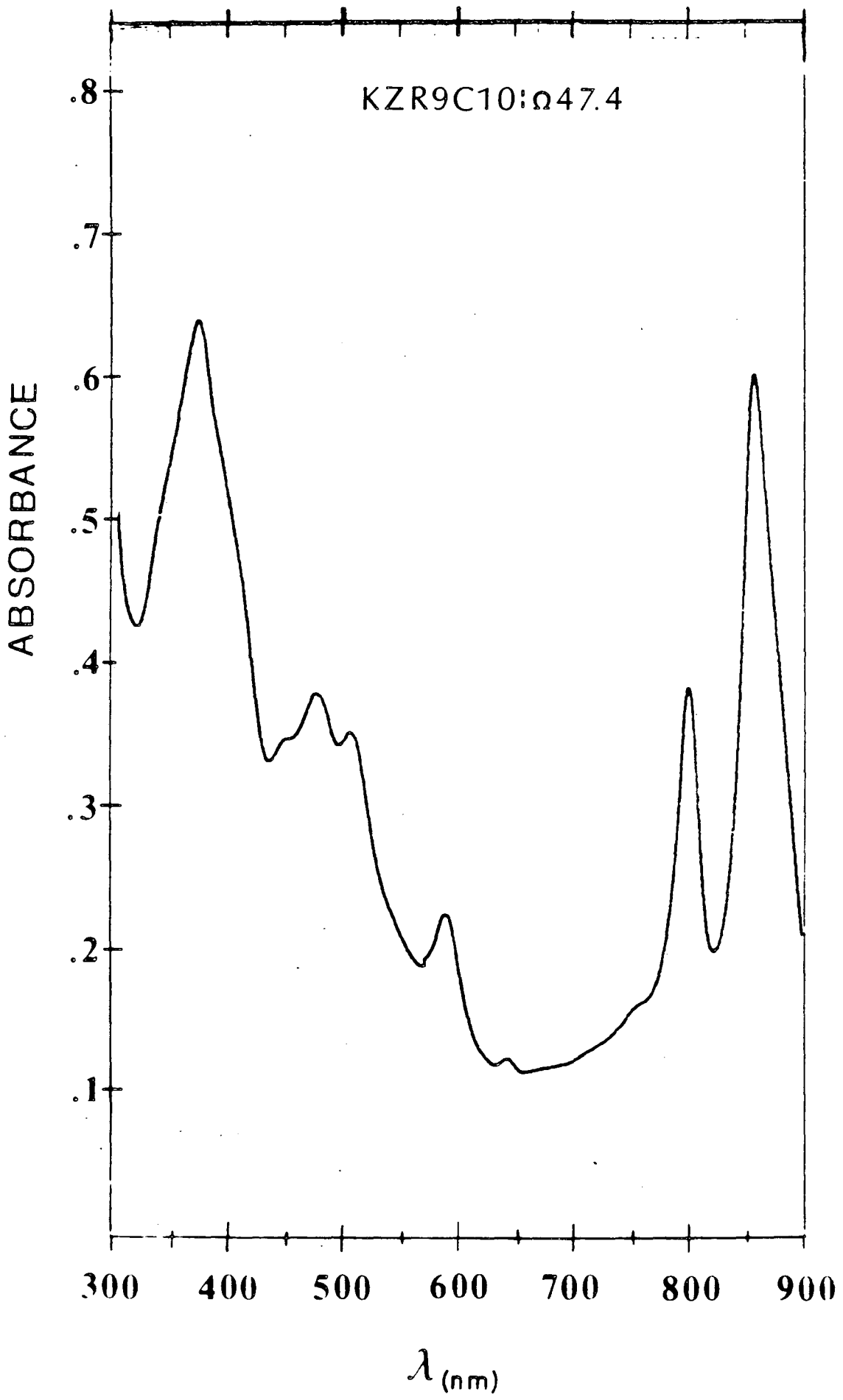
KZR9C10:Ω47.4
ABSORBANCE
.8
.7
.6
.5
.4
.3
.2
.1
300
400
500
600
700
800
900
λ (nm)

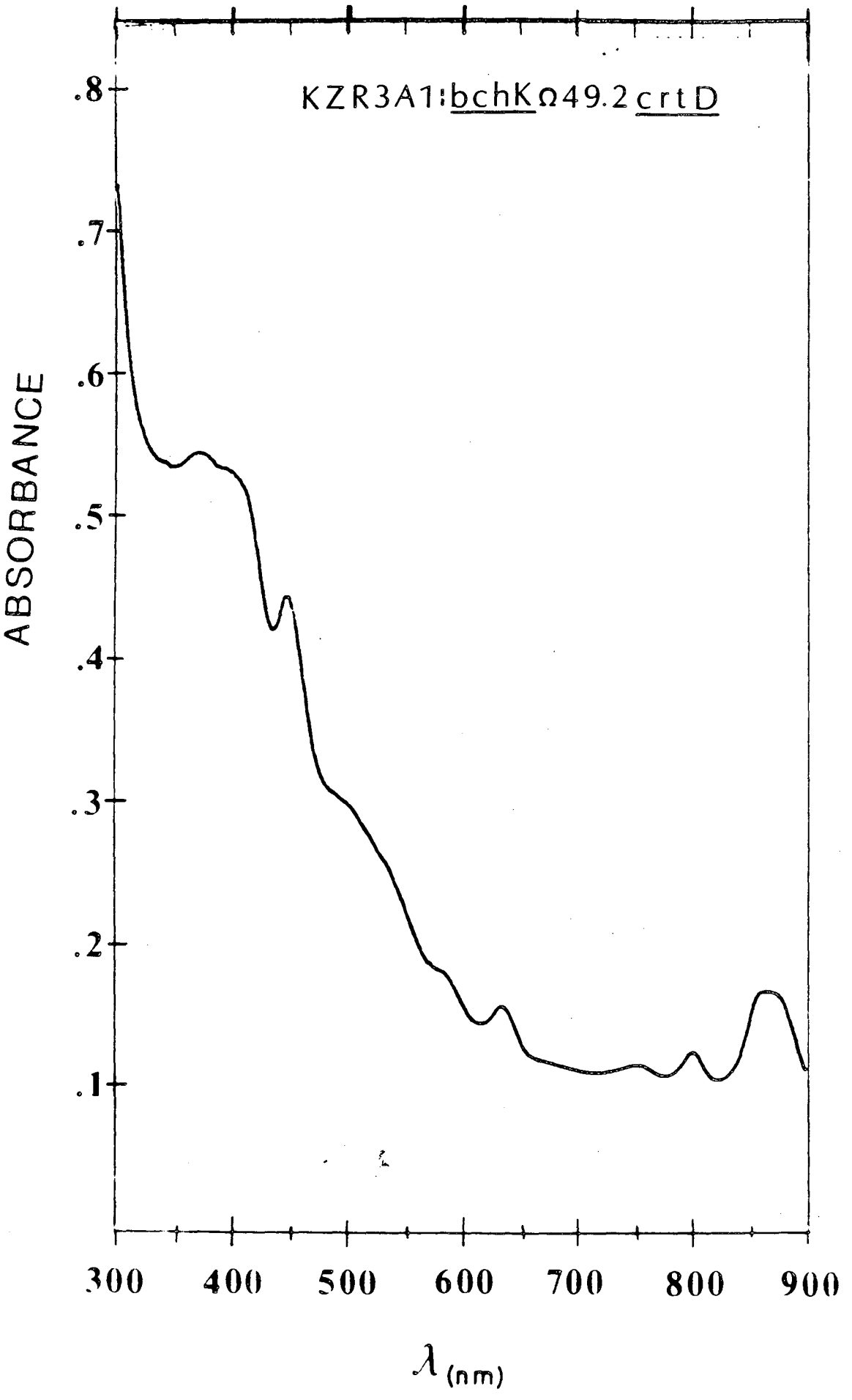
KZR3A1:bchKΩ49.2crtD
ABSORBANCE
.8
.7
.6
.5
.4
.3
.2
.1
300
400
500
600
700
800
900
λ (nm)

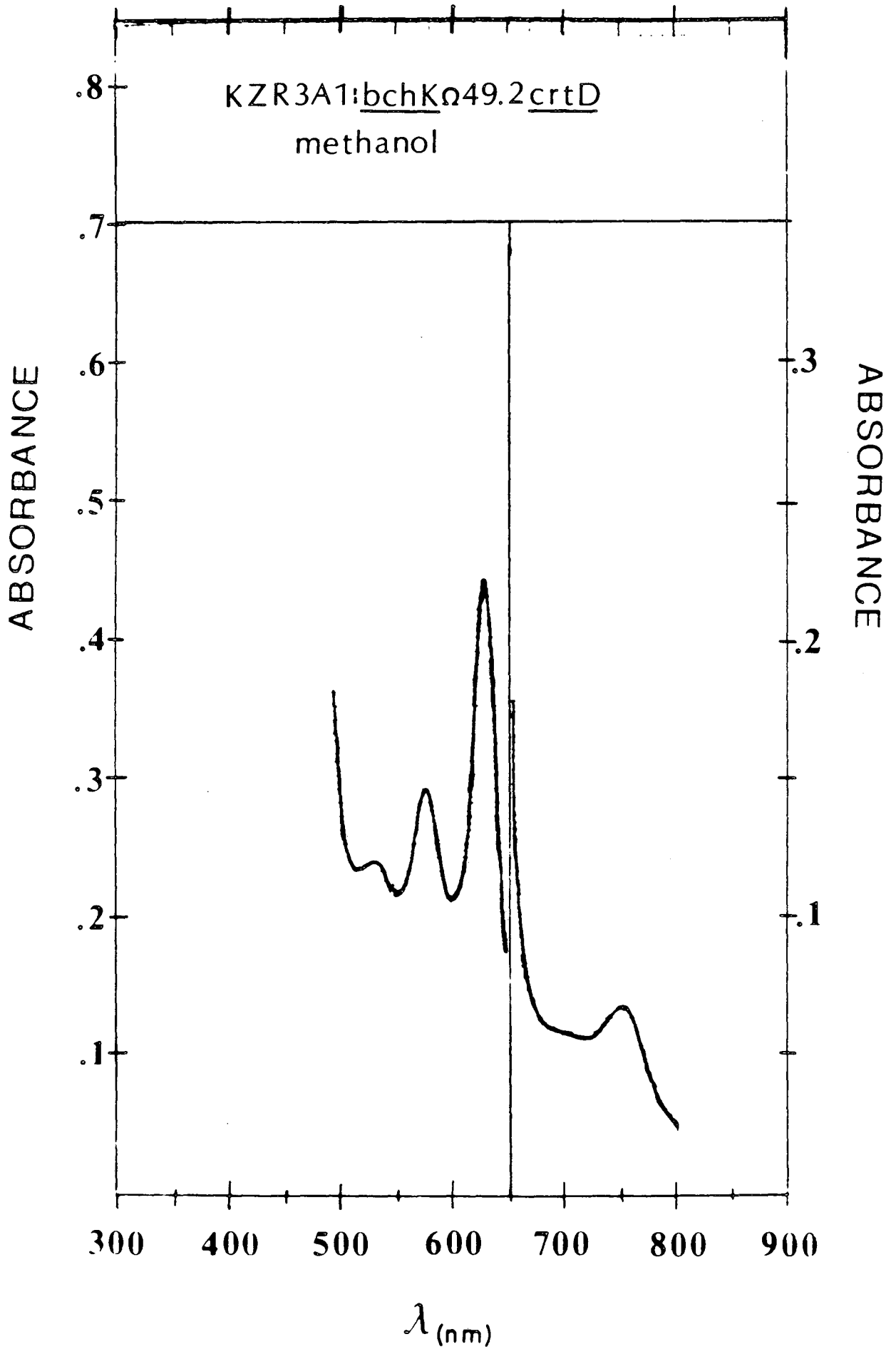
KZR3A1:bchKΩ49.2crtD
methanol
ABSORBANCE
ABSORBANCE
.8
.7
.6
.5
.4
.3
.2
.1
.3
.2
.1
300
400
500
600
700
800
900
λ (nm)

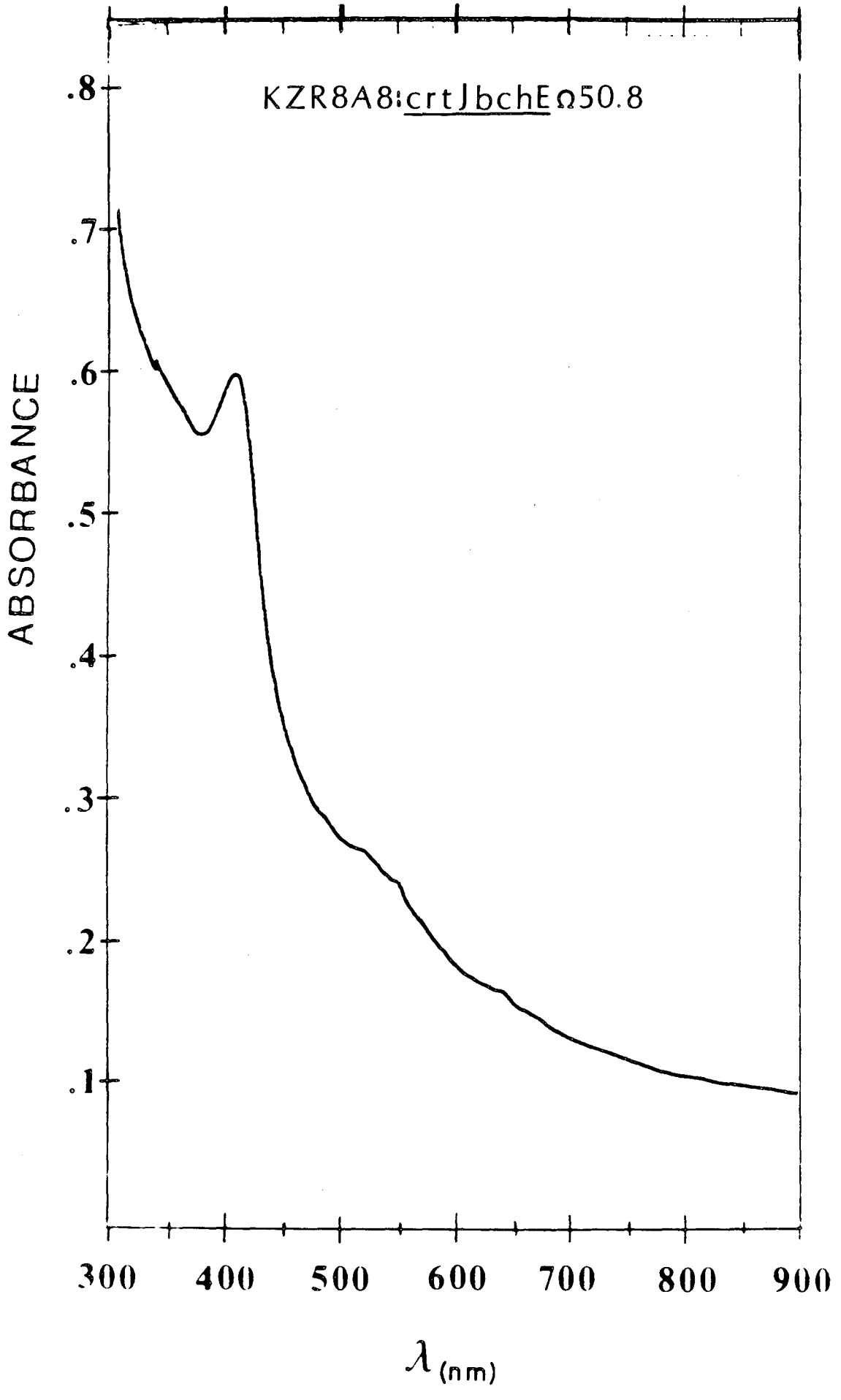
KZR8A8:crtJbchEΩ50.8
ABSORBANCE
.8
.7
.6
.5
.4
.3
.2
.1
300
400
500
600
700
800
900
λ (nm)

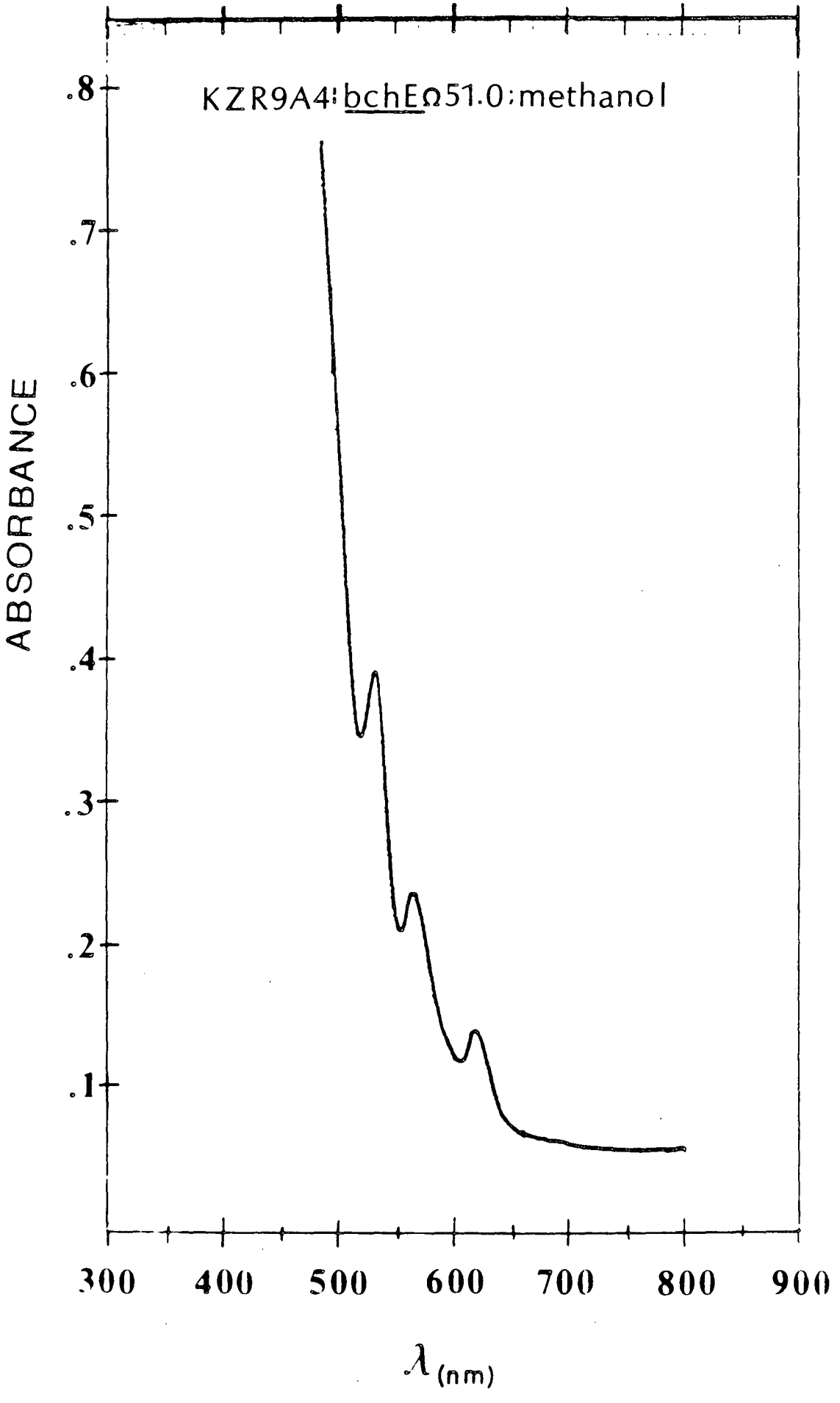
KZR9A4:bchEΩ51.0:methanol
ABSORBANCE
.8
.7
.6
.5
.4
.3
.2
.1
300
400
500
600
700
800
900
λ (nm)

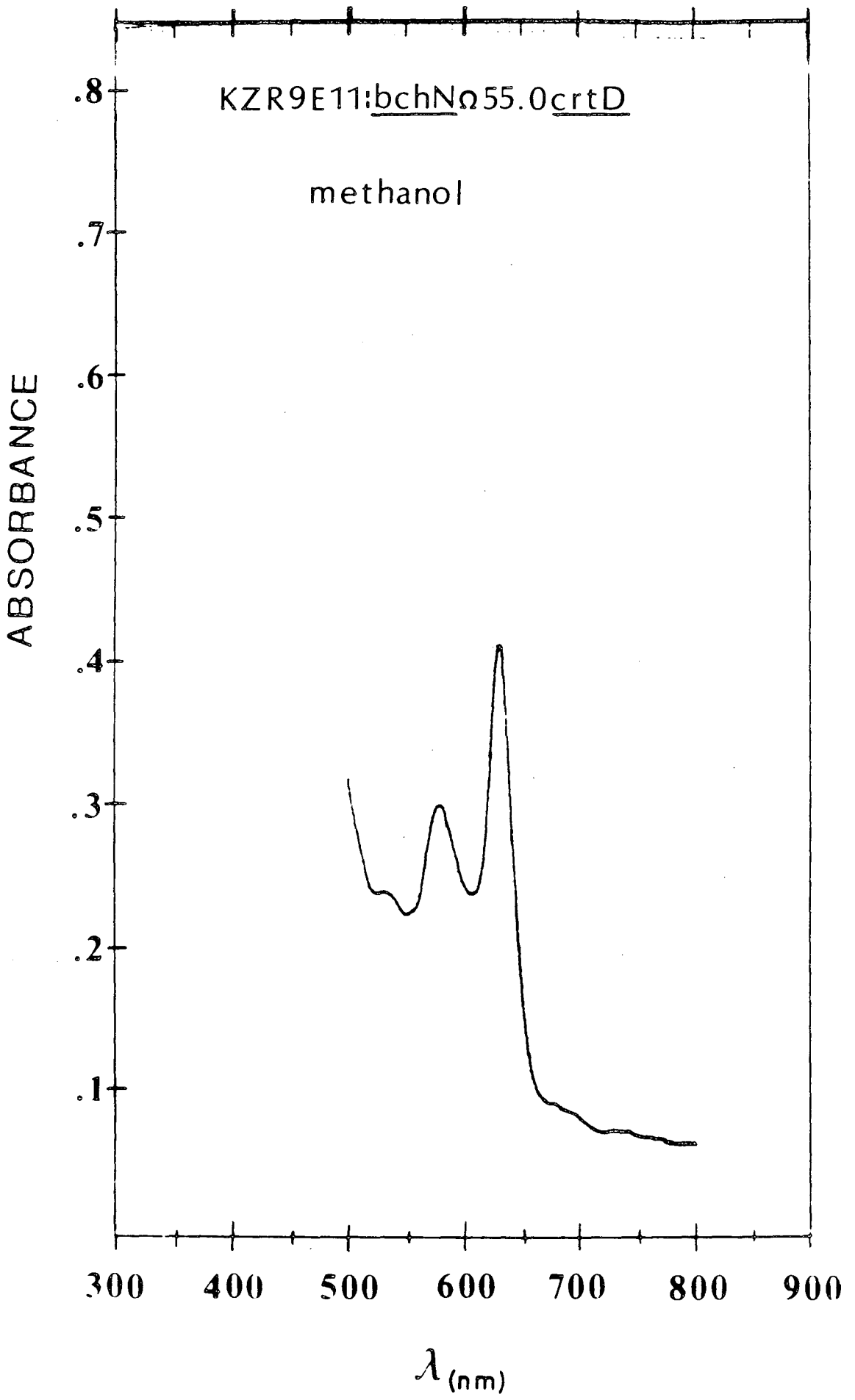
KZR9E11:bchNΩ55.0crtD
methanol
ABSORBANCE
.8
.7
.6
.5
.4
.3
.2
.1
300
400
500
600
700
800
900
λ (nm)

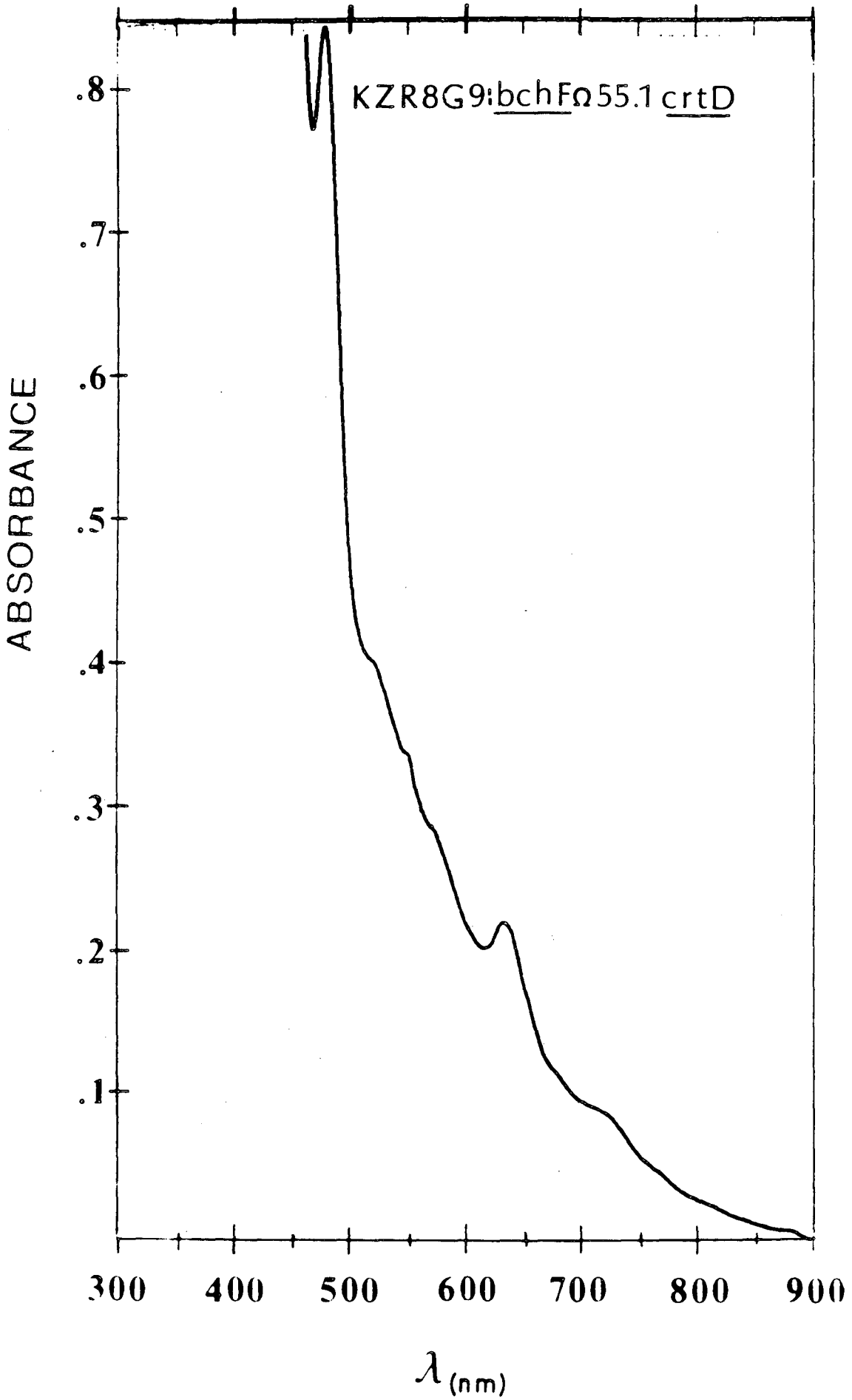
KZR8G9:bchFΩ55.1 crtD
ABSORBANCE
.8
.7
.6
.5
.4
.3
.2
.1
300
400
500
600
700
800
900
λ (nm)

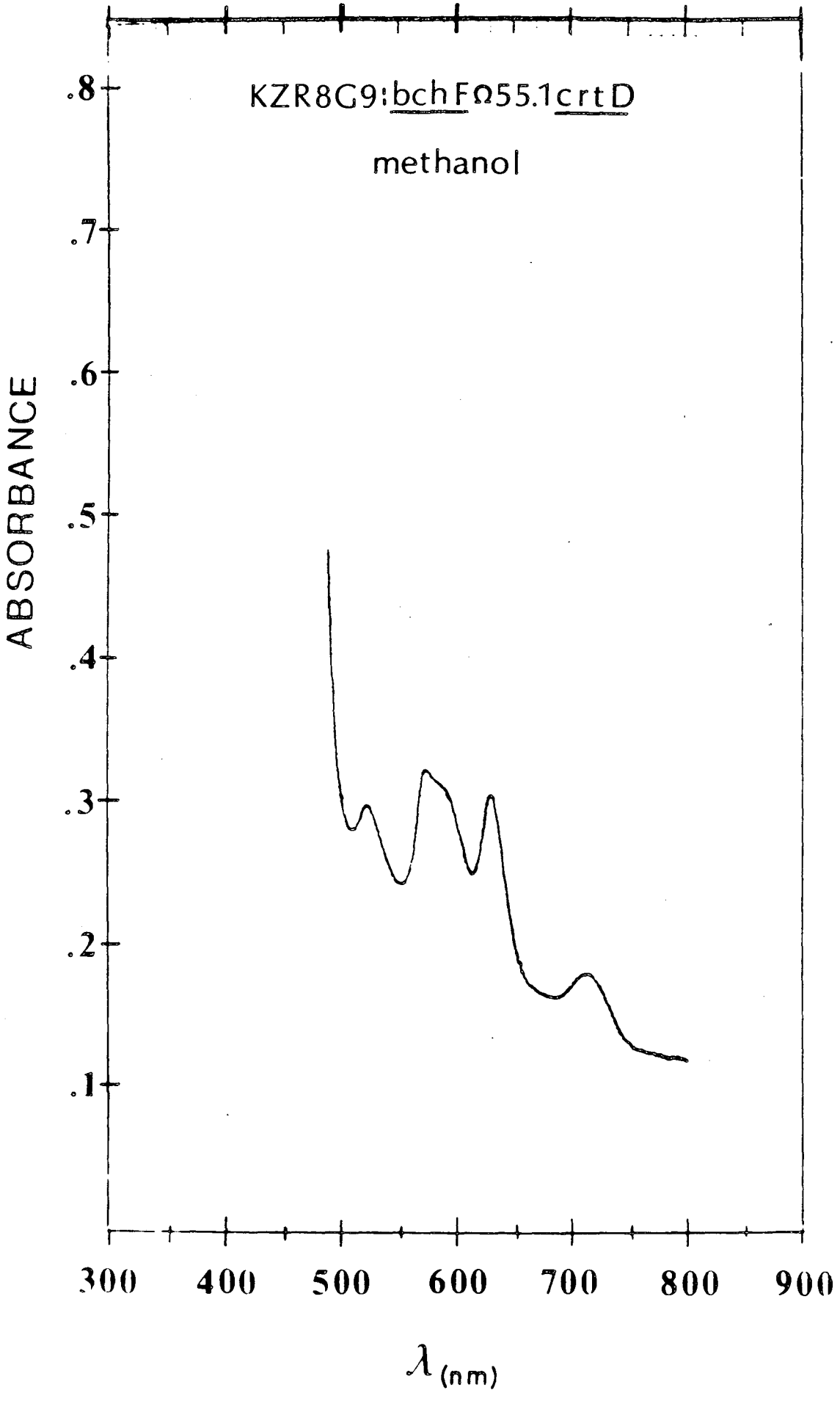
KZR8G9:bchFΩ55.1crtD
methanol
ABSORBANCE
.8
.7
.6
.5
.4
.3
.2
.1
300
400
500
600
700
800
900
λ (nm)

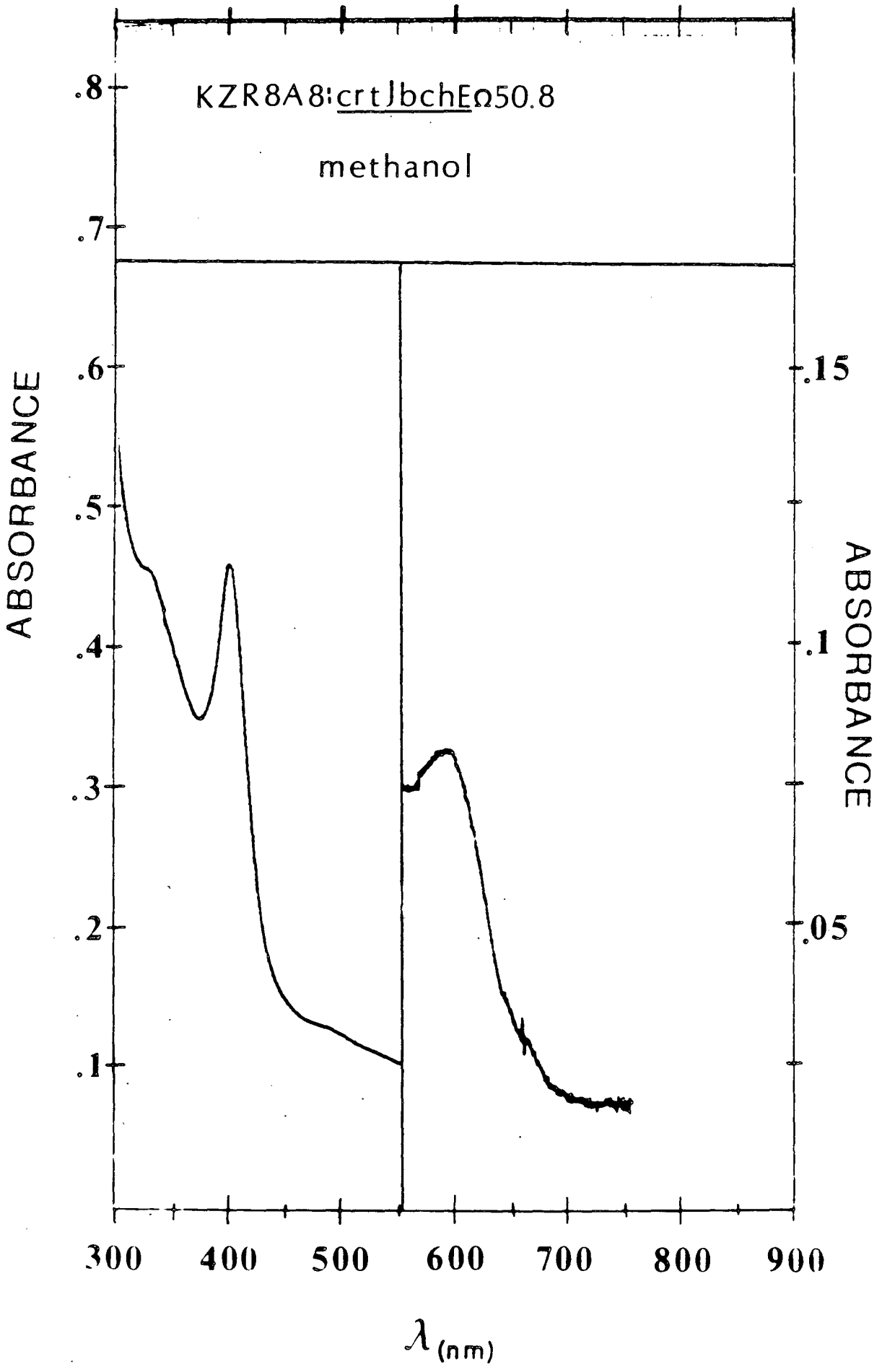
KZR8A8:crtJbchEΩ50.8
methanol
ABSORBANCE
.8
.7
.6
.5
.4
.3
.2
.1
.15
.1
.05
ABSORBANCE
300
400
500
600
700
800
900
λ (nm)

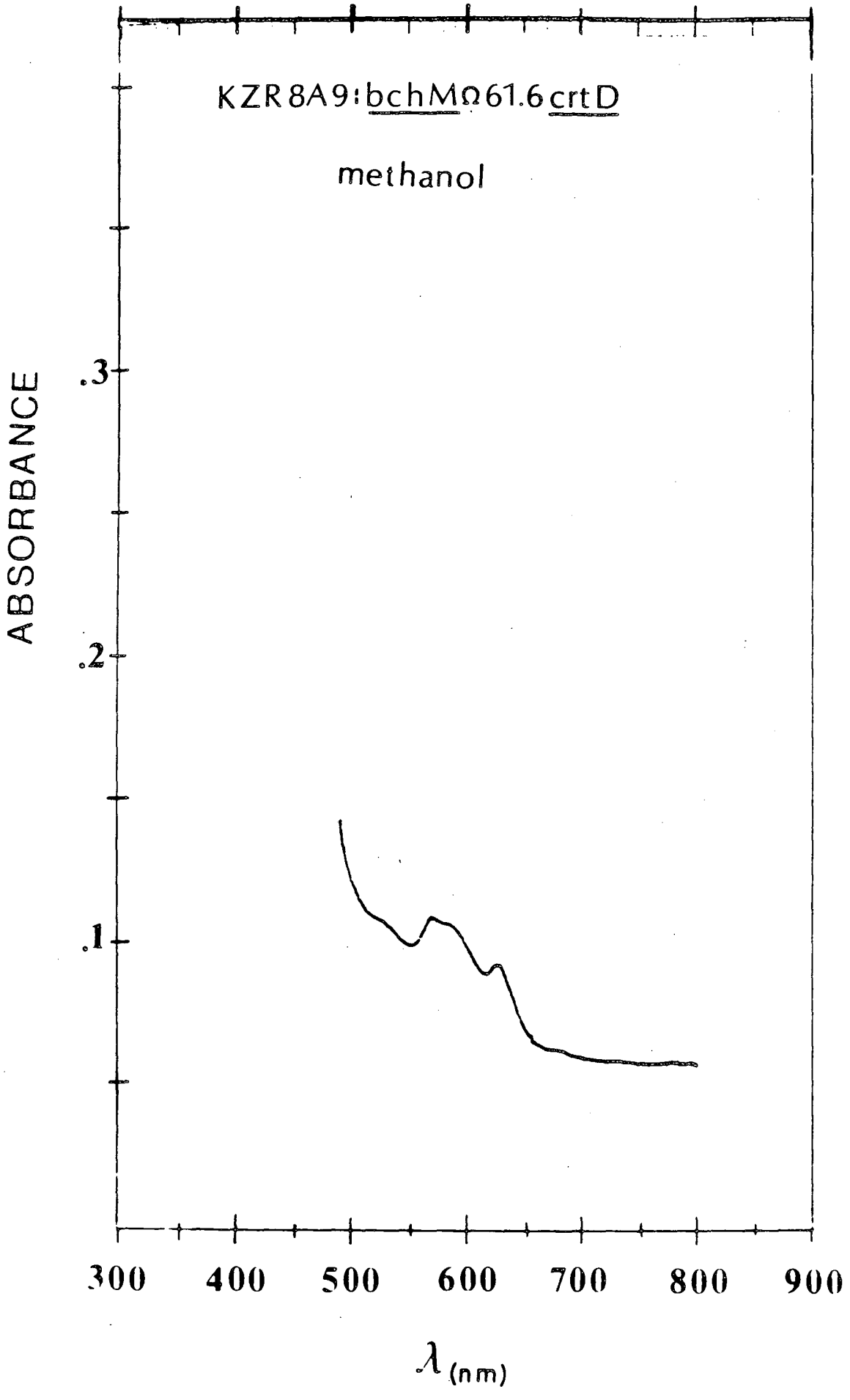
KZR8A9:bchMΩ61.6crtD
methanol
ABSORBANCE
.3
.2
.1
300
400
500
600
700
800
900
λ(nm)

TECHNICAL INFORMATION DEPARTMENT
LAWRENCE BERKELEY LABORATORY
UNIVERSITY OF CALIFORNIA
BERKELEY, CALIFORNIA 94720